Ontario

ONTARIO GEOLOGICAL SURVEY

Open File Report 6093

Precambrian Geology of Denton and Carscallen Townships, Timmins West Area

by

L.A.F. Hall and M.D. Smith

2002

Parts of this publication may be quoted if credit is given. It is recommended that reference to this publication be made in the following form:

Hall, L.A.F. and Smith, M.D. 2002. Precambrian geology of Denton and Carscallen townships, Timmins West area; Ontario Geological Survey, Open File Report 6093, 75p.

© Queen's Printer for Ontario, 2002

© Queen's Printer for Ontario, 2002.

Open File Reports of the Ontario Geological Survey are available for viewing at the Mines Library in Sudbury, at the Mines and Minerals Information Centre in Toronto, and at the regional Mines and Minerals office whose district includes the area covered by the report (see below).

Copies can be purchased at Publication Sales and the office whose district includes the area covered by the report. Although a particular report may not be in stock at locations other than the Publication Sales office in Sudbury, they can generally be obtained within 3 working days. All telephone, fax, mail and e-mail orders should be directed to the Publication Sales office in Sudbury. Use of VISA or MasterCard ensures the fastest possible service. Cheques or money orders should be made payable to the *Minister of Finance.*

Mines and Minerals Information Centre (MMIC) Macdonald Block, Room M2-17 900 Bay St. Toronto, Ontario M7A 1C3	Tel:	(416) 314-3800 1-800-665-4480(toll free inside Ontario)
Mines Library 933 Ramsey Lake Road, Level A3 Sudbury, Ontario P3E 6B5	Tel:	(705) 670-5615
Publication Sales 933 Ramsey Lake Rd., Level A3 Sudbury, Ontario P3E 6B5	Tel: Fax: E-mail:	(705) 670-5691(local) 1-888-415-9845(toll-free) (705) 670-5770 pubsales@ndm.gov.on.ca

Regional Mines and Minerals Offices:

Kenora - Suite 104, 810 Robertson St., Kenora P9N 4J2

Kirkland Lake - 10 Government Rd. E., Kirkland Lake P2N 1A8

Red Lake - Box 324, Ontario Government Building, Red Lake P0V 2M0

Sault Ste. Marie - 70 Foster Dr., Ste. 200, Sault Ste. Marie P6A 6V8

Southern Ontario - P.O. Bag Service 43, Old Troy Rd., Tweed K0K 3J0

Sudbury - Level B3, 933 Ramsey Lake Rd., Sudbury P3E 6B5

Thunder Bay - Suite B002, 435 James St. S., Thunder Bay P7E 6S7

Timmins - Ontario Government Complex, P.O. Bag 3060, Hwy. 101 East, South Porcupine P0N 1H0

Toronto - MMIC, Macdonald Block, Room M2-17, 900 Bay St., Toronto M7A 1C3

This report has not received a technical edit. Discrepancies may occur for which the Ontario Ministry of Northern Development and Mines does not assume any liability. Source references are included in the report and users are urged to verify critical information. Recommendations and statements of opinions expressed are those of the author or authors and are not to be construed as statements of government policy.

If you wish to reproduce any of the text, tables or illustrations in this report, please write for permission to the Team Leader, Publication Services, Ministry of Northern Development and Mines, 933 Ramsey Lake Road, Level B4, Sudbury, Ontario P3E 6B5.

Cette publication est disponible en anglais seulement.

Parts of this report may be quoted if credit is given. It is recommended that reference be made in the following form:

Hall, L.A.F. and Smith, M.D. 2002. Precambrian geology of Denton and Carscallen townships, Timmins West area; Ontario Geological Survey, Open File Report 6093, 75p.

103-00611/

Contents

Abstract xi

Introduction 1
- Scope and Objectives 1
- Location and Access 1
- Previous Geological Work 4
- Acknowledgements 5

Regional Geological Setting 5

Geology of Denton and Carscallen Townships 6
- The Deloro Assemblage (Supracrustal Package A) 8
  - Tholeiitic Mafic Metavolcanic Rocks (map unit 1) 8
  - Tholeiitic Felsic to Intermediate Metavolcanic Rocks (map unit 2) 10
  - Chemical Metasedimentary Rocks (map unit 3) 12
- Kidd-Munro Assemblage (Supracrustal Package B) 14
  - Quartz-Phyric Tholeiitic Felsic Metavolcanic Rocks (map unit 4) 15
  - High Titanium Tholeiitic Mafic Metavolcanic Rocks (map unit 5) 15
- Tisdale Assemblage (Supracrustal Package C) 15
  - Ultramafic Metavolcanic Rocks (unit 6) 17
  - High Magnesium Tholeiitic to Komatiitic Mafic Metavolcanic Rocks (unit 7) 18
  - Calc-Alkalic Intermediate to Felsic Metavolcanic rocks (map unit 8) 18
  - Clastic Metasedimentary Rocks (map unit 9) 19
- Kamiskotia Gabbroic Complex (map unit 10) 21
- Felsic to Intermediate Intrusive Rocks (map unit 11) 21
- Syntectonic Mafic and Ultramafic Intrusive Rocks (map unit 12) 22
- Late Tectonic Felsic to Intermediate Intrusive Rocks (map unit 13) 23
- Felsic and Intermediate Intrusive Rocks (map unit 14) 24
- Mafic Intrusive Rocks 25
  - Matachewan Dikes - (map unit 15) 25
  - Sudbury Dikes - (map unit 16) 25

Geochemistry 25
- Metavolcanic Rocks 27
  - Felsic Metavolcanic Rocks 27
  - Mafic Metavolcanic Rocks 31
  - Ultramafic Metavolcanic Rocks 36

Metamorphism 36

Structural Geology 36
- D_1 38
- D_2 38
- D_3 40
- D_4 40
- Porcupine-Destor Fault Zone (PDFZ) 40
- Late Faults 44

Geochronology 45

Geophysics 46
Airborne Magnetic Surveys 46
Gravity Surveys 47
Magnetic Susceptibility 47
Metavolcanic Rocks 47
Felsic Intrusive Rocks 49
Mafic Intrusive Rocks 49
Economic Geology 49
Gold Mineralization 49
Wire Gold Prospect 50
Larchmont Prospect 50
Jowsey Prospect 51
AuMo Prospects 51
Wakemac Prospect 51
Volcanogenic Massive Sulphide (VMS) Mineralization 53
Platinum Group Element (PGE) Mineralization 53
Recommendations for Mineral Exploration 53
Volcanogenic Massive Sulphide (VMS) Mineralization 53
Gold Mineralization 53
Magmatic Nickel-Copper-Platinum Group Element (PGE) Mineralization 54
References 54
Appendix 1: Geochemical data for 149 rock samples taken from Denton and Carscallen townships 59
Metric Conversion Table 75

FIGURES

1. General geology map of the Timmins area indicating the location of Denton and Carscallen townships 2
2. Access and drainage in Denton and Carscallen townships 3
3. General geology of Denton and Carscallen townships 7
4. Property locations in Denton and Carscallen townships 9
5. Distribution of iron formation (Map unit 3) through Denton and Carscallen townships 13
6. Distribution of Matachewan dikes in Denton and Carscallen townships 26
7. Classification of the metavolcanic rocks of Denton and Carscallen townships 28
8. Chondrite-normalised rare earth element (REE) patterns of the Deloro, Kidd-Munro and Tisdale assemblages felsic metavolcanic rocks 29
9. Chondrite-normalised REE patterns of felsic metavolcanic rocks of the Deloro assemblage compared with those of the Kidd-Munro and Tisdale assemblages 30
10. Geochemical comparison between sample 96JAA-0094, Kidd-Munro assemblage rocks from Denton Township and Kidd-Munro assemblage rocks from Kidd Township 32

11. Chondrite-normalised REE patterns of Deloro, Kidd-Munro and Tisdale assemblages mafic metavolcanic rocks 33
12. Chondrite-normalised REE patterns that compare mafic metavolcanic rocks of the Kidd-Munro assemblage with those of Deloro and Tisdale assemblages 34
13. Chondrite-normalised REE patterns that compare mafic metavolcanic rocks of the Deloro assemblage with those of Tisdale assemblage 35
14. Geochemical characterisation of Tisdale assemblage ultramafic metavolcanic rocks 37
15. U/Pb isochron plot for a syntectonic granodioritic dike in Denton Township 46
16. Frequency distribution histograms of magnetic susceptibility readings taken on rocks of Denton and Carscallen townships 48

PHOTOS

1. Angular chert fragments in Deloro assemblage brecciated pillows at the Wire Gold property 11
2. Chert 'flames' in Deloro assemblage brecciated pillows at the Wire Gold property 11
3. Fiamme in Kidd-Munro assemblage felsic metavolcanic rocks, Carscallen Township 16
4. Flow banding in quartz-phyric felsic metavolcanic rocks of the Kidd-Munro assemblage, Carscallen Township 16
5. Positively weathering polygons on outcrop surface of Tisdale assemblage ultramafic metavolcanic rocks, Denton Township 17
6. Flattened pillows in mafic metavolcanic rocks of the Tisdale assemblage, Denton Township 19
7. Thinly interbedded sandstone and shale of map unit 9c 20
8. Potassium feldspar megacrysts in granodiorite rocks of the Kenogamissi batholith 24
9. Rootless, isoclinal F_1 fold in Tisdale assemblage metasedimentary rocks, Denton Township 39
10. Z-shaped F_2 fold in Tisdale mafic metavolcanic rocks, Denton Township 39
11. Chevron-shaped F_3 folds in Tisdale ultramafic metavolcanic rocks, Denton Township 41
12. Composite set of F_4 kink-bands over-printing Z-shaped F_2 fold in Tisdale assemblage metasedimentary rocks, Denton Township 42
13. Syntectonic granodiorite dikes intruding mylonitized Tisdale assemblage mafic metavolcanic rocks, Denton Township 42
14. Boudinaged and folded syntectonic granodiorite dike, Denton Township 43
15. Folded anisotropy in mylonitized gabbro 43

TABLES

1. Recent exploration activities; Denton and Carscallen townships 5
2. Summary of geological characteristics of properties in Denton and Carscalle[illegible]ships 52

GEOLOGICAL MAP

Map P.3517 Precambrian Geology, Denton and Carscallen Townships ..... back pocket

Abstract

Denton and Carscallen townships are underlain by three distinct assemblages of Neoarchean metavolcanic and metasedimentary rocks: the Deloro, Kidd-Munro and Tisdale assemblages. Intimately interleaved mafic, felsic and intermediate metavolcanic rocks with local iron formation horizons characterise the Deloro assemblage in the map area. A wide section of quartz-phyric, felsic metavolcanic rocks with limited high-iron and high-titanium mafic, metavolcanic flows comprise the Kidd-Munro assemblage and are located in northeast Carscallen Township. The Tisdale assemblage comprises dominantly mafic metavolcanic flows interlayered with ultramafic and felsic metavolcanic rocks and massive to bedded epiclastic metasedimentary rocks. These Tisdale assemblage rocks are exposed primarily in Denton Township.

The Kamiskotia Gabbroic Complex (KGC) intrudes the supracrustal rocks of both the Deloro and Kidd-Munro assemblages in northwest Carscallen Township. The Carlton Lake pluton, a biotite-hornblende granodiorite to tonalite intrusion, occupies much of southwest Carscallen and northwest Denton townships and is interpreted to be temporally and genetically associated with the KGC. Similarly, the Turnbull tonalite in north-central Carscallen is pene-contemporaneous with the KGC. Small, mafic to ultramafic intrusions intrude the Tisdale assemblage rocks in Denton Township, cutting the earliest tectonic fabric present in these supracrustal rocks. The Kenogamissi Batholith intrudes the Tisdale assemblage and the small mafic to ultramafic intrusions and underlies the southern half of Denton Township. Abundant mafic dikes of the Paleoproterozoic Matachewan swarm intrude all of the above rock units. A Mesoproterozoic Sudbury dike is interpreted, from geophysical data, to intrude the Kidd-Munro metavolcanic rocks in northeast Carscallen Township.

Map-scale folds have been interpreted as the earliest deformational feature (D_1) in the map area. Axial planar to these F_1 folds is a penetrative foliation (S_1) present in all the Archean rocks except the small mafic to ultramafic intrusions and the Kenogamissi batholith. Three generations of minor folds overprint S_1 : F_2, primarily Z-shaped, upright folds with a moderately penetrative axial planar foliation (S_2) striking to the east-northeast; F_3, a composite set of shallow dipping crenulations; and F_4, a composite set of upright kink folds. S_1 is typically transposed and forms a composite main foliation with S_2. A west-striking band of mylonite in central Denton Township obliterates and/or replaces these tectonic fabrics. This mylonite zone is interpreted as the main trace of the Porcupine-Destor Fault Zone. Locally, the mylonite cuts S_1 and it is likely to represent a progressive deformation reflected elsewhere by F_2, F_3, F_4.

The Archean rocks in the map area have undergone regional greenschist grade metamorphism. Amphibolite grade metamorphism occurs in proximity to and within the high-strain zone of the Porcupine-Destor Fault as well as in the vicinity of the Carlton Lake pluton.

Mineral exploration activity has been conducted in the map area since 1911. The focus of most of this activity has been gold, however some interest has also been shown in the base metals potential of the area.

Precambrian Geology of Denton and Carscallen Townships, Timmins West Area

L.A.F. Hall and M.D. Smith

Ontario Geological Survey
Open File Report 6093

2002

Introduction

SCOPE AND OBJECTIVES

The Abitibi greenstone belt is one of the world's most economically significant greenstone belts and has been the focus of mineral exploration for nearly a century. Mineral exploration is more challenging as prospectors and geologists are required to work in areas where there is little geoscience information due to extensive overburden and structural complexities. The Precambrian Geoscience Section of the Ontario Geological Survey has been conducting township scale (1:20 000) bedrock mapping in some of the least well-understood parts of the Timmins region to facilitate mineral exploration activities. The current project has focussed on Carscallen and Denton townships as a continuation of bedrock mapping in Bristol and Ogden townships in 2000 (Vaillancourt 2000; Vaillancourt, Pickett and Dinel 2001).

The goals of this project are threefold:

1) to clarify lithostratigraphic uncertainties and to refine the map boundaries;
2) to evaluate mineral potential of an Ontario Living Legacy (OLL) site established in Denton Township;
3) and to ascertain the extent and nature of the regionally significant Porcupine-Destor fault zone (PDFZ).

Nearly three months were spent in the field conducting bedrock mapping and lithogeochemical sampling. Airborne and ground geophysical surveys and diamond-drill hole data were used to aid in the extrapolation of geological contacts across the many large areas obscured by overburden.

LOCATION AND ACCESS

The geographic center of the map area is approximately 30 km southwest of the City of Timmins (Figure 1). Bounded by Latitudes 48° 16' 36" and 48° 27' 02" and Longitudes 81° 35' 41" and 81° 43' 34" the map area covers an almost 200 km^2 area which encompasses Carscallen and Denton townships.

Access to the area is afforded by Highway 101 that bisects it and by numerous forestry roads in variable condition. Well used roads include the Malette Road that extends along the northern boundary of Carscallen Township, the "Old Malette Road" that extends south through Carscallen Township and into Denton Township to Highway 101 and the road to the Star Lake garbage dump south of the highway. The Tatachikapika River flows diagonally across southeast Denton Township providing boat access when there is enough water (Figure 2).

The map area is flat-lying with a total relief of less than 100 m. Lying within the Northern Clay Belt (Hughes 1959) the area is largely covered by surficial deposits with less than 5% bedrock exposure. Quaternary deposits include the Adam Till, covering most of both townships; local eskers, kames and fluvial terraces; and glaciofluvial outwash in Denton Township (Tucker and Richard 1983).

Waterways in Denton Township and southern Carscallen Township drain to the south into the Tatachikapika River. Drainage in northern Denton Township flows to the north feeding the Kamiskotia River. Both the Tatachikapika and Kamiskotia rivers flow north to Hudson Bay.

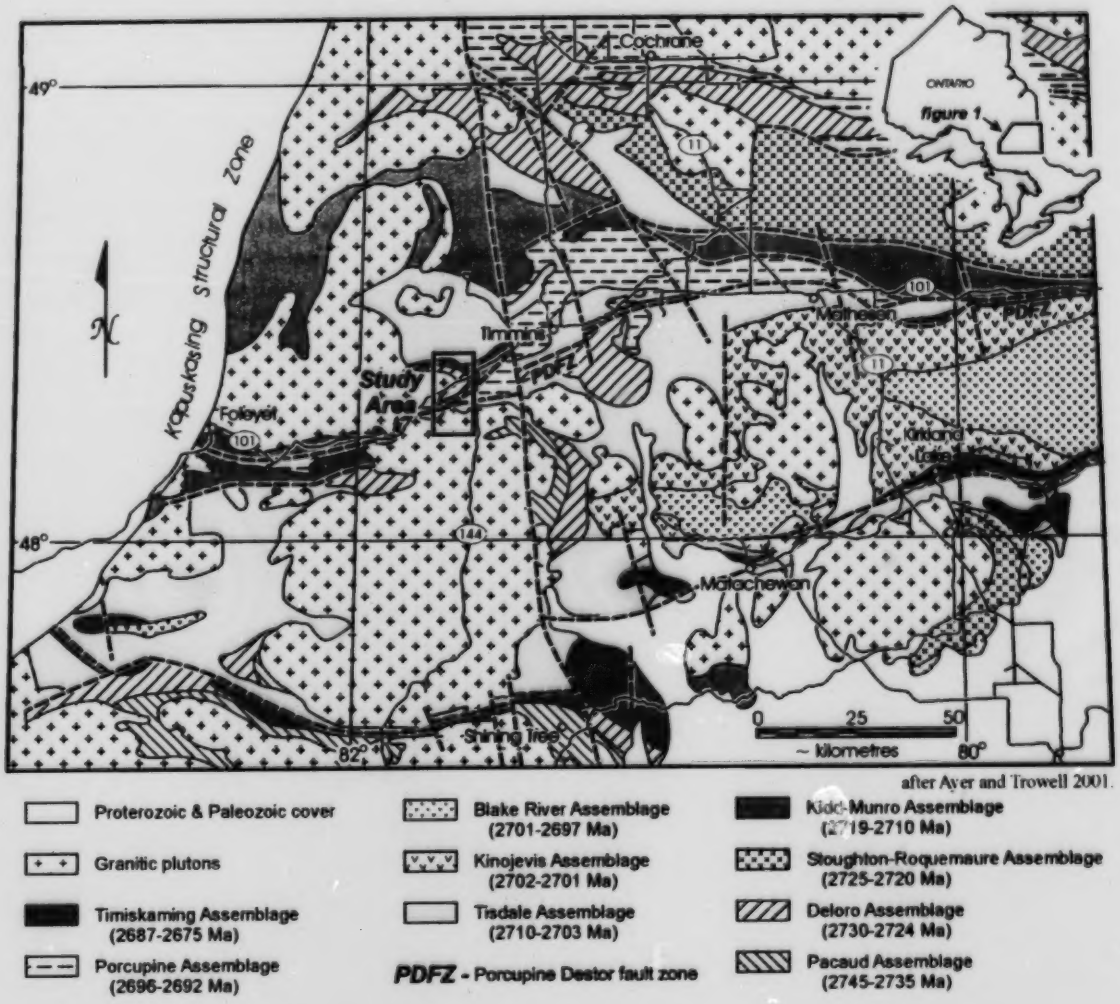

Figure 1. General geology map of the Timmins area indicating the location of Denton and Carscallen townships.

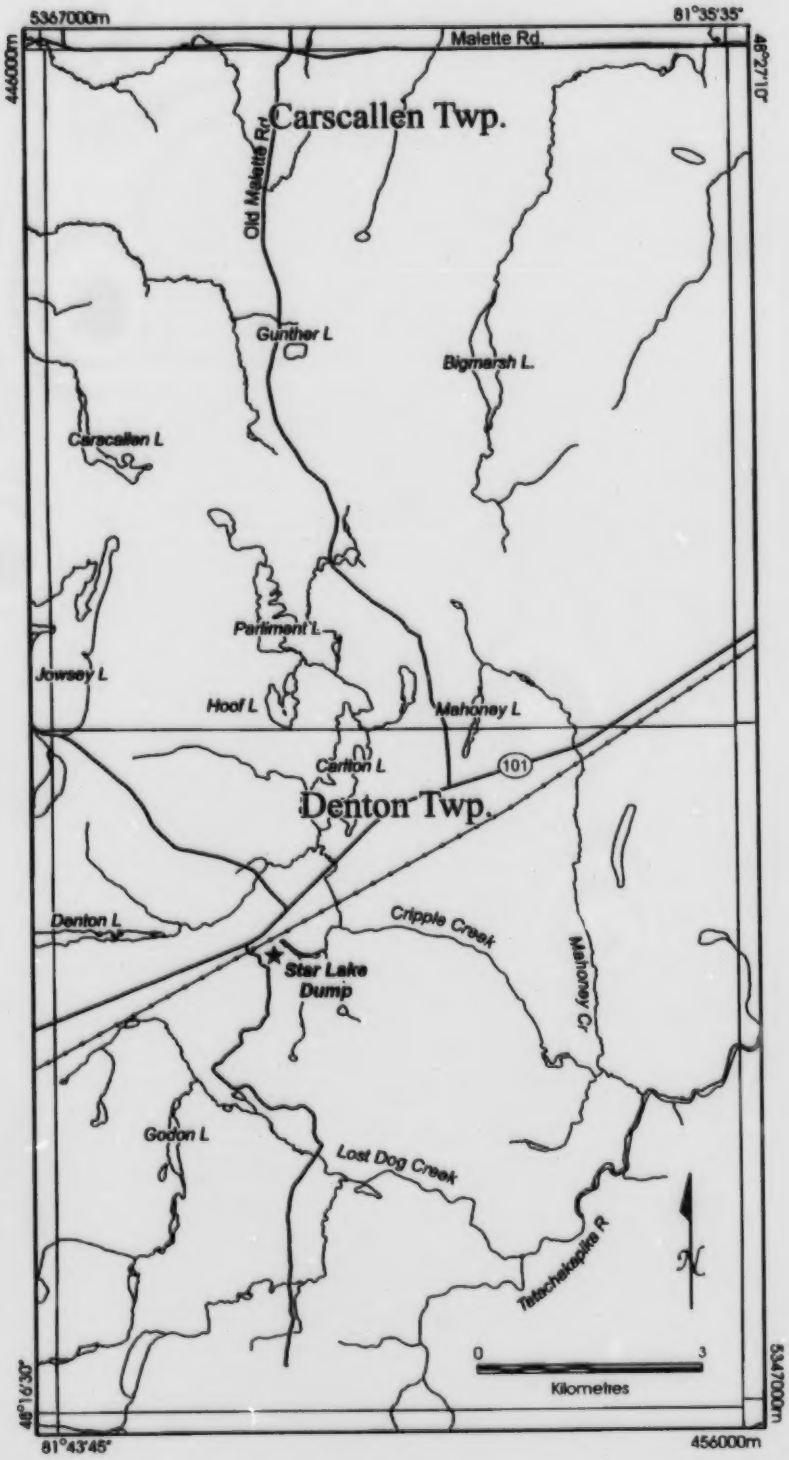

Figure 2. Access and drainage in Denton and Carscallen townships.

Little forestry activity has been conducted in the map area within the last year. Over the last two decades, however, much of the area has been clear-cut and replanted. Jack pine plantations predominate in Denton Township where the land is well drained. Carscallen Township was replanted with spruce, fir and larch as well as pine.

PREVIOUS GEOLOGICAL WORK

Following Wilson's landmark gold discovery of 1909 and the staking rush it precipitated, the Ontario Department of Mines sponsored geological investigations into the Porcupine gold camp (Burrows 1911, 1912; Rogers and Bruce 1911). Included in Burrows' reports (1911, 1912) are descriptions of exposures on claims staked in Denton Township. Rogers and Bruce (1911) conducted a geological survey of part of the 'Cripple Creek Gold Area' of Denton Township along and in proximity to the waterways. Todd (1926) identified a belt of Archean supracrustal rocks along the canoe routes through Denton and Keefer townships. Hawley (1926) mapped Carscallen Township at a scale of 1:47 520 as part of a project which also included Bristol and Ogden townships. All the major lithologies were identified and classified within the accepted geological model of the day based on relative age criteria. Similarly, Denton Township was included in a study that encompassed Keefer to Eldorado townships (Harding and Berry 1938). Mapping was carried out at a scale of 1:63 360.

Ferguson (1959) compiled a 1:15 840 scale geological map for Denton Township using Ontario Department of Mines airborne geophysical magnetic data and assessment file data. Denton Township was also included in regional compilations at 1:254 440 scale using updated airborne geophysical magnetic data (Ginn et al. 1964; Pyke et al. 1973).

More recently, Denton Township was part of a three township bedrock mapping project conducted by Choudhry (1982, 1989) at a scale of 1:15 840. Carscallen Township was included in a geological mapping project of the Kamiskotia area (1:50 000 scale: Barrie 1990, 1992, 2000). A geological compilation of the Timmins area (1:100 000 scale; Ayer and Trowell 1998) applies current lithostratigraphic concepts to the geology of the map area and the surrounding region using new geochronological and lithogeochemical data.

Brisbin (1997) compiled a comprehensive review of the history of the geological work and the development of stratigraphic models for the Timmins region.

Extensive exploration activity has been carried out across the map area by the mineral exploration industry throughout much of the last century. Most of the focus of this activity was gold. After the discovery of the Kidd Creek volcanogenic massive sulphide deposit, however, base metal exploration began to play a more significant role. Although this is a situation that is in constant flux, it should be noted that much of the Crown Land in the map area was staked at the time of preparation of this report.

Recent exploration activities conducted in Carscallen and Denton townships are summarised in Table 1.

Company/Individual	Area	Type of Work
Galata, F.	southwest Denton Twp.; Godon Lake area	Geological mapping, power stripping
Falconbridge Ltd.	northwest Carscallen Twp.; Carscallen Lake area	Diamond drilling, ground geophysics (EM)
Bonhomme, J.C.	Denton Twp.; S of Hwy 101	Diamond drilling, ground geophysics (Mag., IP)
Prospectors Alliance	west Denton Twp.; south of Denton Lake	Ground geophysics (Mag.)
Prospectors Alliance	west Carscallen Twp.; south of Carscallen Lake	Ground geophysics (Mag., IP)
Explorers Alliance	Denton Twp.: Wakemac Property	Ground geophysics (IP)
Explorers Alliance	northwest Carscallen Twp.	Ground geophysics (IP)
Explorers Alliance	Denton Twp.: AuMo (B) Property	Diamond drilling
Explorers Alliance	west Denton Twp.	Diamond drilling
Explorers Alliance	north Carscallen Twp.	Diamond drilling

Abbreviations: EM – electro-magnetic; Mag – magnetic; IP – induced potential

Table 1. Recent exploration activities; Carscallen and Denton townships.

ACKNOWLEDGEMENTS

This project benefited greatly from the able and enthusiastic assistance of M. Smith (senior assistant), S. Thibeault (junior assistant) and L.-K. Dekeyser (junior assistant). S. Josey drafted the figures with an eye to detail and accuracy as well as aesthetics. J. Parker improved this report with his careful and patient editing. C. Vaillancourt and B. Atkinson introduced me to the Timmins area with extensive fieldtrips. C. Vaillancourt, B. Atkinson, J. Ayer and B. Berger offered their time and their insights into the regional geology of the Timmins gold camp. J. Rudd provided assistance with the geophysical interpretation. The opportunity to go underground at the Kidd Creek Mine was afforded by D. Duff (Manager of Geology, Falconbridge Ltd.) and S. Gibbons (Mine Geologist, Falconbridge Ltd.) led a fascinating tour. B. Calhoun (geologist) took the author to some of the more interesting and relevant exposures and properties of the Timmins West area and provided a great deal of assistance with diamond-drill core. L. Bonhomme (prospector) provided data, access to diamond-drill core and perspective on the exploration potential of the map area. I am indebted to them all.

All geochemical data presented in this report were provided by the Geoscience Laboratories, Ontario Geoservices Centre, Sudbury. J. Ketchum of the Jack Satterly Geochonology Laboratory, Royal Ontario Museum provided the geochronological analysis.

Regional Geological Setting

The Abitibi Subprovince of the Superior Province comprises a stratigraphically continuous succession of Neo- to Mesoarchean (2.5 to 2.9 Ga) metavolcanic and metasedimentary rocks interpreted to have developed in an ensimatic basin (Ayer et al. 2001). These supracrustal rocks are intruded by multiple generations of felsic to ultramafic igneous rocks. This intrusive activity extended from the Neoarchean into the late Proterozoic.

Three volcanic and two sedimentary assemblages are exposed in the Timmins region (Ayer et al. 1997, 1999, 2002) (*see* Figure 1). The Deloro assemblage is the oldest (2730-2724 Ma, Ayer et al. 2002) and consists of mafic to felsic, calc-alkalic metavolcanic rocks and associated iron formation (Ayer et al. 1999, 2002). The Kidd-Munro assemblage ranges in age from 2719 Ma to 2710 Ma (Ayer et al. 2002) and

unconformably overlies the Deloro assemblage (Ayer et al. 1999, 2002). The Kidd-Munro assemblage consists of a suite of tholeiitic and komatiitic metavolcanic rocks locally interlayered with rhyolite and a suite of calc-alkalic felsic to intermediate metavolcanic rocks (Ayer et al. 1999). The Tisdale assemblage overlies the Kidd-Munro assemblage and ranges in age from 2710 Ma to 2703 Ma. The base of the Tisdale assemblage consists of tholeiitic mafic to komatiitic metavolcanic rocks locally associated with high-silica rhyolite. Felsic to intermediate, calc-alkalic pyroclastic metavolcanic rocks and local thick accumulations of iron formation form the upper, younger parts of the Tisdale assemblage (Ayer et al. 1999). The Porcupine assemblage is the oldest (2696-2692 Ma, Ayer et al. 2002), lowermost sedimentary package in the area and consists dominantly of turbiditic metasedimentary rocks. The Porcupine assemblage unconformably overlies the metavolcanic assemblages (Ayer et al. 1999). The Timiskaming assemblage unconformably overlies the Porcupine assemblage and consists of coarse clastic metasedimentary rocks (Ayer et al. 1999, 2002).

The Kamiskotia Gabbroic Complex is interpreted to be coeval with the Tisdale assemblage and intrudes the Deloro and Kidd-Munro assemblages (Barrie 1990, 1992, 2000). Several plutons of felsic to intermediate compositions are considered to be comagmatic with the Kamiskotia Gabboic Complex based on similar geochemical characteristics, overlap in U/Pb zircon ages, contact relationships, and textural similarities (Barrie 1990, 1992, 2000). Archean, post-volcanic, felsic plutons and associated dikes intrude all of the assemblages (Pyke 1982). Proterozoic mafic dikes (Matachewan, Abitibi swarms) intrude Archean rocks (Pyke 1982).

The rocks of the Abitibi Subprovince have experienced variable degrees of deformation and metamorphism. Of particular significance in the Timmins region, due to its relationship with gold mineralization (Berger 2001), is the Porcupine-Destor Fault Zone (PDFZ). The fault zone is a major structural features that strikes east-northeast and has been traced along strike for over 450 km across the Abitibi Subprovince (Berger 2001). The PDFZ is offset by numerous north-northwest-striking faults that partition the Abitibi greenstone belt into distinct blocks that display different styles of alteration associated with gold mineralization, deformation and metamorphism (Berger 2001). Early Proterozoic (2454 Ma; Heaman 1988) Matachewan dikes are also offset by the north-northwest-striking faults (Brisbin 1997). The relationship between these late faults and the younger mafic dikes of the Abitibi swarm has not been determined.

Phanerozoic bedrock is not exposed in the Timmins area, therefore, there is no record of the geological history post-dating the late faulting and/or intrusion of the Abitibi dike swarm. Unconsolidated Quaternary glacial deposits and recent terrestrial sedimentary and regolithic deposits cover most of the Precambrian bedrock in the Timmins region.

Geology of Denton and Carscallen Townships

Archean metavolcanic and plutonic rocks and Paleozoic mafic dikes underlie Denton and Carscallen townships. Mafic to ultramafic plutonic rocks of the Kamiskotia Gabbroic Complex occur in the northwest corner of Carscallen Township while felsic metavolcanic rocks dominate the northeast corner. The Carlton Lake Pluton, a large, semi-circular felsic intrusion, lies in the southwest corner of Carscallen Township and the northwest corner of Denton Township. Felsic plutonic rocks underlie the southern third of Denton Township. Mafic metavolcanic-dominated supracrustal rocks underlie the rest of the map area. The regionally significant PDFZ traverses the southern half of Denton Township with a dominantly westward trend. Figure 3 is a simplified sketch of the Archean geology of Denton and Carscallen Townships.

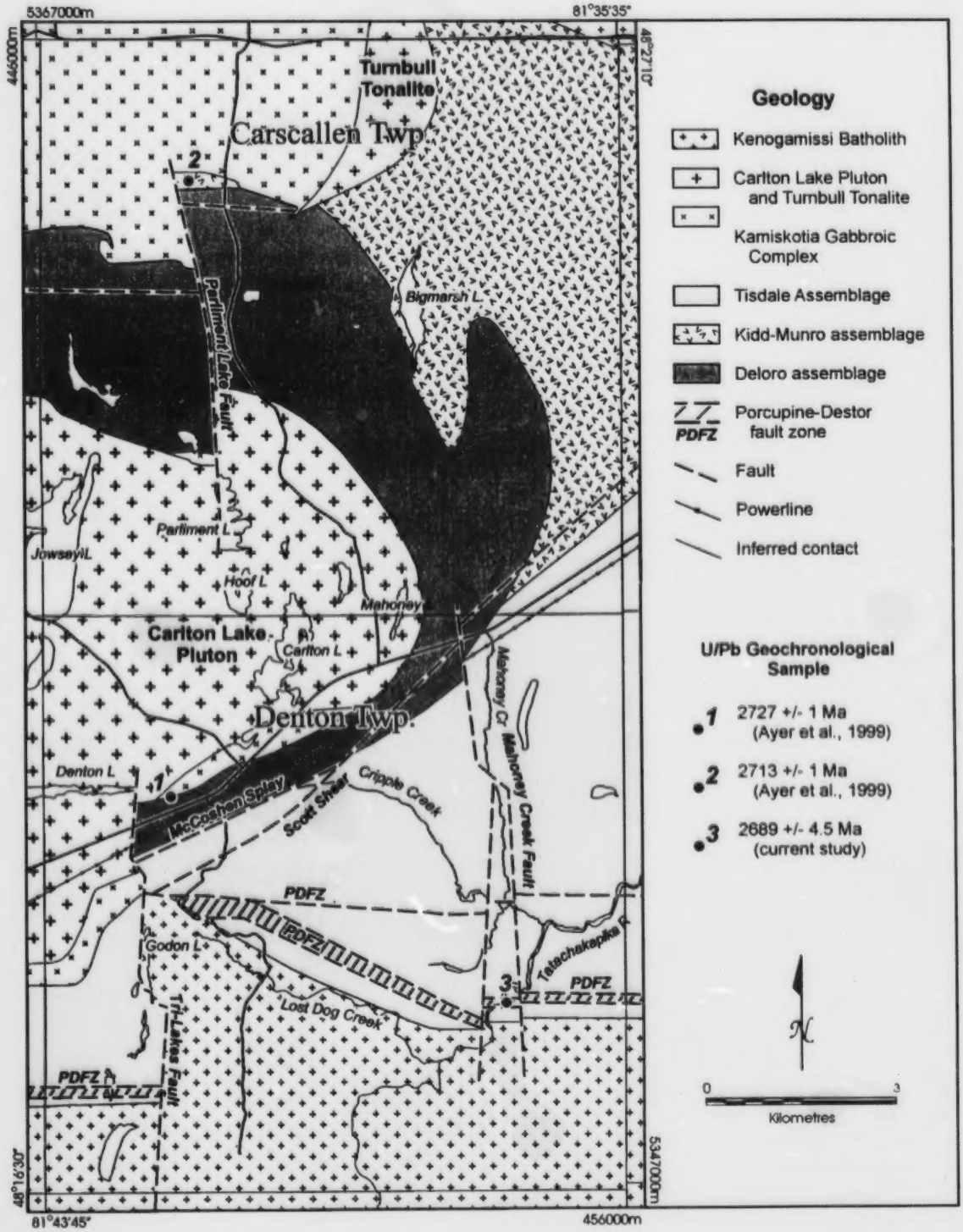

Figure 3. General geology of Denton and Carscallen townships.

Denton and Carscallen townships are underlain by three distinctive metavolcanic and metasedimentary sequences (*see* Figure 3; Map P.3517, back pocket) as well as mafic and felsic intrusions. Identifying the assemblage to which these sequences of supracrustal rocks belong is complicated by the lithologic, stratigraphic and geochemical similarities between the assemblages. Locally intense hydrothermal alteration has also obscured the nature of the metavolcanic and metasedimentary rocks. Structural complexities, including the regionally significant PDFZ, further obscure and offset the assemblages. However, two U-Pb geochronological samples taken in Denton and Carscallen townships (*see* Figure 3) have yielded zircons of Deloro and Kidd-Munro ages respectively (Ayer et al. 1999), indicating that these assemblages at least are present in the field area.

THE DELORO ASSEMBLAGE (SUPRACRUSTAL PACKAGE A)

Supracrustal Package A, herein interpreted as the Deloro assemblage, extends from the western border of Carscallen Township to the western border of Denton Township in a semi-circular, east-facing sequence (*see* Figure 3). The Carlton Lake pluton occupies the core of this semi-circle of metamorphosed supracrustal rocks. The Deloro assemblage is thickest (approximately 3 km) in western Carscallen Township and thins to less than 1 km in western Denton Township.

Intimately interlayered (10 to 100 m) mafic, intermediate and felsic metavolcanic rocks with rare, thin, horizons of chemical metasedimentary rocks characterise the Deloro assemblage. Three separate rock units, within this part of the Deloro assemblage, were identified during bedrock mapping: 1) tholeiitic mafic metavolcanic rocks; 2) tholeiitic felsic to intermediate metavolcanic rocks; and 3) chemical metasedimentary rocks.

The Deloro assemblage rocks in the map area typically display extensive deformation, manifested by a penetrative foliation that is locally folded, crenulated and/or kink-banded. Several of these structural features are recognisable in a single outcrop. The regional greenschist facies metamorphism (Jolly 1974, 1977, 1978; Powell et al. 1990) is manifested through the ubiquitous presence of chlorite and/or sericite that define the main foliation in this assemblage. Garnet porphyroblasts were observed in a few locations. Alteration is variable and includes iron carbonatization, chloritization, silicification and chlorite spots. Chloritization through alteration processes are herein distinguished from metamorphic chlorite development by the brown colour and coarser texture of the altered rocks. Primary igneous textures are preserved in some exposures that are less profoundly deformed and metamorphosed.

Tholeiitic Mafic Metavolcanic Rocks (map unit 1)

Small, flat, glacially scoured exposures of chlorite and/or amphibole phyllite and schist typify the tholeiitic mafic metavolcanic rocks of the Deloro assemblage. Dark green to grey-green on the fresh surface, these rocks are bleached light green-grey to green-buff on weathered surfaces. These rocks are predominantly aphyric but may contain small plagioclase and rare biotite phenocrysts in massive flow horizons.

Relict pillow selvages are discernible in rare outcrops. Pillows are typically flattened, with an aspect ratio in the horizontal surface of between 10:1 and 15:1. At both the Wire Gold property and north of Gunther Lake area (Figures 3 and 4), stripping of cherty iron formation also exposed relatively well-preserved mafic metavolcanic rocks.

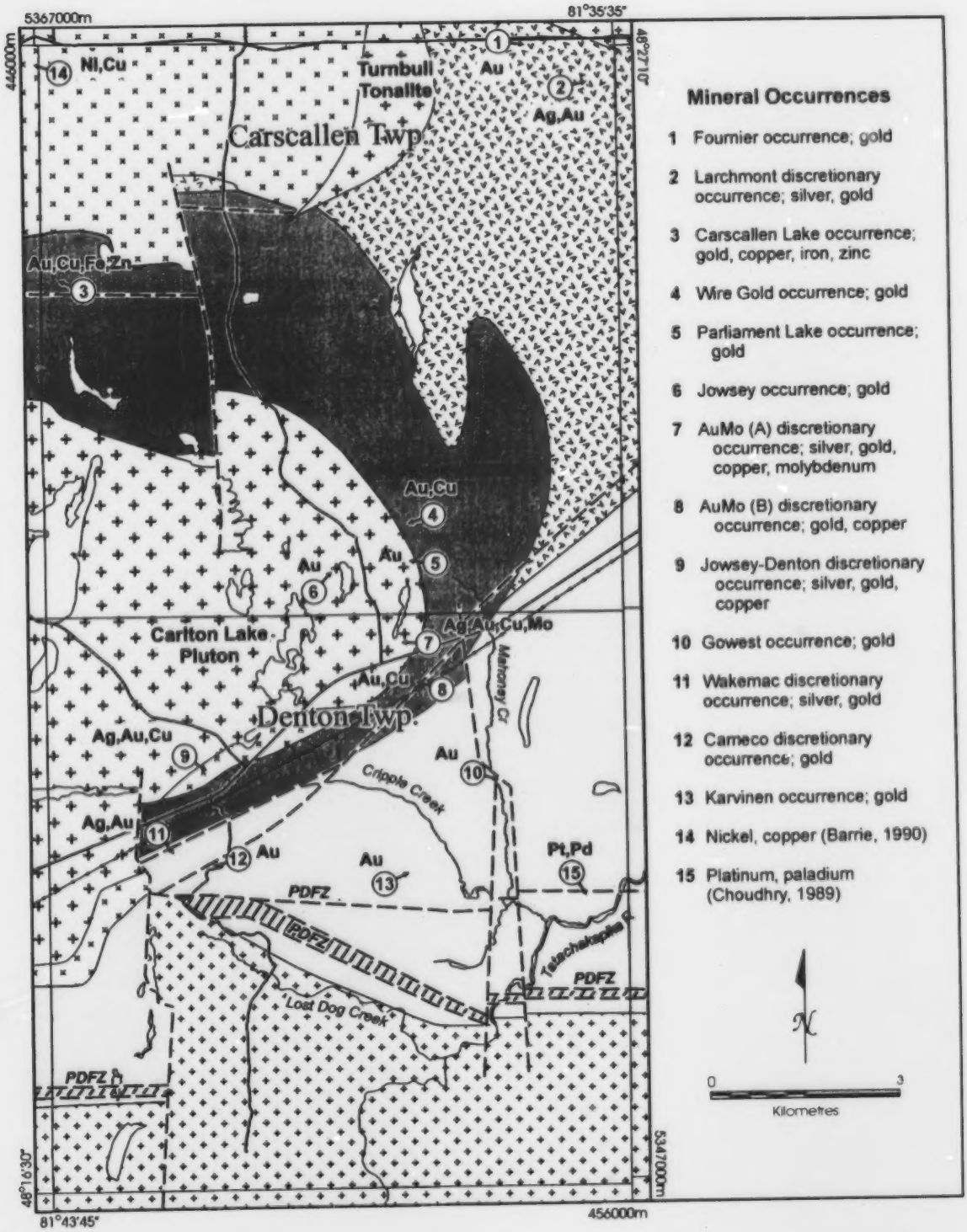

Figure 4. Property locations in Denton and Carscallen townships.

North of Gunther Lake (*see* Figure 3), well-preserved pillows with interstitial cherty material immediately underlie the iron formation. Pillows have an aspect ration of 1:3 to 1:6 at this location. Pillow widths consistently range from 20 to 35 cm, while the lengths of the pillows range from 80 to 200 cm. Quartz-filled, irregularly shaped amygdules are more concentrated on the northeast side of the pillows. Pillow selvages are 2 to 4 cm wide and contain disseminated pyrite. The metavolcanic and metasedimentary rocks are interpreted to face northeast at this location based on pillow cusps/keels and the concentration of amygdules. A mafic to intermediate synvolcanic sill intrudes the top of the iron formation. Mafic to intermediate massive flows overlie it.

At the Wire Gold Property, bleached, angular to rounded, pillow fragments that range from 1 to 70 cm in size are mixed with rare, small (2 to 5 cm), angular chert fragments (Photo 1). This dominantly mafic metavolcanic breccia is interpreted to overlie the cherty iron formation, based on:

a) the presence of chert fragments within the breccia;

b) flame-like structures of chert intruding the breccia (Photo 2); and

c) the mafic breccia truncates iron formation and intrudes the iron formation as a sill-like body, though it retains its fragmental texture.

The mafic breccia is interpreted to be the result of a debris flow event that disrupted the pillowed mafic flows and redeposited them on unlithified chemical sediments.

In thin section the primary mineral assemblage of the mafic metavolcanic rocks of the Deloro assemblage has been obliterated. Amphibolitized mafic rocks in the contact metamorphic aureole of the Carlton Lake pluton consist of hornblende, plagioclase and epidote. Greenschist facies rocks occur outside the contact aureole and dominantly consist of chlorite, epidote and white mica (+/- biotite). Between these end-members are mafic metavolcanic rocks containing both chlorite and hornblende in varied proportions. Plagioclase is limited to rocks with only hornblende. Pyrite and magnetite occur in all thin sections examined.

Thin (<3 m) interbeds of quartz-sericite phyllite and schist occupy less than 10% of the bedrock exposures within the tholeiitic mafic metavolcanic rocks of the Deloro assemblage. These rocks are buff-white weathering and quite distinctive from the surrounding mafic rocks. The felsic to intermediate rocks are primarily aphyric, though rare exposures contain small, feldspar phenocrysts. The felsic to intermediate rocks become more abundant near the contact with the tholeiitic felsic to intermediate metavolcanic rocks of the Deloro assemblage. This contact is gradational and its location is highly interpretive.

Small, dismembered, cherty horizons and pods are exposed within the mafic metavolcanic rocks west and southeast of Carscallen Lake. Magnetite is commonly present, though it accounts for less than 5% of rock in these small occurrences of chemical metasedimentary rocks.

Tholeiitic Felsic to Intermediate Metavolcanic Rocks (map unit 2)

Tholeiitic, felsic to intermediate metavolcanic rocks of the Deloro assemblage are exposed in light-buff outcrops that typically display a well-developed, near-vertical, planar weathering pattern that accentuates the foliation in the rock. Some of the large, prominent, bedrock exposures display a whaleback form.

Photo 1. Angular chert fragments in Deloro assemblage brecciated pillows at the Wire Gold property.

Photo 2. Chert 'flames' in Deloro assemblage brecciated pillows at the Wire Gold property.

The main rock type is quartz-sericite phyllite. The rocks are dark grey, dark buff-grey and dark green-grey on fresh surfaces. The felsic metavolcanic rocks include lapilli-tuff, crystal tuff and massive aphyric rocks. Lithic fragments include locally abundant, angular to rounded lapilli. The rocks are typically aphyric with feldspar-phyric, quartz-feldspar-phyric and sparsely (<1%) quartz-phyric examples. Rocks of intermediate composition are feldspar-biotite-phyric.

Ayer et al. (1999) sampled a quartz-phyric high-silica rhyolite from this sequence for U-Pb zircon age dating in western Denton Township (*see* Figure 3). The sample yielded zircons with an isotopic age of 2727 +/-1 Ma. This age confirms that the rock belongs to the Deloro assemblage.

Mafic sills and massive flows within the felsic to intermediate metavolcanic horizons are common. These 1 to 3 m horizons may be distinguished by their recessive weathering and brown-buff hue.

In thin section the aphyric phyllites typical of the Deloro assemblage felsic metavolcanic rocks consist of very fine, sericite and quartz with limited chlorite and carbonate and a penetrative foliaton. Plagioclase and potassium-feldspar were only identified in porphyritic samples.

Chemical Metasedimentary Rocks (map unit 3)

Chert-rich banded iron formation and closely associated clastic/chemical metasedimentary rocks occur within the Deloro assemblage in the map area (Figure 5). Three different horizons were identified:

1) A 4-5 m horizon of chert-dominated, magnetite +/- pyrrhotite ± chalcopyrite, banded iron formation is associated with mafic metavolcanic rocks near the interpreted stratigraphic top of the mafic-dominated metavolcanic sequence in the Deloro assemblage. This iron formation horizon was traced by bedrock mapping, geophysical interpretation and diamond drilling from north of the Carlton Lake pluton in Carscallen and Whitesides townships and around the pluton into Denton and Keefer townships. A high strain zone in western Carscallen Township transects the iron formation horizon at a low angle, changing the character of the rocks to magnetic, siliceous, schist.

2) Small (< 1 m), structurally dismembered, cherty horizons and pods are exposed within the mafic metavolcanic rocks of the Deloro assemblage, west and southeast of Carscallen Lake and south of the aforementioned iron formation horizon. Magnetite is commonly present though less abundant. It is possible that these occurrences form part of the same iron formation horizon described above, but it is disrupted and repeated by folding and faulting.

3) A thin (1 m wide), discontinuous, folded, banded chert-magnetite horizon occurs within felsic metavolcanic rocks of the Deloro assemblage. The horizon is exposed north of Carscallen Lake in two outcrops and is traceable into Whitesides Township to the west.

Several stripped exposures in Carscallen Township are centered on the thickest iron formation horizon. These include the Wire Gold property (*see* Figure 4), an area north of Gunther Lake (*see* Figure 3) and three smaller areas north of Carscallen Lake (*see* Figure 3) within the high strain zone described within horizon 1 above. The chemical metasedimentary rocks at the Wire Gold and Gunther Lake stripped zones are predominantly banded grey chert and magnetite. Pyrrhotite and chalcopyrite are locally associated with the magnetite bands.

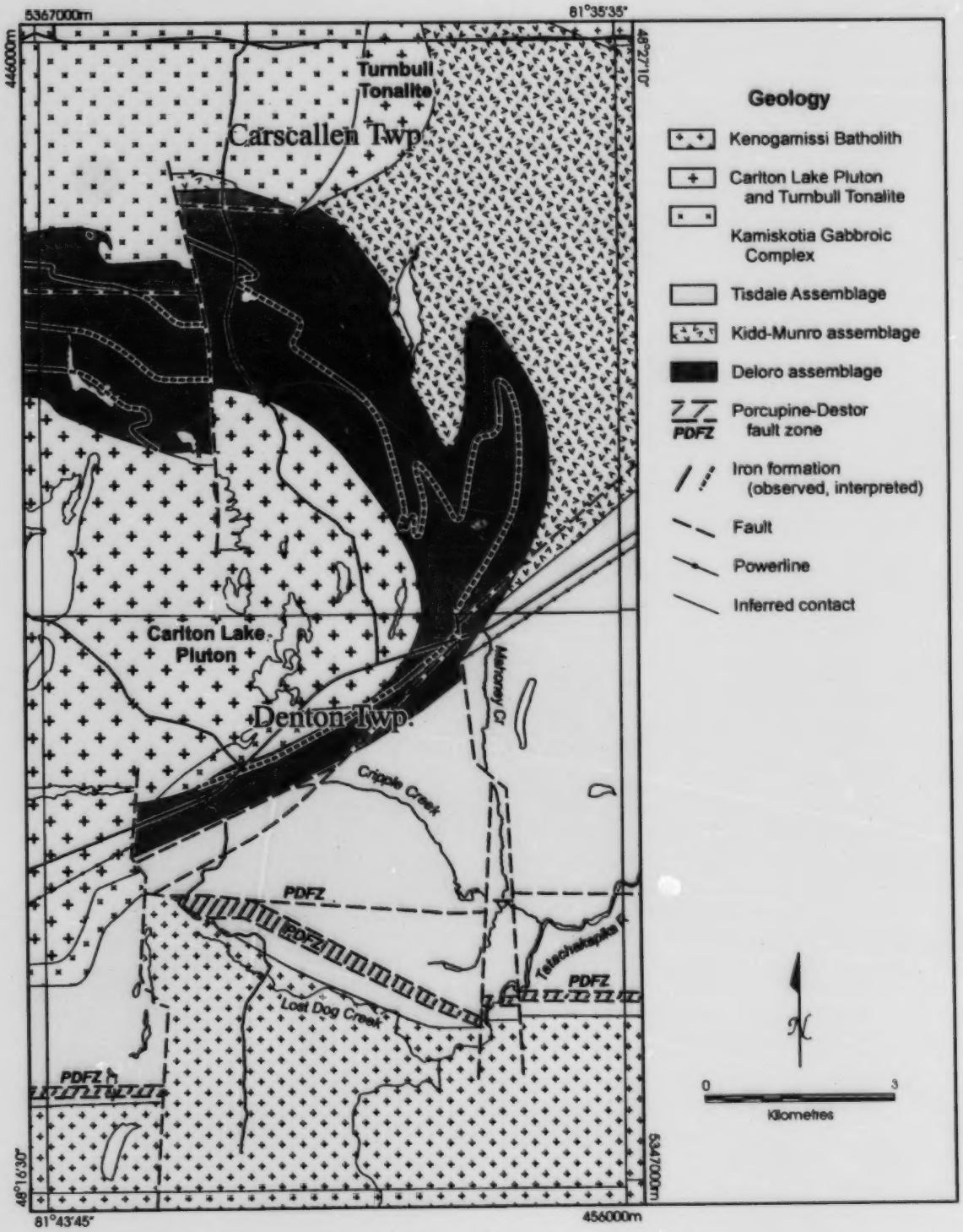

Figure 5. Distribution of iron formation (Map unit 3) through Denton and Carscallen townships.

At Gunther Lake, an intermediate metavolcanic sill with chilled margins intrudes the iron formation horizon sub-concordantly. Light grey chert (10 to 20 cm wide) makes up approximately 80% of the cherty iron formation. Magnetite with up to 10% pyrrhotite occurs in layers that are 2 to 4 cm wide.

At the Wire Gold property, brittle and brittle-ductile faults and folds (both slump and tectonic related folding are interpreted to have occurred) complicate the stratigraphy. However, a single, repeated horizon is interpreted at this locality. Felsic metavolcanic rocks, that underlie the banded iron formation, host disrupted cherty horizons and grade into chemical metasedimentary rocks with a small clay component then abruptly change to the cherty iron formation. As at Gunther Lake, chert horizons (10 to 20 cm wide) are dominant and comprise 75 to 85% of the rock. Most of the iron-rich bands are composed of magnetite (2 to 4 cm wide, with one exceptional horizon 10 cm wide), and contain pyrite, pyrrhotite and chalcopyrite where they are over-printed by brittle faults.

The other stripped outcrops and several other small exposures of the thickest iron formation horizon lie within the high strain zone in western Carscallen Township (*see* Figure 3). This iron formation is dark grey, gossanous, strongly magnetic, very friable and siliceous. The 3 m wide magnetic zone is flanked by highly strained, penetratively foliated and friable, pillowed and massive, mafic, metavolcanic rocks.

Though thinner and typically dismembered, the other two horizons of chert-rich banded iron formation exhibit similar characteristics to the thicker horizon. These units dominantly consist of grey chert with magnetite as the main iron mineral. The horizon hosted by felsic metavolcanic rocks is typically more magnetite-rich and more magnetic than the horizon in the mafic metavolcanic rocks. Some of the latter exposures consist entirely of wispy grey chert.

In thin section, the chemical metasedimentary rocks of the Deloro assemblage consist of quartz and magnetite with trace accessory minerals such as grunerite-cummingtonite, stilpnomelane, biotite and chlorite.

KIDD-MUNRO ASSEMBLAGE (SUPRACRUSTAL PACKAGE B)

A thick sequence of felsic metavolcanic rocks, in the northeast region of the map area, is referred to as Supracrustal Package B (*see* Map P.3517, back pocket). A sample taken from a rhyolite in northern Carscallen township (*see* Figure 3) yielded a U/Pb zircon age of 2713 ± 1 Ma (Ayer et al. 1999), consistent with the general age of the Kidd-Munro assemblage. The rhyolite that was dated is separated from the main sequence by an apophysis of the Kamiskotia Gabbroic Complex (*see* Figure 3). The correlation across the intrusive body is based on textural and compositional considerations as well as lithgeochemical characteristics. It should be noted, however, that the rocks exposed in northeastern Carscallen Township could be part of the Kamiskotia assemblage (Jackson and Fyon 1991) that has been included in the Tisdale assemblage by Ayer et al. (1999).

Two units were distinguished within the Kidd-Munro assemblage: quartz-phyric, tholeiitic felsic metavolcanic rocks and high titanium tholeiitic mafic metavolcanic rocks. The mafic flows occur as relatively limited flow units and dikes within the felsic sequence (*see* Map P.3517, back pocket).

The rocks of the Kidd-Munro assemblage are not as metamorphosed or deformed as Deloro assemblage rocks. A moderately penetrative foliation occurs in high strain zones including fold closures and small shear zones. In these areas the rocks are more sericitized and display a pale appearance on fresh surfaces.

Quartz-Phyric Tholeiitic Felsic Metavolcanic Rocks (map unit 4)

Quartz-phyric, felsic metavolcanic rocks of the Kidd-Munro assemblage are exposed in prominent, large, rounded, light buff to white outcrops. A variety of colours on the fresh surface, including light green, light grey, dark green, dark grey and black appears to reflect the degree of sericitization.

Well preserved metavolcanic and volcano-sedimentary textures, including tuffaceous beds with truncated slump folds, cuspate pumice shards/fiamme (Photo 3), accretionary lapilli, rare bombs and flow banding (Photo 4) are present. Widespread horizons containing abundant quartz phenocrysts are a distinctive feature of the felsic metavolcanic rocks.

In thin section, the felsic metavolcanic rocks consist of a very fine-grained quartz-sericite matrix with coarser-grained accessory chlorite and carbonate hosting abundant quartz and relict feldspar phenocrysts. The quartz phenocrysts are well preserved, however, the feldspar phenocrysts (plagioclase) are variably sericitized.

High Titanium Tholeiitic Mafic Metavolcanic Rocks (map unit 5)

The high titanium tholeiitic mafic metavolcanic rocks of the Kidd-Munro assemblage are only exposed in the northeast corner of Carscallen Township (*see* Map P.3517, back pocket). Outcrops are generally low-lying and flat and the rocks weather to medium blue-green (locally pinkish). These rocks are a distinctive dark blue-green on fresh surfaces. The mafic rocks of the Kidd-Munro assemblage are magnetic which facilitates the correlation of these units across areas of overburden using airborne magnetic geophysical data.

The mafic metavolcanic rocks occur as massive and pillowed flows and porphyritic dikes and sills within the felsic metavolcanic sequence. Pillows are large (up to 3 m) with distinctive, lobate, amoeba-like shapes. Pillow selvages are vibrant blue-green while the pillows are a medium pink-green. Due to the unusual shape of these pillows, neither paleohorizontal nor facing direction is clear, however, an east-northeast facing is tentatively interpreted at one outcrop. Small, euhedral plagioclase phenocrysts were observed in the pillowed flows and one of the dikes contains blue amphibole phenocrysts.

In thin section these rocks consist of plagioclase, chlorite, carbonate, epidote (± quartz ± sericite). The plagioclase occurs as relatively coarse-grained (1 mm), subhedral to anhedral crystals in a finer-grained matrix of chlorite, carbonate, epidote and sericite.

TISDALE ASSEMBLAGE (SUPRACRUSTAL PACKAGE C)

Supracrustal Package C, interpreted herein as Tisdale assemblage, occupies an east-trending, wedge-shaped area in Denton Township. At the eastern border of the map area, the assemblage is almost 10 km wide but narrows to less than 3 km at the western border of Denton Township (*see* Figure 3).

Limited exposure and proximity to the PDFZ have obscured the primary characteristics of the Tisdale assemblage in the map area. However, the distinctive intimate interleaving of mafic and ultramafic metavolcanic rocks of the lowermost suite of the Tisdale assemblage (Ayer et al 1999) is preserved in the rocks. Four rock units have been distinguished: ultramafic metavolcanic rocks, high magnesium tholeiitic to komatiitic mafic metavolcanic rocks, calc-alkalic intermediate to felsic metavolcanic rocks and clastic metasedimentary rocks.

Photo 3. Fiamme in Kidd-Munro assemblage felsic metavolcanic rocks, Carscallen Township.

Photo 4. Flow banding in quartz-phyric felsic metavolcanic rocks of the Kidd-Munro assemblage, Carscallen Township.

Ultramafic Metavolcanic Rocks (unit 6)

Exposures of ultramafic metavolcanic rocks are rare. The characteristic high magnetic susceptibility of these rocks makes possible the use of airborne magnetic geophysical data to interpolate between outcrops. These rocks occur in two distinct modes: prominent, whaleback-shaped outcrops of serpentinite with distinctive elephant-skin texture; and small, low-lying, outcrops of extremely fissile schist. Ultramafic metavolcanic rocks are variably deformed and altered and include aphanitic to fine-grained serpentinites with rare, preserved spinifex that exhibit only a weak foliation; and very friable, talcose schists.

Relatively well preserved, ultramafic metavolcanic rocks with a moderate penetrative foliation are exposed in two areas in eastern Denton Township. At both localities the rocks have a deep (2 to 3 cm) rusty-brown weathering rind and are dark green to black on fresh surfaces. A small patch of relict, 2 to 3 cm long spinifex texture occurs at each locality. An equivocal interpretation of tops to the north was determined at one of the spinifex occurrences. An unusual positive weathering pattern of interlocking polygons occurs on the surface of one of the outcrops (Photo 5). These small ridges are over-printed by the main foliation.

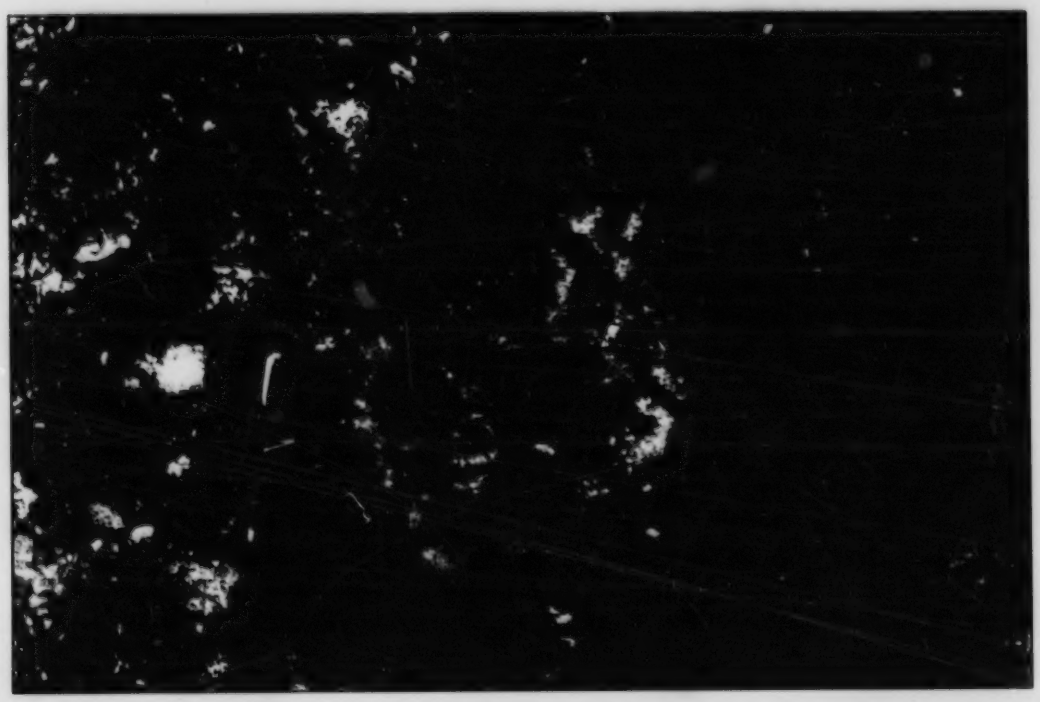

Photo 5. Positively weathering polygons on outcrop surface of Tisdale assemblage ultramafic metavolcanic rocks, Denton Township.

The majority of exposed ultramafic rocks are highly strained. These rocks are extremely penetratively foliated schists and phyllites and primary textures have been obliterated. The weathered surface can be white commonly with green streaks or dark blue to dark green-blue. These different colours are present in the same outcrops in some places. Fresh surfaces are difficult to obtain since these

rocks are very deeply weathered. Schistose ultramafic metavolcanic rocks are exposed in thin layers (everywhere less than 40 m, typically less than 10 m across strike) and are closely flanked by other rock types including clastic metasedimentary rocks and mafic and felsic metavolcanic rocks. Contact relationships are obscured by deformation and depositional contacts are interpreted.

A single, small outcrop, on the west side of the road extending south from the Star Lake garbage dump (*see* Map P.3517, back pocket), is strongly magnetic, very hard and dense. These rocks are thinly (2 to 15 mm) banded, black and tan and interpreted to be ultramafic in composition. A similar rock type is exposed in a thin (2 m) horizon at the east end of the stripped area at the Wakemac property (Figure 4).

In thin section, the better-preserved ultramafic rocks are composed of serpentine (largely replaced by cummingtonite-grunerite in the northern area), chlorite, magnetite and carbonate. The main mineral phase in the schistose ultramafic rocks is white mica interpreted to be talc. Other minerals include chlorite, carbonate, magnetite, and minor quartz in one sample.

High Magnesium Tholeiitic to Komatiitic Mafic Metavolcanic Rocks (unit 7)

Exposures of the mafic metavolcanic rocks of the Tisdale assemblage tend to be flat-lying but deeply incised through weathering. Several of the best exposures in the map area resulted from power stripping. These include stripped areas on the Wakemac, Cameco, Gowest and Karvinen properties and on the Galata claims south of Godon Lake (*see* Figures 3 and 4). The mafic metavolcanic rocks weather to a distinctive dark brown to brown-black. Rare exposures that lack extensive alteration have dark green weathered surfaces. The fresh surface is dark grey-green or black, depending on the minerals that are present.

The mafic metavolcanic rocks display a range of alteration, metamorphism and strain states. The only area where volcanic textures are preserved is in a group of outcrops that extend west from the junction between Cripple Creek and Mahoney Creek (*see* Map P.3517, back pocket). Small, flattened pillows with recessively weathered selvages (Photo 6) were observed in several outcrops. The pillows are so extremely flattened that they impart a banded appearance to the rock in proximity with a mylonitic high strain zone (associated with the PDFZ).

The characteristic mafic metavolcanic rocks are chlorite schists with moderate to extreme carbonate and iron carbonate alteration coupled with extensive deformation. Amphibolites are exposed in a band along the southern extent of the Tisdale assemblage in the map area. Primary volcanic features were not identified in either the chloritic or amphibolite schists.

Calc-Alkalic Intermediate to Felsic Metavolcanic rocks (map unit 8)

Calc-alkalic intermediate to felsic metavolcanic rocks of the Tisdale assemblage are exposed in east-central Denton Township in the vicinity of Cripple Creek and in western Denton Township along the shoreline of the Godon lakes (*see* Map P.3517, back pocket). The best exposures of these rocks are in stripped areas at the Karvinen property (*see* Figure 4). Other felsic metavolcanic horizons, reported in diamond-drill core, are associated with mafic and ultramafic metavolcanic rocks at both the Karvinen and Gowest properties (*see* Figure 4).

Photo 6. Flattened pillows in mafic metavolcanic rocks of the Tisdale assemblage, Denton Township.

The intermediate to felsic metavolcanic rocks are creamy-buff weathering, light grey-green, unaltered, foliated, quartz-sericite schists. Primary textures were not observed. Relict phenocrysts are absent which is interpreted to reflect an aphyric protolith. Minerals identified in thin section include quartz, sericite, plagioclase, chlorite and biotite. Pyrite was identified from a sample taken from a stripped area at the Karvinen property.

Clastic Metasedimentary Rocks (map unit 9)

Clastic metasedimentary rocks of the Tisdale assemblage outcrop within the core of the assemblage in western Denton Township (*see* Map P.3517, back pocket). The outcrops are flat-lying and smooth, larger and less deeply incised than neighbouring outcrops of metavolcanic rocks. The largest exposure of this unit occurs in a stripped area between the Godon lakes that also exposes ultramafic and mafic metavolcanic rocks and gabbroic rocks.

The clastic metasedimentary rocks display a range of characteristics that reflect a high degree of deformation and alteration. Well preserved, metasedimentary rocks are poorly-sorted wackes containing angular feldspar grains; rare, small, fuchsite clasts; horizons rich in quartz crystals; and rare sedimentary structures. Typically massive and unbedded, bedding and graded bedding are locally present. An outcrop on the west side of the northern Godon Lake displays graded bedding and scour marks that indicate facing to the south.

Alteration and deformation have obliterated much of the primary textures of the metasedimentary rocks in the stripped area between the Godon lakes. Some of the interpreted metasedimentary rocks in

this area display thin black and buff laminations interpreted to be structurally imposed rather than a primary sedimentary feature. These laminated rocks are folded and penetratively foliated. Small, mafic intrusive bodies further obscure the nature of the supracrustal rocks in this exposure.

The metasedimentary rocks are interpreted to have been deposited proximal to their source based on the following characteristics: they are poorly sorted; sand grains are angular; and the metasediments have variable compositions that change across relatively short distances. The immature nature, compositional variation and intimate relationship with metavolcanic rocks of various compositions are interpreted to reflect a synvolcanic depositional environment.

Atypical clastic metasedimentary rocks (*see* unit 9c, Map P.3517, back pocket) are exposed in a small outcrop on the west side of Mahoney Creek at the site of a former drill camp at the Gowest property. Interbedded, fine- to medium-grained wacke and shale preserve sedimentary structures despite the presence of a penetrative foliation. Thin beds (1 cm) of medium buff-grey, fine-grained sandstone grade into darker shale beds (2 to 8 cm wide) (Photo 7). Scoured contacts between the sandstone and shale horizons and normal grading indicate a south-facing sequence. These metasedimentary rocks are interpreted to be turbidites. It should be noted that it is likely that these rocks are part of the Porcupine assemblage. However, there is insufficient exposure to assign this unit to a unique map unit. As a result, it is included with the Tisdale assemblage metasedimentary rocks.

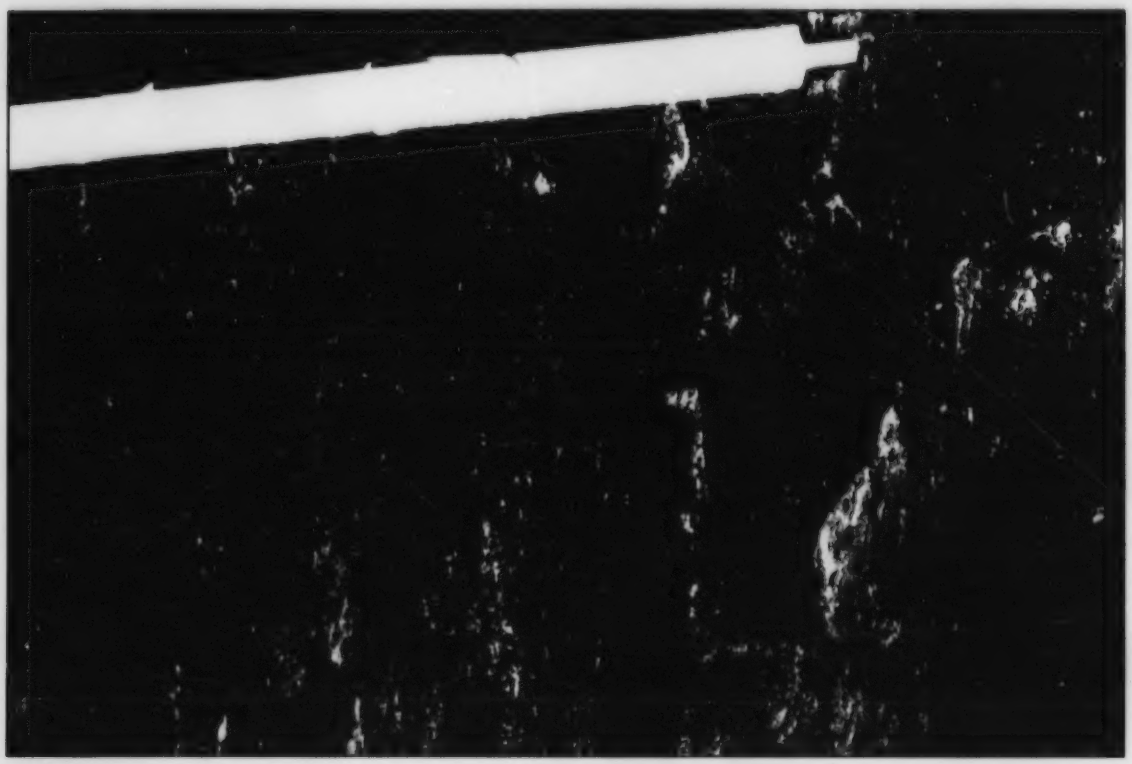

Photo 7. Thinly interbedded sandstone and shale of map unit 9c.

KAMISKOTIA GABBROIC COMPLEX (MAP UNIT 10)

The Kamiskotia Gabbroic Complex (KGC) (Barrie 2000) underlies the northwest corner of Carscallen Township (*see* Figure 3). This compositionally and texturally heterogeneous intrusive body is composed of metamorphosed mafic and ultramafic rocks. The KGC is interpreted to be coeval with the metavolcanic rocks of the Tisdale assemblage based on textural similarities; mutually crosscutting relationships; similar geochemical characteristics; and geochronological data which suggest that the complex is the same age as the metavolcanic rocks (2707 ± 2 Ma; Barrie 1990, 1992, 2000).

Gabbroic rocks that are marginal to the Carlton Lake pluton (*see* Figure 3) are interpreted to be associated with the KGC (*see* Map P.3517, back pocket). These rocks display textural, compositional and geochemical characteristics similar to those found in the main body of the KGC.

The rocks of the KGC have medium pink-brown, brown and grey-brown weathered surfaces and dark green to black fresh surfaces. Rocks with gabbro, gabbro-norite and olivine gabbro compositions display a range of textures from fine-grained ophitic textures to massive medium- to coarse-grained cumulates and pegmatitic phases. Cumulate layering observed elsewhere in the complex (Barrie 1990, 1992, 2000) was not observed in Carscallen Township during the present study. Primary textural and compositional changes were observed across intervals of 10 m or less in most bedrock exposures.

In thin section the mafic rocks dominantly consist of plagioclase, chlorite and epidote with accessory quartz, pyrite and titanite. Barrie (1990, 2000) has reported the presence of olivine, clinopyroxene and plagioclase.

A large outcrop of altered peridotite is exposed 50 m west of the Carscallen-Whitesides township boundary, south of the Malette forestry road (*see* Map P.3517, back pocket). The peridotite is magnetic, weakly foliated and has a red-brown weathered surface and dark green fresh surface. In thin section, the peridotite consists of talc, serpentine, chlorite, and magnetite. Relict olivine, reported by Barrie (1990, 2000), was not observed.

An unusual, plagioclase-megacrystic, mafic intrusion is exposed immediately north of Highway 101 where it intrudes felsic metavolcanic rocks of the Deloro assemblage. Euhedral to subhedral plagioclase phenocrysts exceed 3 cm in diameter. The matrix consists of penetratively foliated chlorite schist. Contacts between this mafic rock and the surrounding metavolcanic rocks are not exposed. The author interprets this unit as a dike or sill related to the KGC based on similar geochemical characteristics. The presence of a large KGC body in close proximity to this small mafic body supports this interpretation.

Mutually crosscutting relationships between the KGC and the Carlton Lake pluton imply an intimate temporal relationship between these two intrusive units. A large apophysis of hornblende tonalite intrudes an interpreted KGC body on the southern margin of the Carlton Lake pluton (*see* Map P.3517, back pocket).

FELSIC TO INTERMEDIATE INTRUSIVE ROCKS (MAP UNIT 11)

The Carlton Lake pluton (CLP) occupies 30 to 35 km^2 of the western half of the map area and straddles the Denton-Carscallen township boundary (*see* Figure 3). The Turnbull Township tonalite (TTT) (an informal name, Barrie 1990, 1992) extends along the eastern margin of the KGC in a band that narrows to the south (*see* Figure 3). Mutually crosscutting relationships between the CLP and KGC and a U/Pb age

of 2706 ± 2 Ma (Barrie 1990, 1992) for the TTT indicate that both intrusions are temporally associated with the KGC.

Rocks of the CLP and TTT are equant, medium- to coarse-grained granitoid rocks that have creamy-white weathered surfaces and light- to medium-grey fresh surfaces. Both intrusions contain rare, small (5 to 70 cm), round, mafic (usually gabbroic) xenoliths. Angular gabbroic xenoliths are abundant in outcrops where the TTT is exposed with the KGC. Subtle grain-size variations between exposures are the only primary textural variations noted in the CLP. The TTT displays some textural heterogeneity with schlieren and small zones of compositional layering (defined by the mafic mineral component).

Both plutons display a range of compositions including biotite-hornblende tonalite, biotite tonalite and biotite granodiorite. Thin section observations confirm that both biotite and hornblende are igneous minerals, however, both are overgrown by chlorite and may be totally replaced by chlorite. The feldspars are extensively sericitized and the quartz grains are polygonal.

Rocks of the CLP and TTT are foliated. However, there are local variations in both the intensity and orientation of the foliation. The secondary mafic minerals such as chlorite are aligned along the foliation.

SYNTECTONIC MAFIC AND ULTRAMAFIC INTRUSIVE ROCKS (MAP UNIT 12)

The syntectonic mafic and ultramafic intrusions can be distinguished from KGC rocks that are marginal to the CLP based on two criteria:

1) The characteristic, extreme textural and compositional variations preserved in the KGC and associated rocks were not observed in the syntectonic gabbroic rocks.
2) The syntectonic intrusions intrude the oldest tectonic fabric observed in the Tisdale assemblage rocks. KGC rocks would not cut a post-depositional fabric since the KGC and Tisdale assemblage are interpreted to be coeval.

Syntectonic gabbroic and peridotitic rocks exposed in Denton Township are not considered to be associated with the KGC. These small and numerous intrusions occur in the same region as the Tisdale assemblage (*see* Figure 3; Map P.3517, back pocket). Rarely exposed intrusive contacts were observed between the gabbroic rocks and Tisdale assemblage rocks. The small plutons are separated into 3 distinct rock types: gabbro (map unit 12a), amphibolite (map unit 12b) and serpentinite (map unit 12c).

The gabbro sub-unit (map unit 12b) is exposed in large, prominent outcrops. Weathered surfaces of the gabbro are speckled dark green-creamy-white. Depressions in outcrops have accumulations of coarse-grained sand derived from the rock (which is unusually crumbly for a gabbro). The weathered surface is 1 to 2 cm thick. Fresh surfaces are dark green to black. The gabbro sub-unit comprises greenschist grade metagabbroic rocks with chlorite and actinolite replacing relict clinopyroxene. Primary igneous textures are preserved in low-strain examples of this unit. Grain size varies from fine-grained at the margins of the intrusions to medium- to coarse-grained in the centre. No pegmatitic or aplitic phases were observed. Well preserved, euhedral, primary clinopyroxene and plagioclase laths are recognisable in areas of low strain. In areas of higher strain, gabbroic rocks are characterised by a well-developed foliation, chlorite is the main mineral phase and is aligned along the foliation.

The amphibolite sub-unit (map unit 12b) is spatially associated with the PDFZ (*see* Figure 3). Amphibolite outcrops are typically small and solitary. The amphibolite sub-unit is an amphibolite grade metagabbro with metamorphic hornblende as the main mafic mineral. The primary igneous textures are locally preserved in the amphibolite sub-unit, however they are typically obliterated by both metamorphic

and structurally imposed textures. The amphibolite is dark grey with reflective surfaces and common metamorphic compositional banding.

One small body of serpentinite is exposed south of the Godon lakes. The serpentinite has a rusty-tan weathered surface, a dark green to dark grey fresh surface and is both soft and friable. A penetrative foliation is crenulated and kink-banded and has obliterated any primary igneous textures. These ultramafic rocks are easily distinguished from the nearby ultramafic metavolcanic rocks of the Tisdale assemblage through their distinctive colour and the relatively large and prominent outcrops.

LATE TECTONIC FELSIC TO INTERMEDIATE INTRUSIVE ROCKS (MAP UNIT 13)

The Kenogamissi batholith (map unit 13) underlies the southern third of Denton Township (i.e. Pyke 1982) (*see* Figure 3; Map P.3517, back pocket). This large granitoid complex lies between the Abitibi and Swayze greenstone belts (Becker, Benn and Ayer 2001). It consists of several units of felsic to intermediate intrusive rock including: hornblende diorite, hornblende tonalite and biotite granodiorite (Becker, Benn and Ayer 2001). Massive, foliated and gneissic textures have been reported (Jackson and Fyon 1991).

In southern Denton Township, white, pale pink, orange and creamy-yellow weathered surfaces reflect variations in composition, textures, strain state and metamorphism in the felsic to intermediate intrusive rocks. Based on crosscutting relationships it is interpreted that at least two phases of intrusion occurred in this area resulting in a locally potassium feldspar-porphyritic granodiorite and a yellowish biotite-hornblende granodiorite.

Pale pink weathering, potassium-feldspar-megacrystic (up to 2 cm) (Photo 8) granodiorite to granite displays a well-developed foliation that locally grades into a weak gneissic banding (1 to 2 cm wide). Biotite, hornblende and/or chlorite define the foliation. White weathering, foliated, fine- to medium-grained, equigranular, biotite ± hornblende granodiorite to tonalite occurs in close proximity to the feldspar porphyritic granodiorite. No contact relationship was observed between these equigranular rocks and the porphyitic rocks. Orange weathering of the equigranular phase occurs in small areas of high strain. The orange colour is interpreted to reflect the presence of hematite.

Creamy-yellow weathering, foliated, fine-grained, biotite ± muscovite granodiorite to tonalite is exposed south of the Tatachikapika River. A small dike of this unit cuts potassium-feldspar megacrystic granodiorite at an outcrop exposure on Lost Dog Creek. This relationship demonstrates that the megacrystic granodiorite phase is older. Both phases are foliated.

Granodioritic to tonalitic dikes intrude syntectonic mafic to ultramafic intrusive rocks (map unit 12) in south-central Denton Township. These dikes are lithologically similar and in close proximity with the main body of the Kenogamissi batholith in Denton Township. They are, therefore, interpreted to arise from this plutonic complex. This provides a constraint on the relative age of these plutonic rocks. A highly strained, pink weathering, muscovite-bearing granite intrudes mylonitic mafic rocks in a lit-par-lit configuration in an outcrop on the Tatachikapika River. This granite was sampled for U/Pb zircon geochronology.

Photo 8. Potassium feldspar megacrysts in granodiorite rocks of the Kenogamissi batholith.

FELSIC AND INTERMEDIATE INTRUSIVE ROCKS (MAP UNIT 14)

Two distinct populations of dikes were observed. One of the dike sets is porphyritic (map unit 14a) whereas the other dikes are coarse-grained and alkalic (map unit 14b). All of these dikes occur in southern and central Denton Township (*see* Map P.3517, back pocket).

Two, large (at least 20 m wide), prominent ash-white to pink weathering quartz, biotite ± feldspar porphyritic dikes intrude Tisdale assemblage and KGC associated rocks. No contact relationships were observed between the porphyritic dikes and the country rocks. The porphyritic rocks are not foliated while the country rocks all are. The unfoliated rocks are, therefore, younger than the deformational event that caused the foliation in the country rocks. The igneous nature, phaneritic character, relative age criteria and straight trends of the porphyritic rocks are interpreted to indicate that these rocks are porphyritic dikes that intrude the country rocks.

A cluster of small (less than 3 m wide), mutually cross-cutting, dark brown weathering alkalic dikes intrude Tisdale assemblage mafic metavolcanic rocks in southwestern Denton Township. Similar, small dikes intrude felsic intrusive rocks of the Kenogamissi batholith in an outcrop on the Tatachikapika River. Both locations are in proximity to mylonite zones associated with the PDFZ. The dikes are folded and weakly foliated but transect the main structural fabric in the outcrops. Dikes are pegmatitic to fine-grained and dominantly consist of phlogopite, plagioclase, actinolite, hornblende, quartz and epidote. It is postulated that these dikes may be genetically linked to alkalic rocks observed in Bristol Township (Barrie 1990, 1992, 2000; Vaillancourt, Picket and Dinel 2000).

MAFIC INTRUSIVE ROCKS

Matachewan Dikes - (map unit 15)

Weakly magnetic diabase dikes of the Paleoproterozoic Matachewan dike swarm intrude all Archean rocks. These dominantly north-northwest-trending dikes are common throughout the map area (Figure 6). The extent of these dikes has been interpreted from airborne geophysical magnetic maps (OGS 1996, 1999) in areas of extensive overburden. These dikes are commonly 10 m wide or less and do not exceed 15 m in width. The dikes are commonly vertical with some subvertical dikes. Rare, small, dikelets intrude the country rocks as subconcordant sills across short distances. An example of this feature is exposed at the west end of the stripped area between the Godon lakes.

The orange-brown weathering Matachewan dikes are dark brown-green on fresh surfaces. The Matachewan dikes are composed of quartz diabase consisting of plagioclase, augite, quartz and magnetite. The grain size of these dikes varies both within and between dikes. The dikes are typically fine-grained to aphanitic at their margins but grain size increases to very coarse at the centre of larger dikes. Two dikes in the map area display the plagioclase-megaporphyritic texture considered diagnostic of the Matachewan swarm. At these outcrops large (up to 6 cm), six-sided, greenish-white plagioclase phenocrysts occupy as much as 60% of the rock.

Matachewan dikes are largely undeformed and unmetamorphosed. Epidote alteration has been observed along joint surfaces in various orientations. Brisbin (1997) observed a Matachewan dike offset by a late brittle fault. The north-northwest-trending faults that extend across the map area may offset these dikes but this was not directly observed.

The Matachewan and Hearst swarms are interpreted to be genetically and temporally linked (Osmani 1991). Based on an isotopic age obtained from a Hearst dike (Heaman 1988), the age of the Matachewan dike swarm is considered to be 2454 ± 2 Ma.

Sudbury Dikes - (map unit 16)

A distinctive, northwest-trending magnetic high across northeast Carscallen Township is indicated on the Ontario airborne magnetic surveys (OGS 1996, 1999). This prominent geophysical feature is interpreted as a Sudbury dike based on its orientation (*see* Map P.3517, back pocket). This unit is not exposed in the map area, which is typical of the recessive weathering Sudbury dike swarm (Osmani 1991).

Olivine diabase is the most typical composition of the Sudbury dikes (Osmani 1991). This swarm has been dated at 1238.5 ± 4 Ma (Krogh et al. 1987) using U/Pb zircon analysis.

Geochemistry

A total of 149 samples were analysed for major oxides and selected trace elements in order to classify and characterise the various rock units of the map area. These analyses were also compared to analyses performed on other rocks of the Timmins area in an effort to correlate the rocks of the map area to the established lithostratigraphy of the Abitibi greenstone belt.

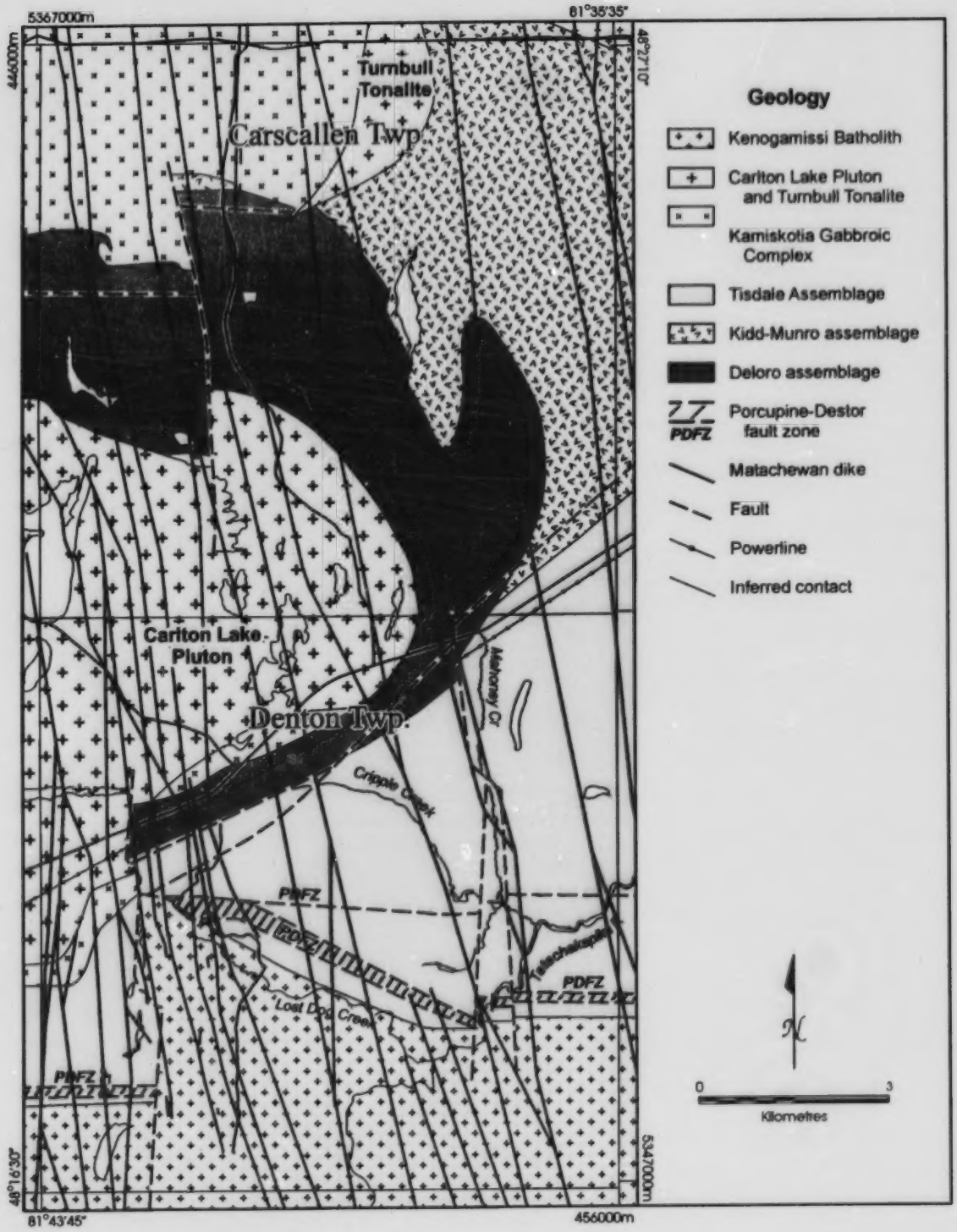

Figure 6. Distribution of Matachewan dikes in Denton and Carscallen townships.

All samples were fed to a small jaw-crusher with steel plates. The crushed sample was then split on a riffle and pulverised by an Al_2O_3 planetary ball mill. Major oxides and selected trace elements were analysed by wavelength dispersive X-ray fluorescence on a fused borate disk and a pressed pellet, respectively. Other trace element analyses were performed with inductively coupled plasma emission mass spectrometry (ICP-MS) using closed beaker digest solution preparation. Fire assay analyses were performed on 27 of the samples and PGE analyses were performed on 13 samples. The results of all analyses are provided in Appendix 1.

METAVOLCANIC ROCKS

Analytical results from the felsic and mafic metavolcanic rocks were plotted separately on Jensen cation plots (Jensen 1976) (Figure 7). This classification scheme is an effective discriminator for subalkalic volcanic rocks that have undergone low-grade metamorphism (Rollinson 1993, p.63) such as those in the map area. The felsic metavolcanic rocks of the three assemblages plot as separate clusters with some overlap (*see* Figure 7a). The felsic rocks of the Deloro assemblage are spread over both the tholeiitic and calc-alkaline fields (*see* Figure 7a). However, considered with data from the mafic metavolcanic rocks of the Deloro assemblage (Figure 7b) they are interpreted to define a calc-alkalic trend. Felsic metavolcanic rocks of the Tisdale assemblage plot in a fairly tight cluster in the calc-alkalic field (*see* Figure 7a). Mafic metavolcanic rocks of the Tisdale assemblage plot in two clusters (*see* Figure 7b), one in each of the high-iron and high-magnesium tholeiitic fields (with some over-lap into the calc-alkalic field). There is limited overlap between the Deloro and Tisdale metavolcanic rocks supporting the premise that these packages are distinct.

Both samples of the felsic unit of the Kidd-Munro assemblage (*see* Figure 7a) overlap with the Deloro assemblage rocks on the Jensen cation plot (Jensen 1976). The two mafic Kidd-Munro assemblage samples are well separated on the Jensen diagram (*see* Figure 7b) but neither overlap with clusters of the other two supracrustal packages. No distinct chemical trends are discernible due to a paucity of samples from the Kidd-Munro assemblage.

Felsic Metavolcanic Rocks

Comparisons of chondrite-normalised rare earth element (REE) plots (Sun and McDonough 1989) were made (Figures 8 and 9) to ascertain whether the felsic metavolcanic rocks of the Kidd-Munro assemblage are chemically distinct from those of the other two assemblages. Deloro assemblage rocks display two distinct patterns and were divided into Deloro A and Deloro B groups and compared with other felsic rocks separately. The REE patterns of Deloro A felsic metavolcanic rocks (*see* Figure 8a) are steep with greater depletion in the heavy REEs than the REE patterns of Deloro B felsic metavolcanic rocks (*see* Figure 8b). Both groups have negative europium anomalies. The REE patterns of the Kidd-Munro and Tisdale assemblage felsic metavolcanic rocks are represented on Figures 8c and 8d, respectively. Deloro A and Kidd-Munro rocks display very similar REE patterns, however, the Deloro A rocks have lower total REEs than the Kidd-Munro rocks (*see* Figure 9a). Similarly, the REE patterns of Tisdale felsic metavolcanic rocks are similar to the Deloro A and Kidd-Munro patterns but have lower total REEs (*see* Figures 9c and 9e, respectively). The Tisdale rocks are further distinguished by a weak negative europium anomaly. These distinct REE patterns support the premise that there are three distinct felsic metavolcanic sequences in the map area.

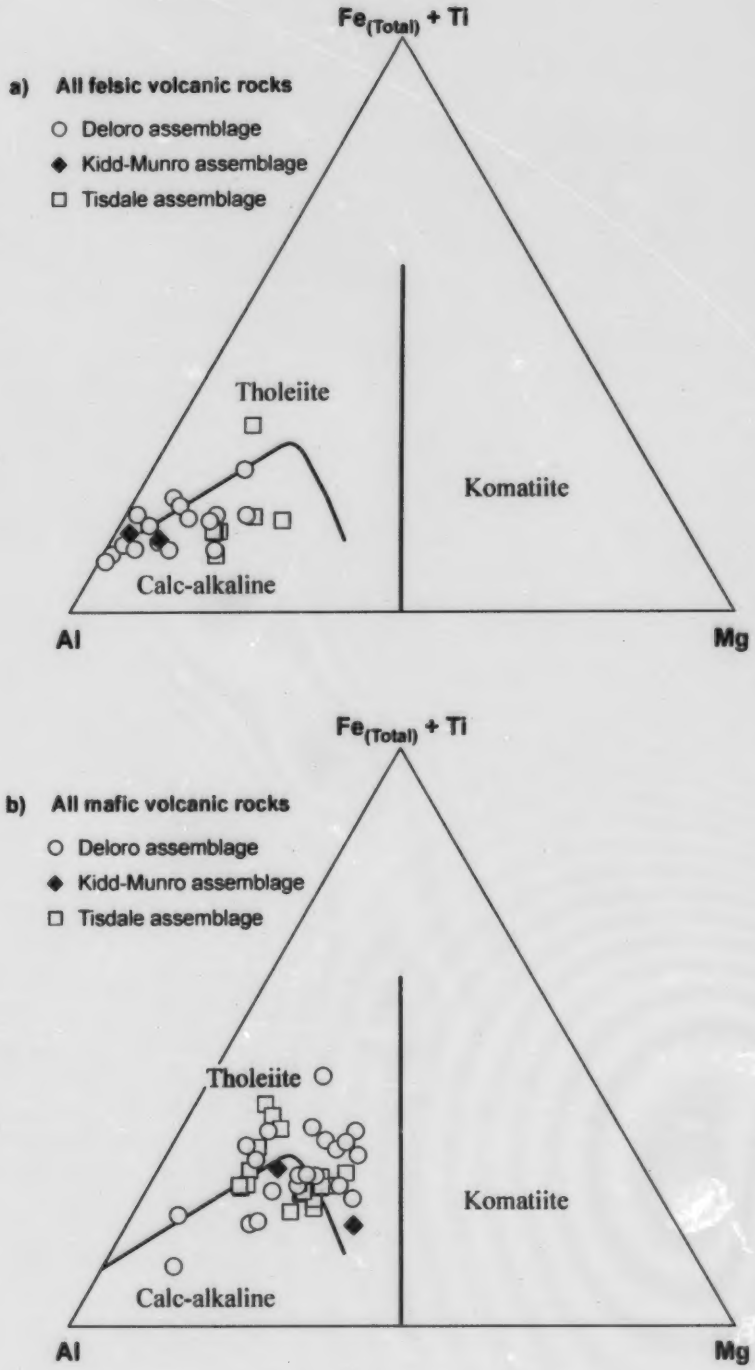

Figure 7. Classification of the metavolcanic rocks of Denton and Carscallen townships using a Jensen diagram (1976).

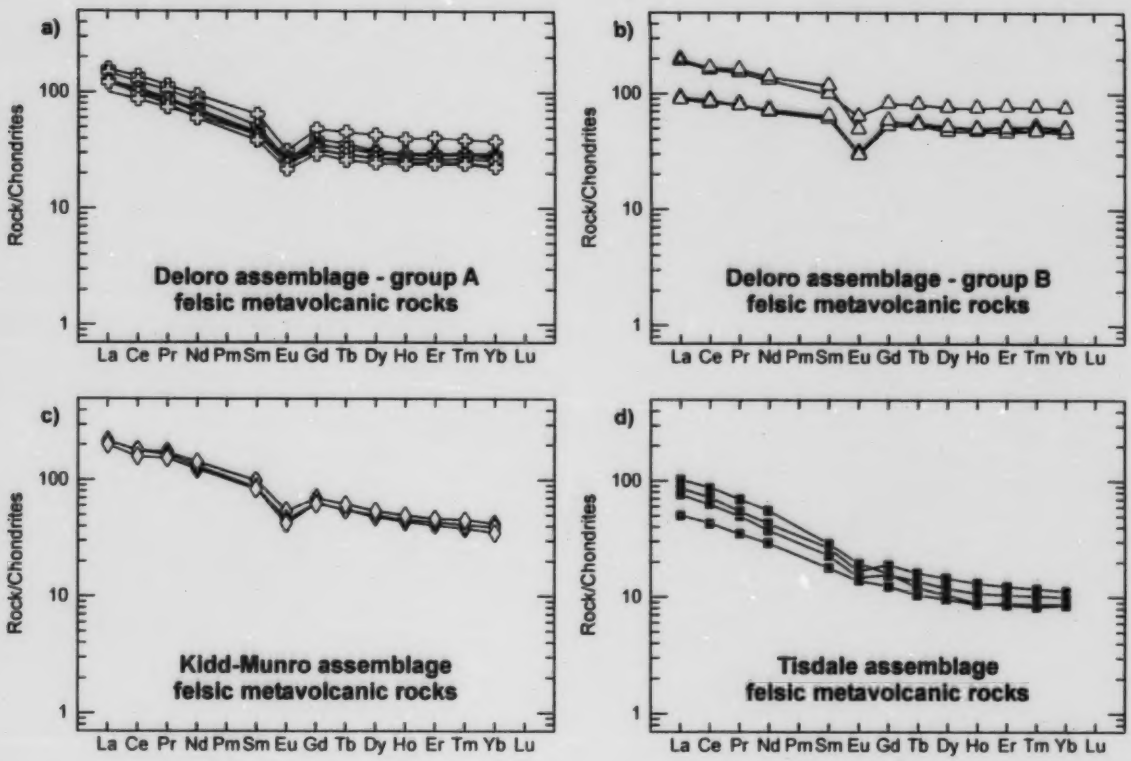

Figure 8. Chondrite-normalised rare earth element (REE) patterns of the Deloro, Kidd-Munro and Tisdale assemblages felsic metavolcanic rocks. Normalising values from Sun and McDonough (1989).

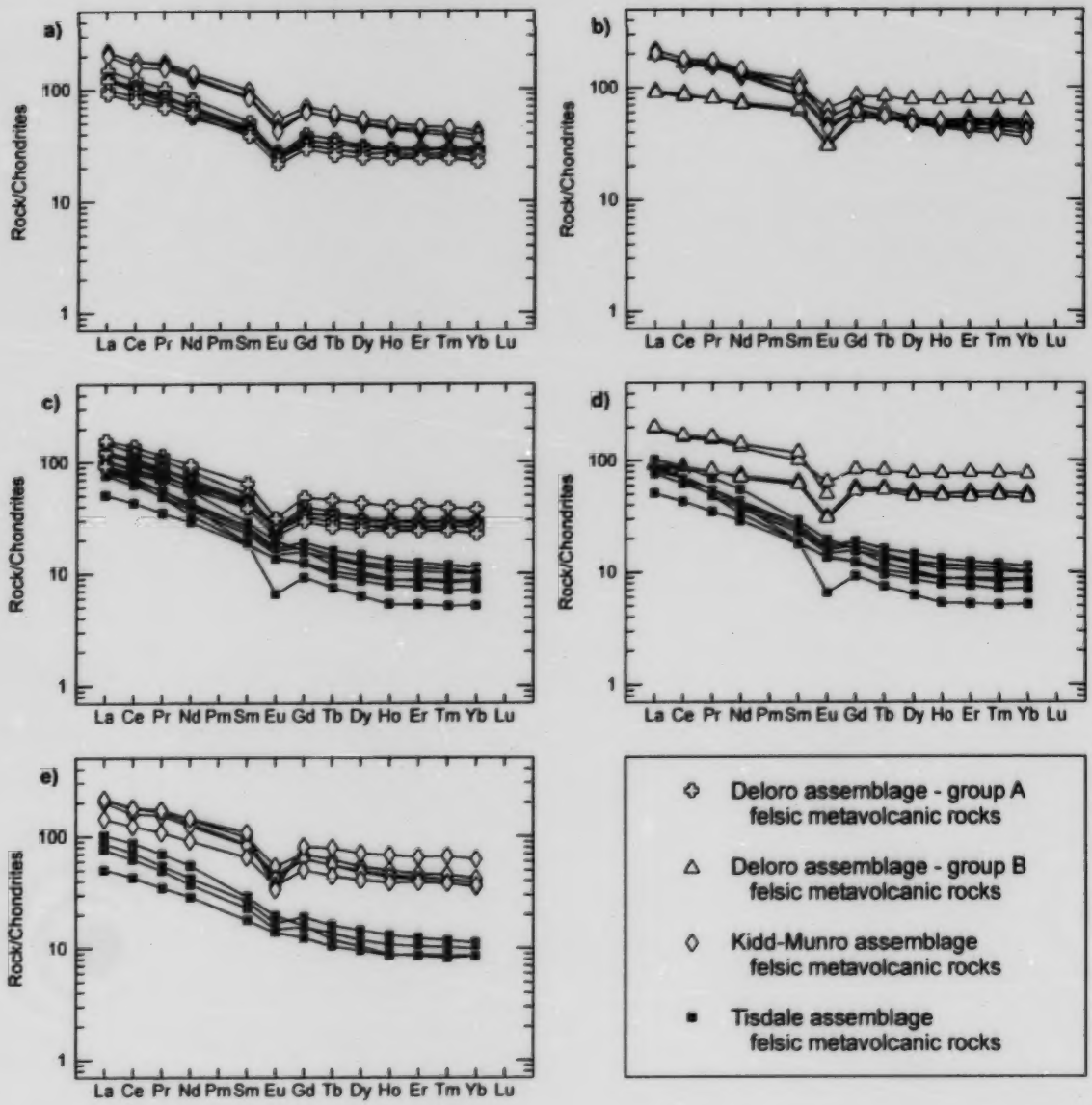

Figure 9. Chondrite-normalised REE patterns of felsic metavolcanic rocks of the Deloro assemblage compared with those of the Kidd-Munro and Tisdale assemblages. Normalising values from Sun and McDonough (1989).

A geochemical comparison was also made between the rhyolite sample that yielded a Kidd-Munro age (2713 Ma; Ayer et al. 1999, sample 96JAA-0094) and other samples (from northeast Carscallen Township) collected from units that the author has interpreted to be Kidd-Munro assemblage (Figure 10). The dated rhyolite unit is separated from the rest of the Kidd-Munro assemblage by an apophysis of the KGC (*see* Figure 3) as well as 30 km^2 of overburden cover. Also included in these comparisons are data from Kidd-Munro assemblage rocks outside the map area (Ontario Geological Survey 2001b). Although proportionally lower, the REE pattern of the dated rhyolite sample (96JAA-0094) resembles the REE patterns of the Kidd-Munro assemblage almost exactly (Figure 10a). The authors interpret the lower total REEs in sample 96JAA-0094 to be the result of a higher degree of fractionation than the samples from northeast Carscallen Township based on the La/Yb ratio (Figure 10b). There is also a profound overlap in the REE patterns of the Kidd-Munro rocks from the map area and those from Kidd Township (*see* Figure 10a). These similarities support the interpretation that the felsic metavolcanic rocks in northeast Carscallen Township are part of the Kidd-Munro assemblage.

Mafic Metavolcanic Rocks

Chondrite-normalized (Sun and McDonough 1989) REE data were analysed to characterise and distinguish the mafic metavolcanic rocks of the map area (Figure 11). REE patterns indicate that the Deloro and Tisdale assemblage mafic rocks each exhibit two distinct groupings of REE patterns. Deloro A mafic rocks have REE patterns with flat, gentle, negative slopes whereas Deloro B mafic rocks display slightly concave, steeper REE patterns with negative slopes (*see* Figure 11a and 11b). The total REE values of both groups of Deloro mafic metavolcanic rocks lie within a narrow range. The REE patterns of Tisdale A mafic metavolcanic rocks are relatively flat with slightly depleted light REEs and consistent total REE contents with the exception of one sample that has higher total REE values (*see* Figure 11d). Tisdale B rocks are characterised by REE patterns with a moderately steep negative slope in the light REEs and a flatter pattern in the middle and heavy REEs (*see* Figure 11e). The REE patterns of the two Kidd-Munro assemblage samples are somewhat similar in that they both display a moderately steep, negative slope (*see* Figure 11c). However, one of the samples has higher total REEs, a steeper slope and a weak positive europium anomaly whereas the other sample has a weak negative europium anomaly.

Comparisons of the chondrite-normalized REE patterns between the assemblages (Figures 12 and 13) reveal that each assemblage is geochemically distinct from the others. Figure 12 illustrates the Kidd-Munro assemblage REE patterns superimposed on the REE patterns for Deloro A, Deloro B, Tisdale A and Tisdale B samples. Deloro B and Tisdale B both have similar REE patterns to one of the mafic Kidd-Munro samples (*see* Figures 12b and 12d). However, Deloro B has a slightly shallower negative slope in the heavy REEs and no europium anomaly (*see* Figure 12b). Tisdale B also lacks a significant europium anomaly (*see* Figure 12d). Figure 13 compares the REE patterns of the Deloro groups with the Tisdale groups. Deloro A and Tisdale A are similar, but Tisdale A patterns bow up slightly and, with the exception of one sample, have lower total REEs than the Deloro A group (*see* Figure 13a). The REE patterns for the Deloro B group are similar to the Tisdale B group, however, the Tisdale B group has slightly shallower slopes (*see* Figure 13d). These distinctions support the separation of the mafic metavolcanic rocks into the three assemblages.

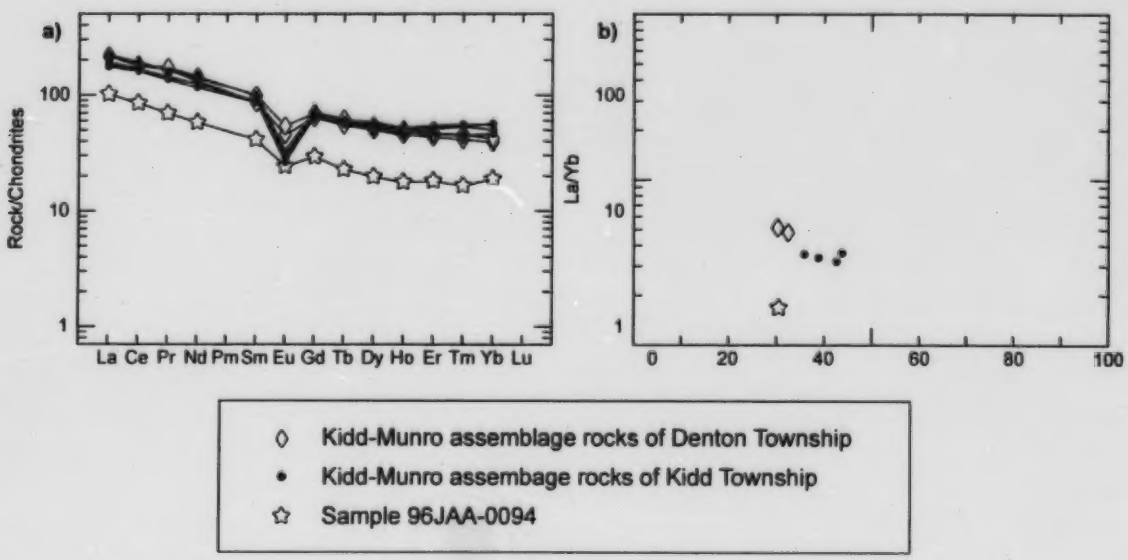

Figure 10. Geochemical comparison between sample 96JAA-0094, Kidd-Munro assemblage rocks from Denton Township and Kidd-Munro assemblage rocks from Kidd Township.

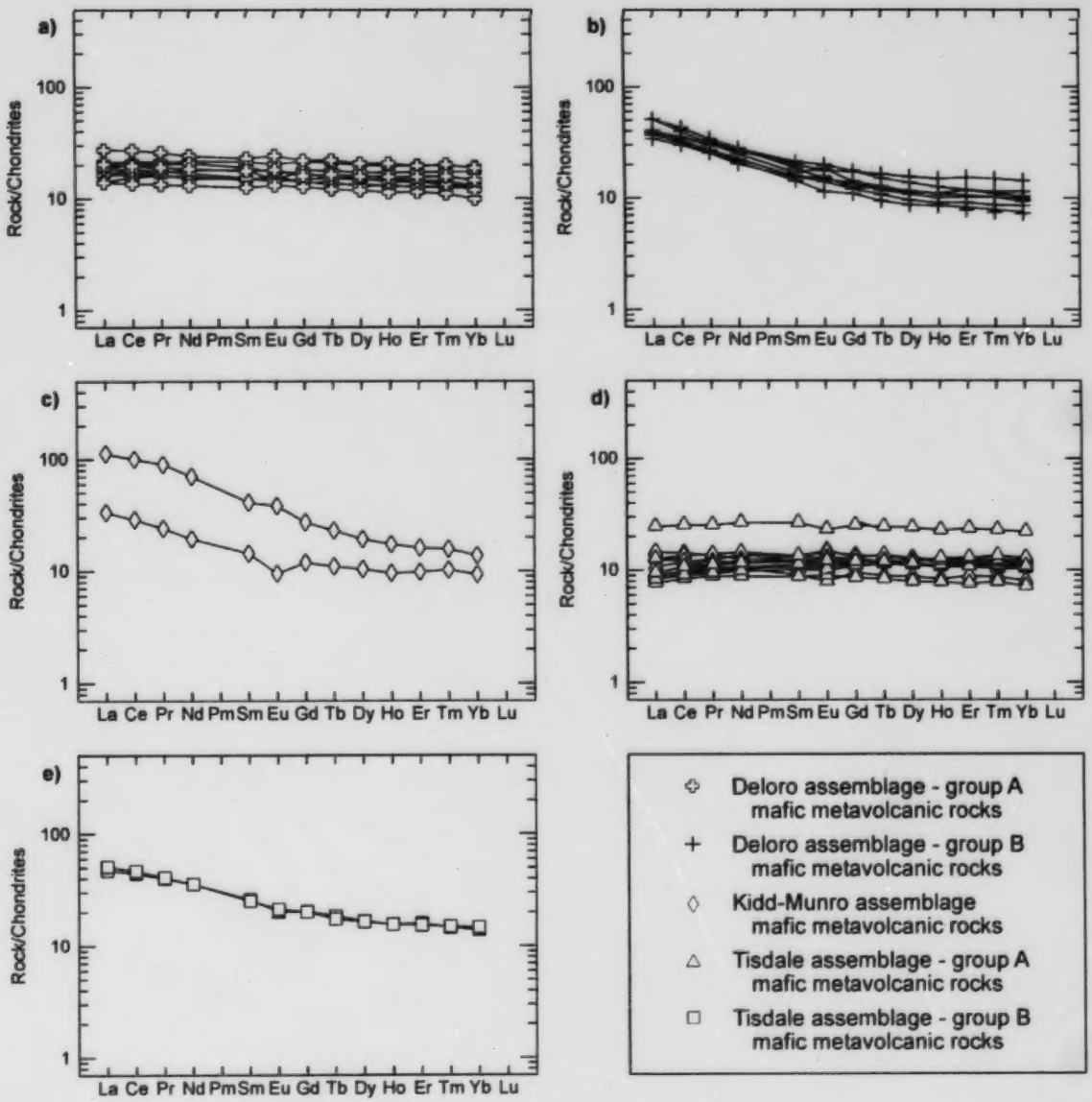
a)
b)
c)
d)
e)
Rock/Chondrites
100
10
1
La Ce Pr Nd Pm Sm Eu Gd Tb Dy Ho Er Tm Yb Lu
Deloro assemblage - group A mafic metavolcanic rocks
Deloro assemblage - group B mafic metavolcanic rocks
Kidd-Munro assemblage mafic metavolcanic rocks
Tisdale assemblage - group A mafic metavolcanic rocks
Tisdale assemblage - group B mafic metavolcanic rocks

Figure 11. Chondrite-normalised REE patterns of Deloro, Kidd-Munro and Tisdale assemblages mafic metavolcanic rocks. Normalising values from Sun and McDonough (1989).

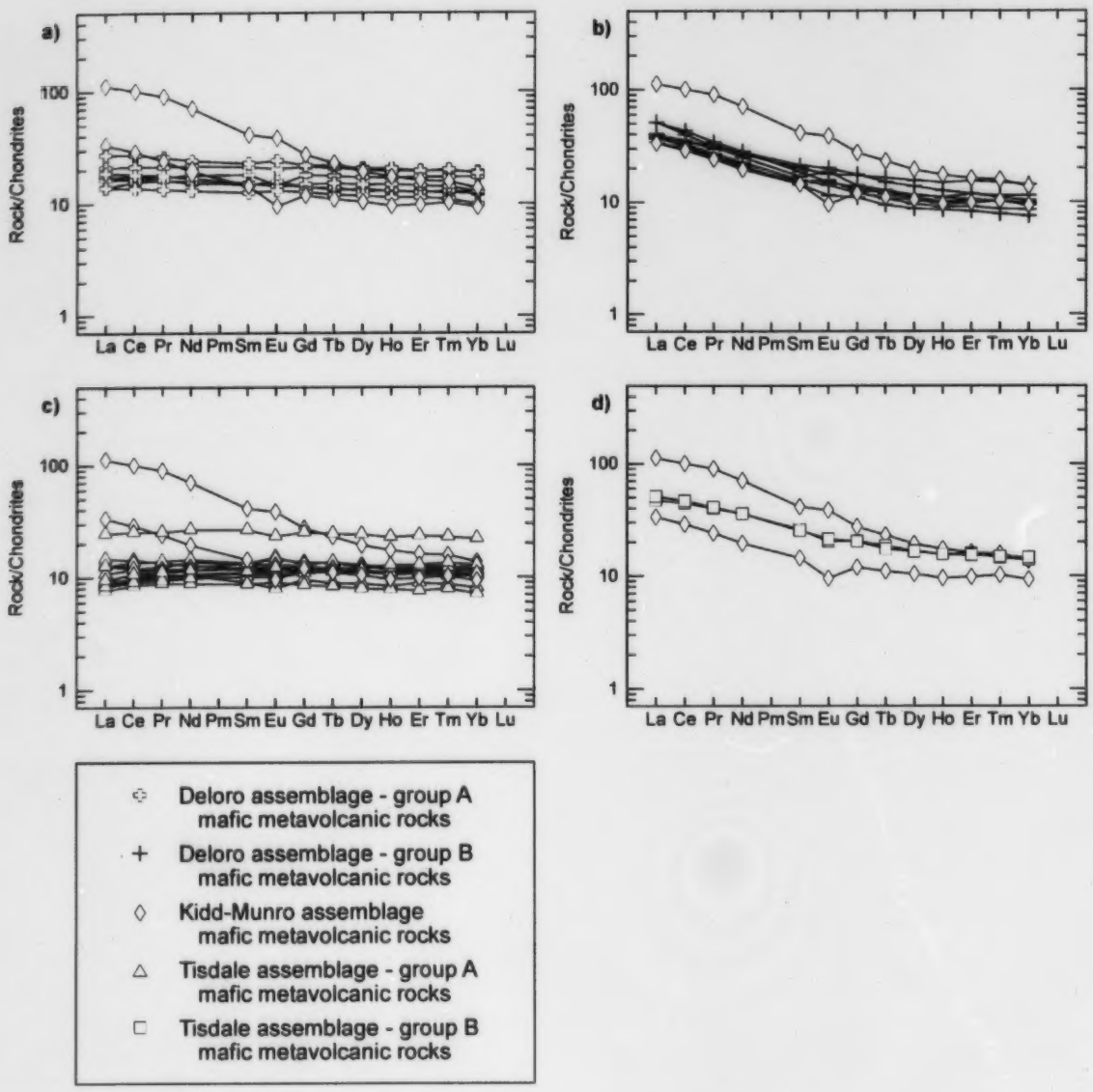
a)
b)
c)
d)
Rock/Chondrites
100
10
1
La Ce Pr Nd Pm Sm Eu Gd Tb Dy Ho Er Tm Yb Lu
Deloro assemblage - group A mafic metavolcanic rocks
Deloro assemblage - group B mafic metavolcanic rocks
Kidd-Munro assemblage mafic metavolcanic rocks
Tisdale assemblage - group A mafic metavolcanic rocks
Tisdale assemblage - group B mafic metavolcanic rocks

Figure 12. Chondrite-normalised REE patterns that compare mafic metavolcanic rocks of the Kidd-Munro assemblage with those of Deloro and Tisdale assemblages. Normalising values from Sun and McDonough (1989).

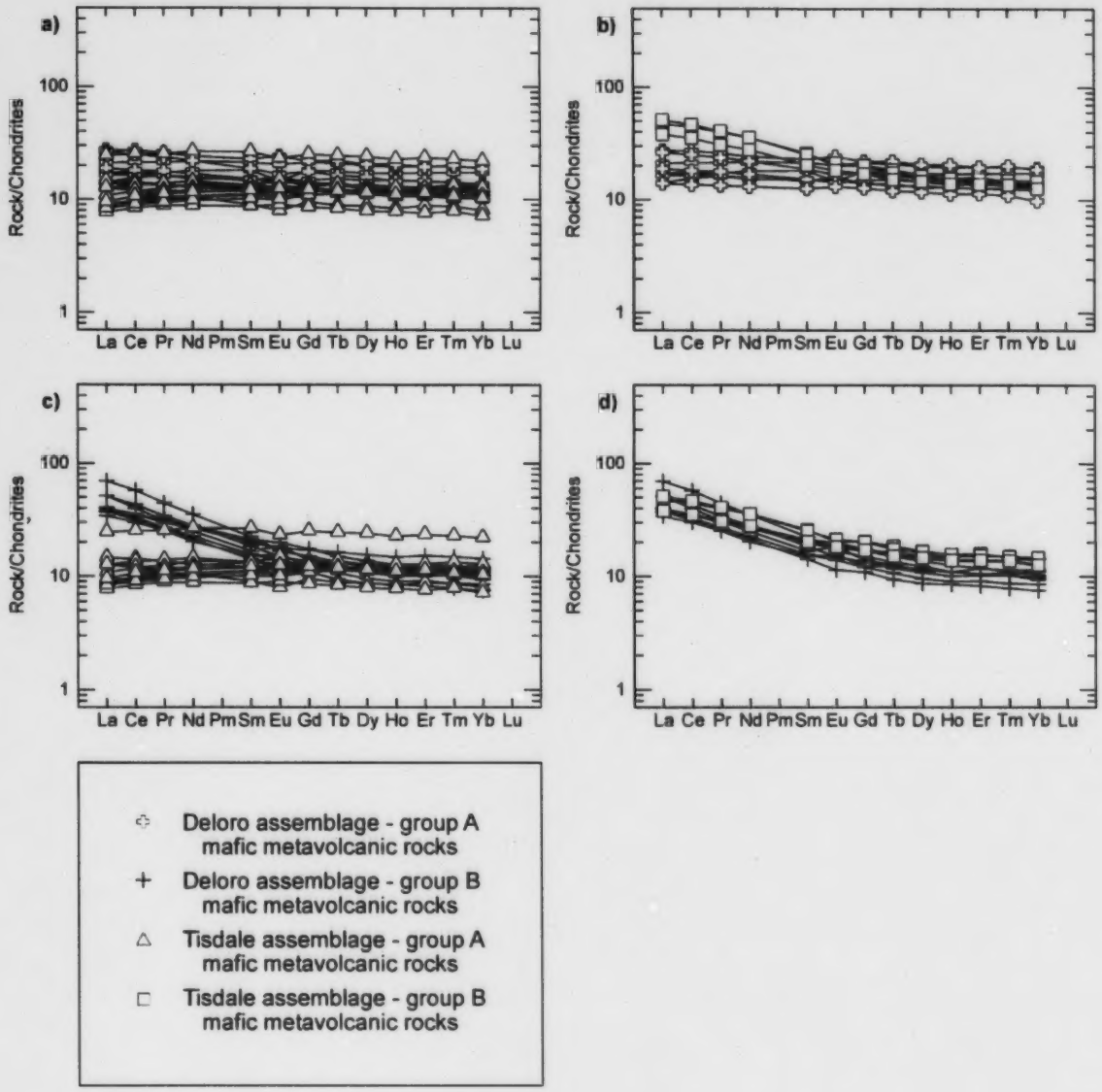
a)
b)
c)
d)
Rock/Chondrites
100
10
1
La Ce Pr Nd Pm Sm Eu Gd Tb Dy Ho Er Tm Yb Lu
Deloro assemblage - group A mafic metavolcanic rocks
Deloro assemblage - group B mafic metavolcanic rocks
Tisdale assemblage - group A mafic metavolcanic rocks
Tisdale assemblage - group B mafic metavolcanic rocks

Figure 13. Chondrite-normalised REE patterns that compare mafic metavolcanic rocks of the Deloro assemblage with those of Tisdale assemblage. Normalising values from Sun and McDonough (1989).

Ultramafic Metavolcanic Rocks

The ultramafic metavolcanic rocks plot as a komatiitic trend on the Jensen cation plot (Figure 14a) across the peridotitic komatiite and basaltic komatiite fields. These rocks display typical chondrite-normalised REE patterns for ultramafic rocks with depleted light REE and a shallow positive slope that increases toward the heavy REE (Figure 14b). All samples have low total REE values, however, there is little overlap in the values between samples. Two of the samples express negative europium anomalies. A third sample has a weak positive europium anomaly. This variation at europium may be due to the affects of hydrothermal alteration.

Metamorphism

The supracrustal rocks of the Abitibi greenstone belt have undergone sub-greenschist to greenschist facies regional metamorphism. Amphibolite facies metamorphism occurs in proximity to large granitoid plutons (Jolly 1974, 1977, 1978; Powell et al. 1990).

The dominant metamorphic mineral assemblage in the map area is actinolite ± chlorite + plagioclase + quartz + epidote ± white mica. This is consistent with the regional greenschist facies metamorphism recorded elsewhere in the Abitibi (Jolly 1974, 1977, 1978; Powell et al. 1990). Higher-grade metamorphic mineral assemblages are present in other parts of the map area.

In west Carscallen Township, between the KGC and the CLP (*see* Figure 3), amphibolite facies metamorphism is recorded in some of the mafic and felsic metavolcanic rocks. Assemblages in this area include hornblende + plagioclase ± garnet ± biotite ± white mica ± quartz. This elevated metamorphic grade is herein interpreted to be a result of an increased thermal gradient due to the intrusion of the two plutons.

In central to southern Denton Township, hornblende + plagioclase ± actinolite ± biotite ± white mica define the amphibolite facies metamorphism observed in metagabbroic and metavolcanic rocks. The amphibolitized rocks of this area lie between and within the two mylonitic splays of the Porcupine-Destor fault zone (*see* Figure 3). East of the 'Tri-Lakes Fault' amphibolite grade metamorphism was not observed. It is interpreted that this area of elevated metamorphic grade reflects rocks brought to surface from greater depths along the Porcupine-Destor fault.

Structural Geology

The impacts of four deformation episodes (D_1, D_2, D_3 and D_4) have been recognised in the map area. These manifest themselves as folds with distinctive morphologies and orientations. Planar fabrics are associated with some folds and display a range of characteristics that seem to reflect rock type characteristics as well as the degree of deformation. Distinct zones of mylonitized rock were recognised during bedrock mapping. The large, west-striking mylonite zones are interpreted to represent the Porcupine-Destor Fault zone (PDFZ). Three, vertical, essentially north-striking faults have been identified in the map area. These faults are correlated with the Mattagami River fault and are associated with significant displacement of stratigraphy (*see* Map P.3517, back pocket). Numerous, small, brittle-ductile shear zones have also been identified throughout the map area and are commonly associated with sulphide mineralization.

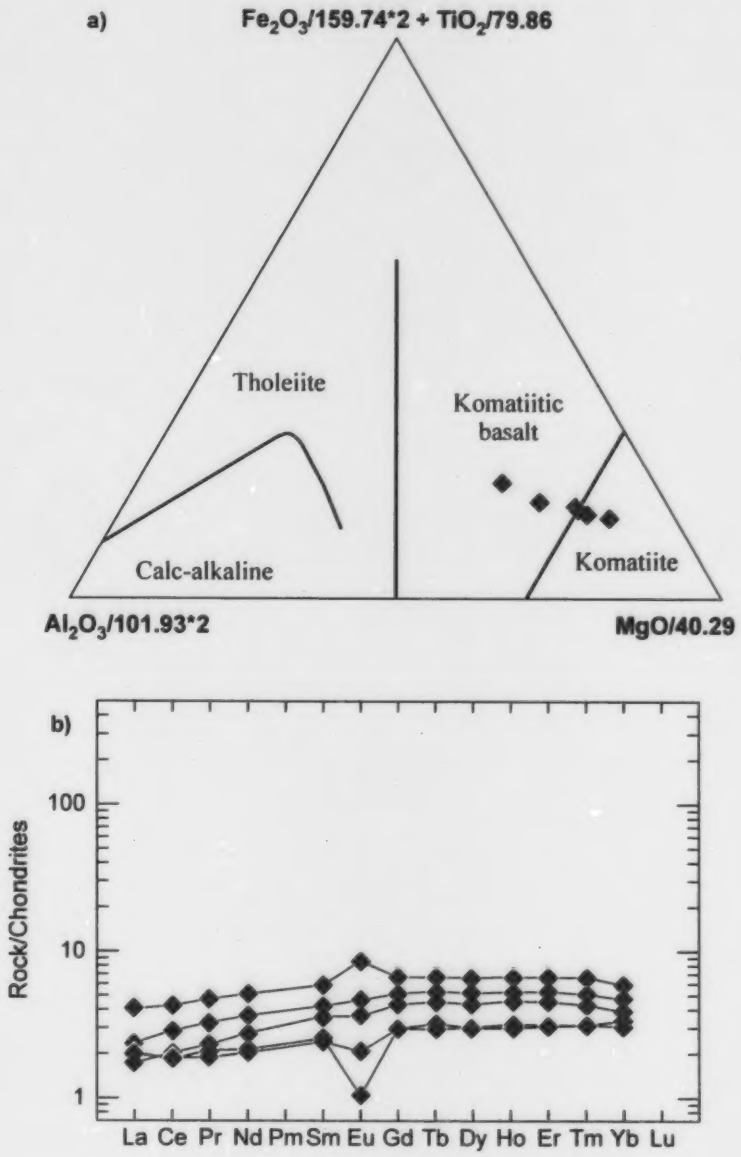

Figure 14. Geochemical characterisation of Tisdale assemblage ultramafic metavolcanic rocks.

For the purposes of this work, the term mylonite is used to connote highly strained rocks with an imposed planar fabric and significant grain-size reduction.

D_1

D_1 is the earliest recognised deformational episode in the map area and is most easily recognised in metavolcanic rocks of the Deloro and Tisdale assemblages. This deformational event is manifested by a penetrative foliation and by mesoscopic and megascopic folds.

A penetrative foliation (S_1) is the primary manifestation of D_1. S_1 is commonly transposed into the plane of the later S_2 foliation such that they form a composite main foliation on most outcrop surfaces. All of the supracrustal rocks of the map area display this foliation to varying degrees. It is least well developed in the metavolcanic rocks in northeast Carscallen Township where it tends to be more concentrated in small (tens of metres wide) zones of high strain. This foliation is weakly developed in the intrusive rocks of both the KGC and the CLP where the foliation occurs in a variety of orientations (*see* Map P.3517; back pocket). This variation is consistent for competent plutonic rocks, especially those surrounded by less competent supracrustal rocks. It is unclear which deformational episode is related to the earliest foliation recognised in the Kenogamissi batholith.

Rare, tight (folds with interlimb angles of 30 to 0 degrees; Ramsey and Huber 1987, p.313) to isoclinal folds (F_1) are associated with D_1. Mesoscopic-scale F_1 folds are rootless (Photo 9) and locally display an axial planar foliation. These folds are rare or difficult to discern as they typically occur in rocks that lack planar inhomogeneities (i.e. bedding). The map-scale synforms and the interpreted synform-antiform pair depicted on Map P.3517 (back pocket), in Denton and Carscallen townships, respectively, are interpreted as F_1 folds. It is further postulated that the intrusion of the CLP is associated with this earliest fold event in Carscallen Township based on the fact that the Deloro assemblage iron formation (map unit 3) can be traced around the margin of the CLP (*see* Figure 5).

The presence of the foliation in all of supracrustal rocks and the plutonic rocks of the CLP and KGC requires that this deformational event post-dated the development of these rocks. The youngest rock unit in the map area that contains the S_1 foliation is the KGC (U/Pb age of 2707 ± 2 Ma; Barrie 1990, 1992, 2000). D_1 must, therefore, have developed after the emplacement of the KGC.

D_2

The most readily identifiable deformational features are associated with D_2. These include a well developed foliation (S_2) and common, widespread folds (F_2; Photo 10).

Typically, S_1 and S_2 form a composite foliation, however, the foliations are sub-parallel to oblique at or near the closures of F_2 folds. S_2 is the obvious, more spaced, deeply weathered foliation on the outcrop surface whereas S_1 is the more penetrative foliation.

F_2 folds are tight to close (folds with interlimb angles of 70 to 30 degrees; Ramsey and Huber 1987, p.313), asymmetric (usually Z-shaped) folds observed at microscopic, mesoscopic and megascopic scales. The axial surface traces of these folds commonly strike east-northeast. The hinges fan about a vertical orientation (i.e. they plunge in an array of orientations that range from moderate to the east-northeast through vertical to steep to the west). On the outcrop and microscopic scales the F_2 folds are easily distinguished from F_1 folds as they fold the pre-existing S_1 foliation. In southwest Denton Township the

Photo 9. Rootless, isoclinal F_1 fold in Tisdale assemblage metasedimentary rocks, Denton Township.

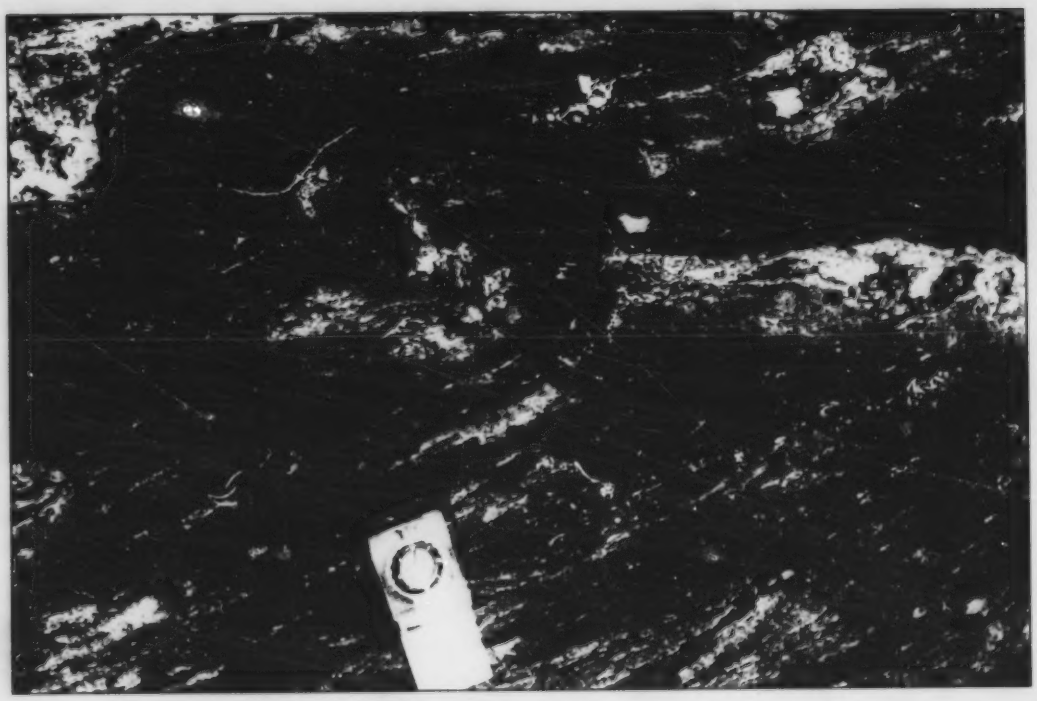

Photo 10. Z-shaped F_2 fold in Tisdale mafic metavolcanic rocks, Denton Township.

contacts between lithologic units have been affected by an F_1-F_2 interference pattern (Type 3; Ramsey and Huber 1987, p.492) that is highlighted on Map P.3517 (back pocket) through the bend in the synform trace.

D_3

D_3 is only locally developed. A set of crenulations (F_3) can be observed on S_1, S_2 and S_1/S_2 composite foliation surfaces, especially in highly sericitized and chloritized rocks. The hinges of these crenulations are near horizontal. This makes them easily distinguishable from folds that are related to other deformational episodes. The folds vary locally in intensity and morphology. Most typically they form a faint crenulation lineation that is hard to discern unless the surface is well lit. However, F_3 also locally occurs as relatively large (a period of up to 20 cm), open folds with round, chevron-shaped (Photo 11), box-shaped or sub-angular conjugate sets. No axial planar foliation was recognised with the F_3 folds.

D_4

D_4 is manifested as kink folds (F_4) with steeply dipping hinges and near vertical axial planes. The kink-bands are typically between 4 and 15 cm wide. Although conjugate sets are present, Z-shaped asymmetries are dominant. These F_4 kinks can be distinguished from F_2 minor folds by the absence of an axial planar foliation, size, variable orientation, relative isolation from each other and by their local occurrence as conjugate sets (Photo 12). Jointing in the CLP (*see* Map P.3517, back pocket) may be another feature resulting from D_4.

PORCUPINE-DESTOR FAULT ZONE (PDFZ)

Two parallel, west-trending zones of mylonitized rocks cut the eastern half of southern Denton Township (*see* Figure 3; Map P.3517, back pocket). A wide, northwest-trending mylonite zone connects the southern mylonite zone with the northern zone. The southern zone is truncated and the northern zone becomes wider at the intersection with the northwest-trending zone. The two fault zones are amalgamated into one zone in the western part of the township. The widest exposed section of mylonite is in the west part of Denton Township where it is approximately 500 m wide. The mylonite zones are interpreted to be the result of at least one of the deformation episodes related to the protracted deformational history of the PDFZ.

The mylonite zones contain intimately interleaved rock units consisting of amphibolites and chlorite-feldspar rocks. Coarse-grained gabbro (*see* Map P.3517, back pocket) can be traced into the mylonitic amphibolites through a progression of grain size reduction and planar fabric development. Chlorite-feldspar rocks (dubbed the 'pink and green mylonite') are tentatively correlated to the epiclastic metasedimentary rocks associated with the Tisdale metavolcanic rocks in the vicinity of the Godon lakes. It is likely, however, that there is also a metavolcanic component in the mylonite zone; however, the primary features have been obliterated by the intense deformation. Possible mafic metavolcanic rocks of the Tisdale assemblage accompany deformed gabbros within the mylonite.

Photo 11. Chevron-shaped F_3 folds in Tisdale ultramafic metavolcanic rocks, Denton Township.

Two types of granitoid dikes with different relative ages cut the rocks within the mylonite zones. An early suite of tonalitic to granodioritic dikes lies within the main mylonitic fabric. It is interpreted that these dikes were intruded prior to the episode of high strain that created the fabric. A later suite of granodiorite dikes transects the mylonitic fabric (Photo 13). These transecting dikes are folded and boudinaged within the mylonite zone (Photo 14). Such relationships indicate that these late dikes intruded during mylonite development. A sample of one the later granodioritic dikes was collected for U-Pb zircon age-dating.

Folded anisotropies (Photo 15), boudinaged and rotated dykes, local C-S fabrics and asymmetric flow patterns about passive markers all indicate a dextral transpressive sense of movement within the mylonite zones. Stretching lineations are variable, with three main groups of orientations associated with

Photo 12. Composite set of F_4 kink-bands over-printing Z-shaped F_2 fold in Tisdale assemblage metasedimentary rocks, Denton Township.

Photo 13. Syntectonic granodiorite dikes intruding mylonitized Tisdale assemblage mafic metavolcanic rocks, Denton Township.

Photo 14. Boudinaged and folded syntectonic granodiorite dike, Denton Township.

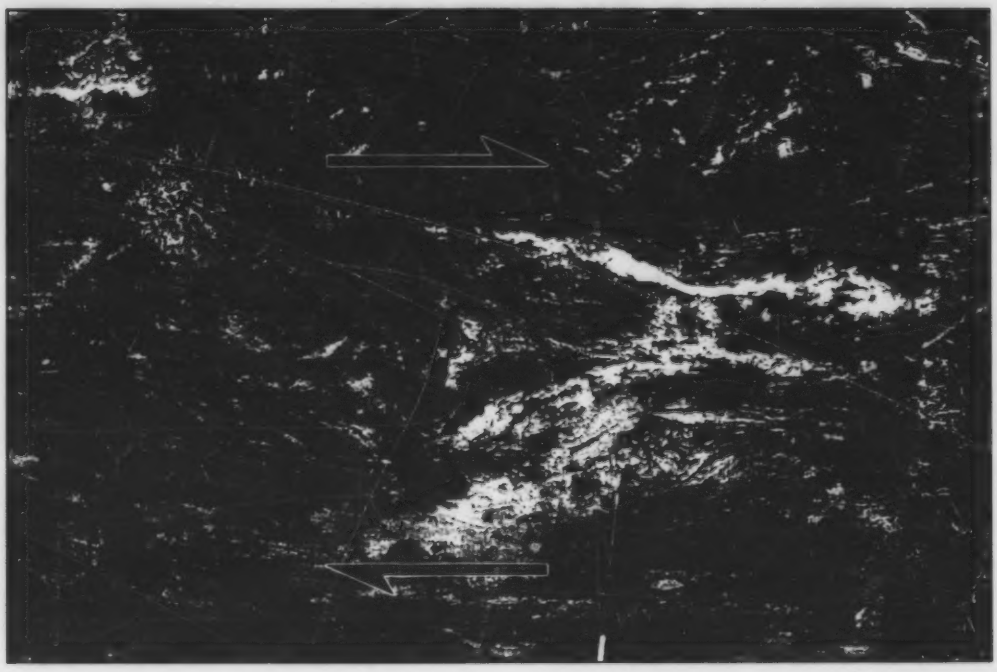

Photo 15. Folded anisotropy in mylonitized gabbro. Dextral sense of shear.

different segments of the mylonite zones. This is consistent with findings in other curved transpressional shear zones (Lin 2000; Lin and Jiang 2001).

The mylonite zones are interpreted to be temporally associated with the D_2 deformation in the rocks north of the zones. The absence of overprinting F_2 folds suggests that this mylonitic fabric must have developed either syn- or post-D_2. The dominant Z-asymmetry of F_2 folds supports a dextral transcurrent regime. The absence of overprinting D_3 crenulations would suggest that the mylonitic fabric was not present during D_3. The non-ubiquitous nature of F_3, however, renders this argument less compelling. A set of northwest-striking fractures that overprint the mylonitic fabric are correlated with D_4.

LATE FAULTS

Three late, north-striking faults cut the rocks of the map area. To simplify their description, these faults are assigned informal names: the 'Tri-Lakes fault', the 'Mahoney Creek fault' and the 'Parliment Lake fault'. The locations of these faults are indicated on Figure 3. These faults are interpreted to be related to the Mattagami River fault.

The Tri-Lakes fault offsets rocks of the Tisdale assemblage, CLP, and mylonitized rocks of the PDFZ near the west margin of Denton Township (*see* Figure 3). Mylonitized granodiorite is exposed on the west side of Godon Lake. The shear zone is steeply-dipping, south-striking and flanked to the west by a north-striking topographic lineament that is consistent with the expression of brittle and brittle-ductile faults. Shear-bands, rotated and boudinaged epidotized zones and folded veins all indicate sinistral transcurrent movement. No stretching lineations were observed. Further south on Godon Lake, a discrete shear zone striking to the northwest and dipping steeply to the northeast cuts gabbroic rocks. This shear zone accommodates a southeastward step in the general north strike of the fault (*see* Figure 3). The relative position of the mylonitic rocks of the Porcupine-Destor fault zone and contacts between supracrustal rocks and the CLP indicate an approximately 2 km, horizontal, sinistral offset across the Tri-Lakes fault. A paucity of outcrop required geophysical data and airphoto interpretation to trace the Tri-Lakes fault to the north and south of where it is exposed at Godon Lake.

Small, discrete, north-striking, steeply dipping, sinistral shear zones in southeast Denton Township (*see* Map P.3517, back pocket) form the interpreted Mahoney Creek fault (*see* Figure 3). Similar to the Tri-Lakes fault, the Mahoney Creek fault steps to the southeast through a zone of accommodation that is exposed in one of the shear zones. Offsets in observed and geophysically interpreted ultramafic metavolcanic horizons resulted in the interpretation of a sub-parallel splay fault associated with the Mahoney Creek fault. No exposed shear zones were observed in association with this splay. The interpreted presence of Porcupine assemblage metasedimentary rocks (*see* map unit 9c; Map P.3517, back pocket) on only the east side of the Mahoney Creek fault may indicate that there is a component of vertical movement (west side up) across the fault. This vertical displacement is interpreted to have resulted in the preferential erosion of this upper stratigraphic unit from the west side of the fault. The general lack of exposure in the area, however, makes this interpretation somewhat tenuous.

The identification and location of the Parliment Lake fault (*see* Figure 3) is based entirely on air-photo and geophysical interpretation. This interpretation is supported, however, by the geographical distribution of exposures of the Deloro assemblage, KGC and CLP. All of these units display apparent sinistral offset across the interpreted trace of the Parliment Lake fault. The trace of the iron formation (map unit 3) within the Deloro assemblage (*see* Figure 5) is an especially useful marker horizon.

An east-northeast striking high strain zone, the Scott shear (Pyke 1980) affects the rocks of the Wakemac (McCoshen splay) and Cameco properties in Denton Township (*see* Figures 3 and 4). This near vertical shear zone is characterised by an intense penetrative foliation and Z-shaped folds consistent with F_2. The closures of these folds, that represent small zones of dilation within an overall transpressive environment, host quartz-iron carbonate veins. The Scott shear can be traced west through the AuMo (B) property and beyond (*see* Figures 3 and 4). The Scott shear may be offset to the north by the Mahoney Creek fault such that it can be linked with the Bristol fault in Bristol Township.

A near vertical, west-northwest-striking high strain zone transects the Deloro assemblage metavolcanic rocks and iron formation between the KGC and CLP. This high strain zone crosses the contact between the mafic-dominated (map unit 1) and felsic-dominated (map unit 2) metavolcanic rocks. In this zone, the rocks display a profound penetrative foliation that locally results in highly fissile outcrops. The high strain zone has also deformed the iron formation (map unit 3). The high strain zone is intersected and offset by the Parliment Lake fault but does not appear to be affected by the F_1 fold event that affected the iron formation. This suggests that the high strain zone is post-D_1 but pre-Parliment Lake fault.

Small brittle-ductile shear zones occur in the vicinity of the CLP. These shear zones are typically less than 1.5 m wide and cut the tonalitic and granodioritic rocks of the CLP as well as the metavolcanic and chemical metasedimentary rocks of the Deloro assemblage. There appears to be a spatial relationship between the faults and late porphyritic dikes within the CLP. The dikes seem to localise the shearing, due perhaps to a competency contrast between the dikes and the surrounding coarse-grained, plutonic rocks. Intensive silicification and sulphide mineralization are associated with these small, late faults.

Geochronology

Numerous, parallel to sub-parallel, pink weathering, granodioritic dikes intrude mylonitized mafic rock in an outcrop exposure on the Tatachikapika River (*see* Photo 13) in what has been described (Harding and Berry 1938) as a lit-par-lit configuration. Relative age criteria indicate that the granodiorite dikes were emplaced during a period of dextral transpressive displacement along the Porcupine-Destor fault zone. As such, a U/Pb zircon age determination for these dikes provides a constraint on the timing of movement along the PDFZ. A granodiorite dike was sampled at this location to achieve this end.

Seven single-grain analyses give concordant to strongly discordant $^{207}Pb/^{206}Pb$ ages, as shown on Figure 15. Four analyses, including one concordant grain, define a lead-loss line (with a 41% probability of fit) with an upper intercept age of 2711 ± 2.3 Ma; a second concordant analysis yielded an age of 2701 ± 2.8 Ma; a third concordant analysis give an age of 2689.3 ± 4.5 Ma.

These data can be interpreted in several ways. However, through consideration of the local geological perspective and our understanding of the ages of other rocks in the vicinity of the sample location, the author supports the following interpretation. The two older ages reflect inheritance in the granodiorite dike, while the younger age reflects the emplacement age for the dike. The 2711 ± 2.3 Ma age is interpreted to be inherited from the deformed mafic metavolcanic rocks into which the dike intruded. This is consistent with the interpretation that mafic country rocks are Tisdale assemblage. The presence of multiple zircon grains defining the discordia line would reflect the intimate relationship between the mafic metavolcanic rocks and the felsic dikes (*see* Photo 13). The multi-phase Kenogamissi batholith is exposed to the southwest of the sample location. The 2701 ± 2.8 Ma age is consistent with some age determinations obtained from this batholith (J. Ayer, Ontario Geological Survey, unpublished data, 2002) through which the dikes may have passed. The range of ages within error for the concordant

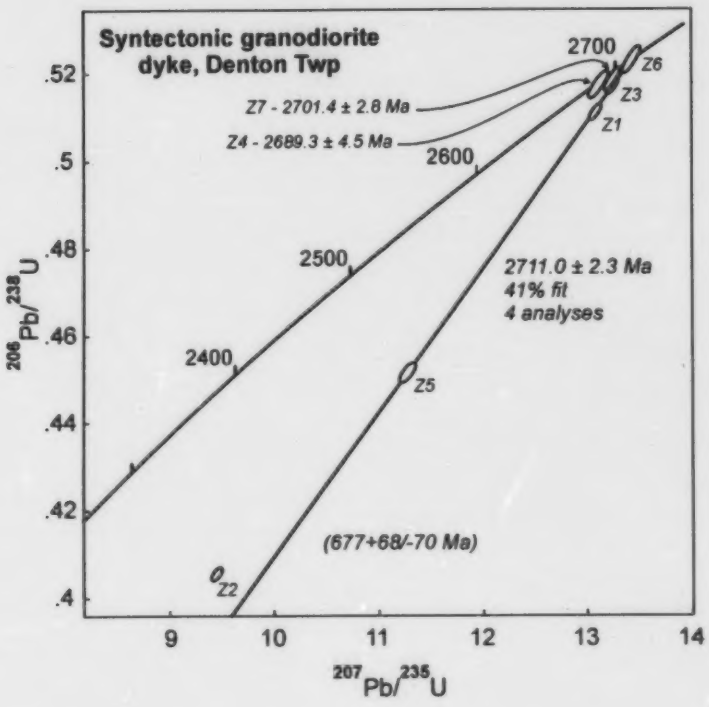

Figure 15. U/Pb isochron plot for a syntectonic granodioritic dike in Denton Township.

zircon analysis of 2689.3 ± 4.5 Ma overlaps with the timing of the deposition of the Porcupine and Timiskaming assemblages (Ayer et al. 1999, 2002). This interpretation is supported by observations elsewhere in the Timmins area that indicate that deformation along the PDFZ affected both the Porcupine and Timiskaming assemblages (Benn et al. 2001). This would require that the emplacement of the syntectonic dike was at least coeval (if not more recent than) with the deposition of the Porcupine and Timiskaming assemblages. The 2689.3 ± 4.5 Ma age also overlaps with the emplacement of several quartz-feldspar porphyry intrusions in the Timmins area (2687 Ma; J. Ayer , OGS, unpublished data, 2002). This can be interpreted to reflect a possible association between the porphyries and the granodiorite dike (J. Ayer, OGS, personal communication, 2002).

Geophysics

AIRBORNE MAGNETIC SURVEYS

The airborne geophysical total magnetic field data were acquired in 1988 as part of the Timmins airborne electromagnetic survey (OGS 1996, 1999). The survey was flown with a nominal line spacing of 200 m with an orientation of 000°. The magnetic sensor was flown at a nominal terrain clearance of approximately 70 m.

The total magnetic field values range from approximately 2 800 nT to 3 200 nT with an average background of 2 840 nT. This relatively low dynamic range is consistent with relatively low overall ferromagnetic mineralization (magnetite and pyrrhotite) and is consistent with the magnetic susceptibility measurements taken in the field. The highest amplitude responses correlate with Tisdale assemblage ultramafic metavolcanic rocks (map unit 6), Deloro assemblage iron formation (map unit 3) and diabase dikes of the Matachewan (map unit 15) and Abitibi (map unit 16) swarms. The mafic metavolcanic rocks of the Deloro and Tisdale assemblages do not produce a strong magnetic response, indicating a lack of ferromagnetic mineralization. As a result of this, coupled with the presence of strongly magnetic diabase dikes, it is virtually impossible to distinguish the mafic metavolcanic rocks from the felsic metavolcanic rocks.

The CLP (map unit 11a) can be delineated by the airborne geophysical magnetic data set. A relative magnetic low appears to coincide with the margin of the pluton. The highly variable response in the interior of the pluton is consistent with the magnetic susceptibility measurements taken in the field. It is further complicated by the presence of Matachewan diabase dikes.

GRAVITY SURVEYS

The gravity data set is part of the regional provincial data set that was recently augmented by the Timmins Collaborative Gravity Survey Project (OGS 2001). The ground stations were spaced 1 to 1.5 km apart over most of the survey area. The data resolution is excellent for application to a regional geologic study such as this one.

The gravity data set was useful in discriminating relatively dense mafic to ultramafic units from felsic rocks. The data also provided a sense of the relative proportion of these denser units.

MAGNETIC SUSCEPTIBILITY

Magnetic susceptibility was measured at the outcrop by portable magnetic susceptibility meters. All outcrop measurements were made with a KT-9 magnetic susceptibility meter (MSM) manufactured by Exploranium Radiation Detection Systems. The instrument measures the true magnetic susceptibility in a range of 0.01×10^{-3} to 999×10^{-3} (dimensionless SI units) and was operated in the "pin-mode" to reduce errors introduced by measuring on uneven surfaces (Exploranium Radiation Detection Systems, KT-9 Users Guide). At every outcrop a minimum of five measurements of each rock type were recorded with exceptional cases warranting more measurements due to variability in magnetic susceptibility. Median values have been calculated and are interpreted in most cases to represent a characteristic magnetic susceptibility for each rock type.

Metavolcanic Rocks

The mafic metavolcanic rocks have a weakly defined bimodal frequency distribution with a wide range of values ($0.2 - >100 \times 10^{-3}$) (Figure 16). Most of the readings fall in the range of $0.4 - 2.0 \times 10^{-3}$ with an overall median value of 0.72×10^{-3}. The higher magnetic susceptibilities tend to be confined to the Kidd-Munro assemblage mafic metavolcanic rocks (map unit 5) in the northeast corner of Carscallen Township.

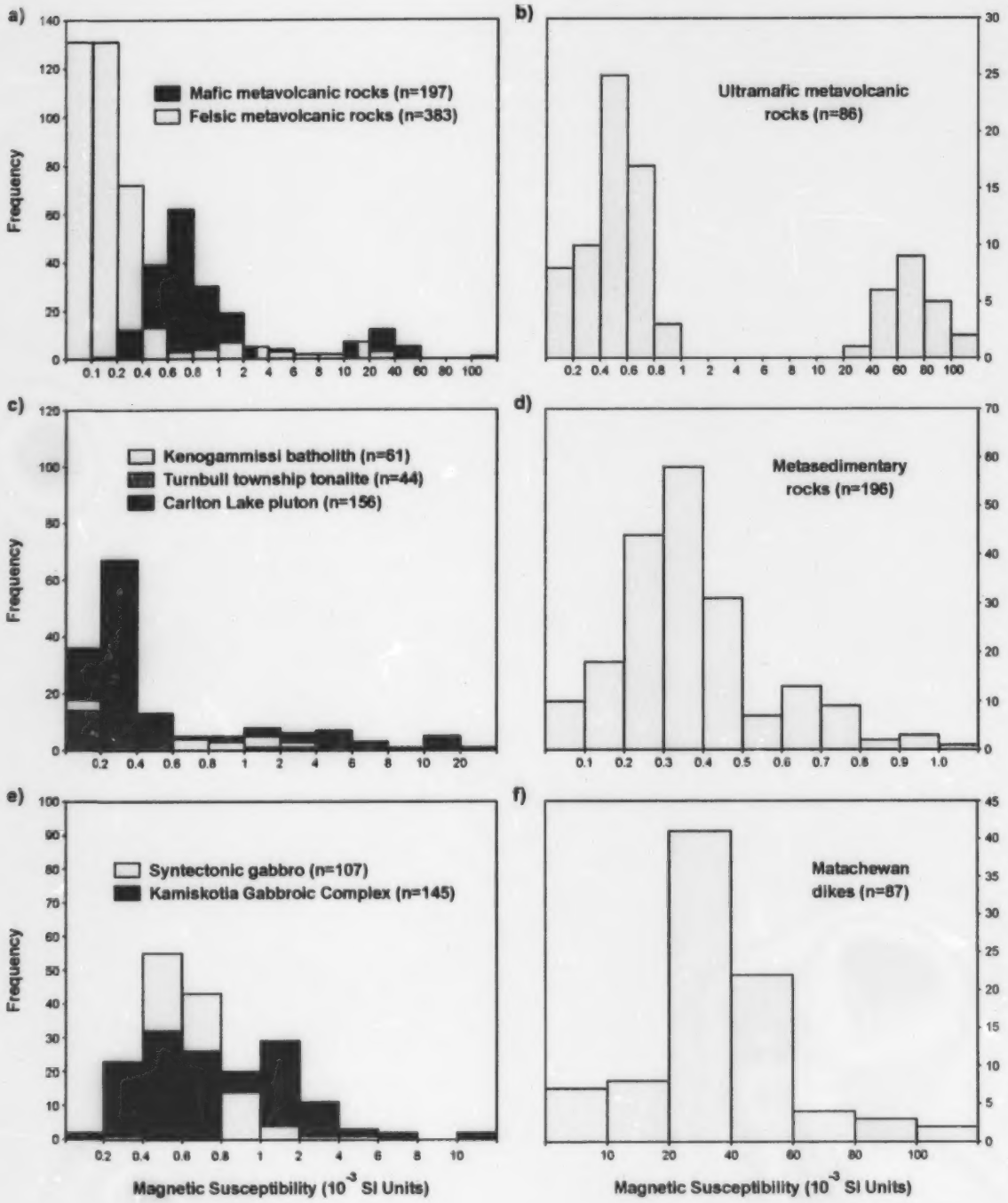

Figure 16. Frequency distribution histograms of magnetic susceptibility readings taken on rocks of Denton and Carscallen townships.

The felsic metavolcanic rocks show a weakly defined bimodal distribution (*see* Figure 16a). Almost all the values are $<0.4 \times 10^{-3}$ with a characteristic median of 0.15×10^{-3}. The felsic metavolcanic rocks of the Deloro (map unit 2) and Tisdale (map unit 8) assemblages yield MSM readings of 0.1 to 0.4×10^{-3}. The felsic metavolcanic rocks of the Kidd-Munro (map unit 4) assemblage yield a bimodal MSM population; one non-magnetic population with readings of $<0.1 \times 10^{-3}$ whereas the other is moderately magnetic ranging from $0.4 - 40 \times 10^{-3}$.

The ultramafic metavolcanic rocks of the Tisdale assemblage (map unit 6) possess a well-defined bimodal frequency distribution with peaks centered on the ranges of $0.4 - 0.6 \times 10^{-3}$ and $60 - 80 \times 10^{-3}$ (*see* Figure 16b).

Felsic Intrusive Rocks

Within the map area there are three, felsic intrusive bodies: the CLP (map unit 11a); TTT (map unit 11b); and Kenogamissi Batholith (map unit 13). The CLP has a wide range of magnetic susceptibilities (up to 40×10^{-3}) but a lower median of 0.29×10^{-3} (*see* Figure 16c). The higher MSM readings seem to be local variations within the pluton and are not restricted to distinctive areas. Dramatic variations were recorded within metres of each other and no visible distinctions were observed to account for these variations. Similarly, the TTT yielded a relatively large range of values and an identical median value. This further supports the interpretation of a genetic link between the CLP and TTT. In the southern region of Denton Township the Kenogamissi Batholith yielded MSM values ranging from $0.05 - 2.95 \times 10^{-3}$ with a median of 0.36×10^{-3} (*see* Figure 16c).

Mafic Intrusive Rocks

Various phases of the KGC (map unit 10) produced a relatively flat frequency distribution pattern in the range of $0.2 - 2.0 \times 10^{-3}$ and a characteristic median of 0.77×10^{-3} (*see* Figure 16e). Anomalous high magnetic susceptibilities came from gabbroic phases with visible magnetic grains present. The syntectonic mafic to ultramafic intrusive rocks (map unit 12) yield a median magnetic susceptibility of 0.62×10^{-3}, distinctly lower than the KGC and the range of values tends to be more restricted to $0.4 - 0.8 \times 10^{-3}$ (*see* Figure 16e).

The Matachewan diabase dikes (map unit 15) provide an excellent example of a unimodal distribution and a median magnetic susceptibility that can be utilised to characterise them. The mafic dikes possess a median magnetic susceptibility of 33.8×10^{-3} with 72% of the readings falling in the range of $20 - 60 \times 10^{-3}$ (*see* Figure 16f).

Economic Geology

GOLD MINERALIZATION

Numerous mineral properties are situated in Carscallen and Denton townships (*see* Figure 4; Map P.3517, back pocket). The majority of these are gold properties. As early as 1911, gold-bearing quartz veins were reported in both 'gray biotite granite' and 'greenish and grayish schists' in Denton Township (Burrows 1911, 1912). Gold mineralization is associated with a diversity of rock types, assemblages,

structures and alteration characteristics in the map area. Table 2 summarises the geological characteristics of the gold properties indicated on Figure 4. Some of the general characteristics of gold properties in the map area are as follows:

- host rocks include metavolcanic rocks of all assemblages, iron formation and granodioritic rocks of the CLP;
- wall rock alteration dominantly consists of chloritization, silicification and variable late iron-carbonatization;
- gold is commonly associated with sulphide minerals such as pyrite and arsenopyrite;
- gold occurs with disseminated sulphide mineralization and quartz-carbonate or quartz-chlorite veins that may or may not be deformed;
- gold is hosted by D_2 and D_3 structures such as folds and shear zones and by late brittle faults.

The observations above indicate that gold mineralizing events occurred relatively late in the tectonic history of Carscallen-Denton townships area. Examples of the diverse geologic environments which host gold mineralization are described below, followed by Table 2 that summarises the geological settings of each of the gold properties in Denton and Carscallen townships.

Wire Gold Prospect

Extensive exploration activity including stripping, trenching and sampling have been conducted at the Wire Gold prospect (*see* Figure 4; Map P.3517, back pocket) since the reported discovery of wire gold at this locality (Harding and Berry 1938). The prospect is underlain by Deloro assemblage mafic metavolcanic flows and breccias; cherty banded iron formation; and an enigmatic unit interpreted as a synvolcanic, intermediate sill. Relationships between these rock types are complicated by syndepositional, slump folds as well as later tectonic folds and faults. Quartz-calcite veins are associated with late brittle faulting. The wire gold was reported to occur in open-space fillings (vugs) in the veins.

Larchmont Prospect

Stripping, sampling and various ground geophysical surveys have been conducted over the Larchmont prospect in the northeast corner of Carscallen Township (Figure 4; Map P.3517, back pocket). Kidd-Munro assemblage felsic metavolcanic rocks underlie the prospect. However, they have been interpreted to be part of the Kamiskotia assemblage (Pyke and Cunnison 1997; L. Bonhomme, Prospector, unpublished data). Quartz porphyry dikes intrude the felsic metavolcanic rocks and have geochemical characteristics that are similar to their host rocks (*see* Appendix 1; samples 01LAH-219A, 01LAH-0225, 01LAH-0226). Assays of samples collected from quartz-carbonate ± chalcopyrite ± pyrite ± chlorite ± tourmaline veins on the property have resulted in trace values of gold (Bradlow 1965). However, 'native gold' has been reported at this locality (Hawley 1926).

Jowsey Prospect

Exploration activity conducted on the Jowsey prospect (Figure 4; Map P.3517, back pocket) includes trenching and sampling. Quartz-feldspar porphyry dikes intrude granodioritic rocks of the CLP. Brittle-ductile shear zones and associated quartz and quartz-chlorite veins are localised at dike margins but also extend across the dikes. Massive zones of pyrite ± arsenopyrite, up to 40 cm wide, occur in the shear zones. Alteration of ferromagnesian mafic minerals in the granodioritic host rocks imparts a "bleached" appearance to the sheared host rocks. A sample of mineralized, sheared quartz-feldspar porphyry dike rock collected by the author from a trench assayed 0.02 ounce gold per ton (Appendix 1; sample 01LAH-0012).

AuMo Prospects

The AuMo (B) prospect has been distinguished from the AuMo (A) prospect on the basis of contrasting geological settings (*see* Figure 4; Map P.3517, back pocket). The AuMo (A) prospect is similar to the Jowsey prospect and is hosted by granodioritic rocks of the CLP which have been intruded by quartz-feldspar porphyry dikes and deformed by brittle-ductile faults. Foliated siliceous, chloritic and graphitic schists characterise the rocks of AuMo (B). These are interpreted as felsic and mafic metavolcanic rocks and possible metasedimentary rocks, respectively, of the Deloro assemblage. Cherty iron formation has also been reported on the property (L. Bonhomme, Prospector, personal communication, 2001). The penetrative foliation in the host rocks at the AuMo (B) prospect is related to the Scott shear zone (*see* Figures 3 and 4) which extends across the property. Trenching and stripping has exposed gossan zones with "bleached", siliceous wall-rocks in the highly strained rocks. Massive and stringer sulphide mineralization within these shear zones consist of pyrite with limited chalcopyrite (Hogg 1946).

Wakemac Prospect

The Wakemac prospect (*see* Figure 4; Map P.3517, back pocket) is a large stripped area with several trenches and diamond-drill holes. The property is underlain by foliated, intimately interlayered, mafic and ultramafic metavolcanic rocks that have been extensively chloritized and iron carbonatized. These rocks are interpreted to be part of the Tisdale assemblage. Two ultramafic horizons are magnetic, hard, vitreous and display an unusual black-tan lamination (1 to 4 mm spacing). The McCoshen splay of the Scott shear zone (*see* Figures 3 and 4) extends across the Wakemac property (Pyke 1980) and is responsible for the strong deformation in the area. F_2 and F_3 folds were observed by the author on this property. Iron carbonate veins are concentrated in the closures of F_2 folds.

Occurrence Name	Host Lithology	Local Structures	Mineralization Type	Associated Minerals	Wall Rock Alteration
Larchmont (Four Corners)	Kidd-Munro quartz-phyric rhyolite, cut by quartz porphyry dikes	quartz veins	disseminated to stringer sulphides	silver	sericitization silicification
Fournier	Kidd-Munro mafic metavolcanics, cut by quartz porphyry dikes	quartz veins	disseminated to stringer sulphides	pyrite	sericitization
Carscallen Lake (Lucky Strike)	Deloro mafic metavolcanic rocks and banded iron formation	shear zone with penetrative foliation	"massive" sulphides	pyrrhotite pyrite chalcopyrite sphalerite	sulphidation
Wire Gold (Aberdeen; Jowsey; Beanland-Hurst)	Deloro banded iron formation	brittle faults and associated quartz-calcite veins	wire gold in quartz-calcite veins iron formation	sulphide horizons	silicification
Parliment Lake	CLP cut by porphyry dykes	variably striking brittle faults cutting porhyry dykes and granodiorite	massive to stringer sulphides with quartz-chlorite veins	pyrite	silicification sulphidation chloritization
Jowsey	CLP cut by porphyry dykes	variably striking brittle faults cutting porhyry dykes and granodiorite	massive to stringer sulphides with quartz-chlorite veins	pyrite arsenopyrite	silicification sulphidation chloritization
AuMo (A) (Hazelton)	CLP cut by porphyry dykes	variably striking brittle faults cutting porhyry dykes and granodiorite	massive to stringer sulphides with quartz-chlorite veins	silver pyrite arsenopyrite molybdenite chalcopyrite sphalerite	silicification sulphidation chloritization
AuMo (B)	Deloro assemblage metavolcanic rocks and iron formation	very penetrative east-striking shear zone	massive, stringer and disseminated sulphide minerals	pyrite chalcopyrite arsenopyrite	silicification sulphidation
Jowsey-Denton (Denton #4-83; Brown-McDade)	KGC associated gabbroic rock	brittle faults with associated quartz veins	rare disseminated sulphides	pyrite	limited sulphidation
Gowest (Halpenny; Mahoney Creek)	Tisdale assemblage komatiites	east-striking shear zone associated with PDFZ	disseminated to stringer sulphide minerals	pyrite arsenopyrite	serpentinization carbonatization (calcite)
Wakemac (McCoshen)	Tisdale assemblage mafic metavolcanic rocks	very penetrative foliation and F_2 and F_3 folds; Scott shear zone	massive to disseminated sulphide minerals	pyrite arsenopyrite	iron carbon-atization chloritization
Cameco	Tisdale assemblage komatiites	very penetrative foliation and F_2 folds	quartz and quartz-carbonate veins associated with F_2 fold closures; disseminated sulphide minerals	pyrite arsenopyrite	iron carbon-atization
Karvinen	Tisdale assemblage mafic and felsic metavolcanic rocks and epiclastic metasedimentary rocks	very penetrative foliation; F_2 folds	quartz and quartz-carbonate veins associated with F_2 fold closures; disseminated sulphide minerals	pyrite arsenopyrite	iron carbon-atization

Abbreviations: PDFZ – Porcupine-Destor fault zone

Table 2. Summary of geological characteristics of gold properties in Denton and Carscallen townships.

VOLCANOGENIC MASSIVE SULPHIDE (VMS) MINERALIZATION

In 1964, Lucky Strike Exploration Ltd. reported a 117.5-foot intersection of massive pyrrhotite and pyrite in core from a diamond drill-hole on the Carscallen Lake property. The mineralization was reported to be associated with mafic metavolcanic rocks and cherty, magnetite iron formation and is interpreted to occur within the Deloro assemblage. This mineralized horizon was sampled and analyzed for gold (with one 10' intersection running approximately 0.05 ounce gold per ton (Patsch 1964)), but only a small portion of it was analyzed for base metals (e.g. copper, zinc). The iron formation in the Deloro assemblage (*see* Figure 5) is being reassessed for copper-zinc potential including work on the Dea-Barnes properties (that straddle the Whitesides-Carscallen township boundary), the Gunther Lake and Wire Gold properties (*see* Figure 4).

The confirmed presence of Kidd-Munro assemblage FIIIb rhyolite (Ayer et al. 1999) in northern Carscallen Township indicates that the area may have potential to host volcanogenic massive sulphide (VMS) mineralization. Explorers Alliance Corporation has been diamond-drilling geophysical targets for VMS potential in northern Carscallen Township (Bonhomme and Calhoun 2000, 2001). Local zones of sericitic ± chloritic ± epidotitic alteration occur in the felsic metavolcanic rocks of the Kidd-Munro assemblage in northern Carscallen Township. These zones are associated with areas of small brittle fractures and local intensification of the weak regional foliation.

PLATINUM GROUP ELEMENT (PGE) MINERALIZATION

Magmatic sulphide mineralization in the KGC (*see* Figure 4, occurrence 14), in the form of net-textured chalcopyrite and pyrrhotite, contain elevated nickel and copper values but lack significant platinum group element (PGE) enrichment (Barrie 1992). In eastern Denton Township, a sample from a small, highly strained gabbro (*see* Figure 4, occurrence 15) was reported to have analyzed (sample 81AGC-0125, Table 2 in Choudhry 1989) 26 ppm Pt and 19 ppm Pd.

Recommendations for Mineral Exploration

VOLCANOGENIC MASSIVE SULPHIDE (VMS) MINERALIZATION

The Kidd Creek VMS deposit is located approximately 30 km northeast of the map area and is hosted by Kidd-Munro assemblage F111b felsic metavolcanic rocks (Prior et al. 1999). The confirmed presence of felsic metavolcanic rocks of the Kidd-Munro assemblage in northern Carscallen Township (Ayer et al. 1999), suggests that the area has the potential to host VMS mineralization. The interpreted extension of the assemblage across Carscallen Township is equivocal. However, the FIIIb felsic metavolcanic rocks in northeast Carscallen Township remain prospective for VMS mineralization even if they are not correlative with the Kidd-Munro assemblage.

GOLD MINERALIZATION

To date, no producing gold mines have been developed in the map area. However, there is potential for further gold discoveries in the vicinity of the Porcupine-Destor fault zone which extends through the map area (*see* Figure 3;Map P.3517, back pocket) since this structure is associated with major gold deposits

elsewhere in the Abitibi greenstone belt. Gold exploration in the map area should also focus on iron carbonatized mafic and ultramafic metavolcanic rocks and deformed and sulphidized iron formation units.

MAGMATIC NICKEL-COPPER-PLATINUM GROUP ELEMENT (PGE) MINERALIZATION

The geochemical signature of the KGC is interpreted to be the result of a partial melt of primitive mantle (Barrie 2000) which is a favourable indicator for magmatic nickel-copper-PGE mineralization. However, Barrie (2000) notes that poorly developed primary modal layering in the KGC suggests an absence of magma chamber processes conducive to the formation and accumulation of such mineralization. This contention is supported by the low nickel, copper and PGE values obtained from mineralized gabbros sampled by Barrie (2000). However, an extensive, closely spaced, sampling program across the stratigraphy of the intrusion has yet to be conducted. Such a program may be required to detect PGE mineralization.

The anomalous platinum and palladium values reported by Choudhry (1989) in eastern Denton Township are considered to be significantly elevated, however, they have not been reproduced by the author. These values were obtained from a sample that was collected from one of the many small syntectonic mafic and ultramafic intrusions (map unit 12) in the map area. The author sampled (Appendix 1; sample 01LAH-0077A) the same intrusion sampled by Choudry (1989) but was unable to duplicate or verify the analytical results reported by Choudry (1989). Samples collected by the author did not analyze above the detection limit for Pd or Pt.

References

Ayer, J.A. and Trowell, N.F. 1998. Geological compilation of the Timmins area, Abitibi greenstone belt; Ontario Geological Survey, Preliminary Map P.3379, scale 1:100 000.

———2001. The Abitibi Greenstone Belt: a program update; *in* Summary of Field Work and Other Activities 2001, Ontario Geological Survey, Open File Report 6070, p.4.1 to 4.9.

Ayre, J.A., Amelin, Y., Corfu, F., Kamo, S., Ketchum, J., Kwok, K and Trowell, N., submitted. Evolution of the Abitibi greenstone belt based on U-Pb geochronology and Nb isotopes: early interation between plume and subduction volcanism followed by sedimentation, folding and plutonism; Precambrian Research.

Ayer, J.A., Trowell, N.F., Madon, Z. and Corfu. 1997. Geological compilation of the Abitibi greenstone belt in Ontario: the correlation of metallogenic potential with stratigraphy; *in* Summary of Field Work and Other Activities 1997, Ontario Geological Survey, Miscellaneous Paper 168, p.3-9.

Ayer, J.A., Trowell, N.F., Madon, Z., Kamo, S., Kwok, Y.Y. and Amelin, Y. 1999. Compilation of the Abitibi greenstone belt in the Timmins-Kirkland Lake area: Revisions to stratigraphy and new geochronological results; *in* Summary of Field Work and Other Activities 1998, Ontario Geological Survey, Open File Report 6000, p.4.1 to 4.14.

Barrie, C.T. 1990. The geology of the Kamiskotia area; Ontario Geological Survey, Preliminary Map 3396, scale 1:50 000.

———1992. The geology of the Kamiskotia area; Ontario Geological Survey, Open File Report 5829, p.180.

———2000. The geology of the Kamiskotia area; Ontario Geological Survey, Study 59, p.79.

Barrie, C.T. and Corfu, F. 1999. The Kidd-Munro extension project: results of U-Pb geochronology for year 1; *in* Summary of Field Work and Other Activities 1998, Ontario Geological Survey, Miscellaneous Paper 169, p.74-81.

Becker, J.K., Benn, K. and Ayer, J.A. 2001. Emplacement and deformation history of the Kenogamissi batholith and surrounding Swayze greenstone belt, *in* Summary of Field Work and Other Activities 2001, Ontario Geological Survey, Open File Report 6070, p12-1 to 12-8.

Benn, K., Ayer, J., Berger, B.R., Vaillancourt, C., Dinel, É. and Luinstra, B. 2001. Structural style and kinematics of the Porcupine-Destor Deformation Zone, Abitibi Greenstone Belt, Ontario; *in* Summary of Field Work and Other Activities 2001, Ontario Geological Survey, Open File Report 6070, p.6-1 to 6-13.

Bleeker, W. and Parrish, R.R. 1996. Stratigraphy and U-Pb zircon geochronology of Kidd Creek: implications for the formation of giant volcanogenic massive sulphide deposits and tectonic history of the Abitibi greenstone belt; Canadian Journal of Earth Sciences, v. 33, p. 1213-1231.

Bonhomme, L. and Calhoun, R. 2000. Summary Report of 1998-1999 Exploration Activities on the Kamiskotia Joint Venture for Explorers Alliance Corporation; unpublished report, Explorers Alliance Corp., p.21.

Bonhomme, L. and Calhoun, R. 2001. Summary Report of 2000 Exploration Activities on the Kamiskotia Joint Venture for Explorers Alliance Corporation; unpublished report, Explorers Alliance Corp., p.26.

Bradlow, P. 1965. Report on drill program, Larchmont property, Larchmont Mines Ltd.; Timmins Resident Geologist's office, Carscallen Township, assessment file AFRI# 42A05NE359, 6p.

Brisbin, D.I. 1997. Geological Setting of Gold Deposits in the Porcupine Gold Camp Timmins, Ontario; unpublished PhD thesis, Queen's University, Kingston, Ontario, 523p.

Burrows, A.G. 1911. The Porcupine Gold Area; Ontario Bureau of Mines, Annual Report 20, pt. 2, p. 3-33.

Burrows, A.G. 1912. The Porcupine Gold Area; Ontario Bureau of Mines, Annual Report 22, pt. 1, p. 205-249.

Choudhry, A.G. 1982. Precambrian geology of Denton Township, Cochrane District; Ontario Geological Survey, Preliminary Map P.2501, scale 1:15 840.

———1989. The geology of Keefer, Denton and Thorneloe townships, District of Cochrane; Ontario Geological Survey, Open File Report 5699, p.164.

Corfu, F. 1993. The evolution of the southern Abitibi greenstone belt in light of precise U-Pb geochronology; Economic Geology, v.88, p.1323-1340.

Ferguson, S.A. 1959. Denton Township, District of Cochrane; Ontario Department of Mines, Map P.28, scale 1:63 360.

Ginn, R.M., Savage, W.S., Thomson, R. and Thomson, J.E. 1964. Timmins-Kirklad Lake Sheet, Cochrane, Sudbury and Timiskaming District; Ontario Department of Mines, Map 2046, scale 1:253 440.

Harding, W.D and Berry L.G. 1938. Geology of the Keefer-Eldorado Area; Ontario Department of Mines, Annual Report 47, pt. 3, p. 1-26.

Hawley, J.E. 1926. Ogden, Bristol and Carscallen Townships, Cochrane District; Ontario Department of Mines, Annual Report 35, pt. 6., p. 1-36.

Heaman, L.M. 1988. A precise U-Pb zircon age for a Hearst dyke; *in* Geological Association of Canada-Mineralogical Association of Canada Annual Meeting, Program with Abstracts, v. 13, p. A53.

Hogg, N. 1946. Report on diamond drilling program, AuMo property, Aumo Porcupine Gold Mines, Ltd.; Timmins Resident Geologist's office, Denton Township, assessment file RGID# T-10. 6p.

Hughes, O.L. 1959. Surficail Geology of Smooth Rock and Iroquois Falls Map-Areas, Cochrane District, Ontario; Ph.D. dissertation, University of Kansas, Lawrence, 190p.

Jackson, S.L. and Fyon, J.A. 1991. The western Abitibi subprovince of Ontario; *in* Geology of Ontario, Ontario Geological Survey, Special Volume 4, Part 1, p.405-484.

Jensen, L.S. 1976. A new cation plot for classifying subalkalic volcanic rocks; Ontario Division of Mines, MP 66, 22p.

Jolly, W.T. 1974. Regional metamorphic zonation as an aid in study of Archean terrains, Abitibi region, Ontario; Canadian Mineralogist, v.12, p.499-508.

——— 1977. Metamorphic history of the Archean Abitibi belt: sample distribution and partial metamorphic zonation; *in* Report of Activities, Part A, Geological Survey of Canada, Paper 77-1A, p.191-196.

——— 1987. Metamorphic history of the Archean Abitibi belt; *in* Metamorphism in the Canadian Shield, Geological Survey of Canada, Paper 78-10. P.63-78.

Krogh, T.E., Corfu, F., Davis, D.W, Dunning, G.R., Heaman, L.M., Kamo, S.L., Machado, N., Greenhough, J.D., and Nakamura, E. 1987. Precise U-Pb isotopic ages of diabase dikes and mafic to ultramafic rocks using trace amounts of baddeleyite and zircon; *in* Mafic Dike Swarms, Geological Association o Canada, Special Paper 34, p.147-152.

Lesher, C.M., Goodwin, A.M., Campbell, I.H., and Gorton, M.P. 1986. Trace-element geochemistry of ore-associated and barren, felsic metavolcanic rocks in the Superior Province, Canada; Canadian Journal of Earth Science, v.23, p.222-237.

Ontario Geological Survey 1996. Timmins Area, Ontario airborne magnetic and electromagnetic surveys, processed data and derived products, Archean and Proterozoic "greenstone" belts; ERLIS Data set CD-ROM 1004, Ontario Geological Survey, Sudbury.

Ontario Geological Survey 1999. Single Master Gravity and Aeromagnetic Data for Ontario, Geosoft Format; ERLIS Data set CD-ROM 1036, Ontario Geological Survey, Sudbury.

Ontario Geological Survey 2001. Regional ground gravity survey from the Timmins Collaborative Gravity Survey Project; Ontario Geological Survey, Miscellaneous Release Data 79.

Ontario Geological Survey 2001b. Whole rock lithogeochemical data of prospective versus barren volcanic belts for volcanogenic massive sulphide (VMS) deposits, Superior province Ontario: Operation Treasure Hunt; Ontario Geological Survey, Miscellaneous Release Data 85.

Osmani, I.A. 1991. Proterozoic Mafic Dike Swarms in the Superior Province of Ontario; *in* Geology of Ontario, Ontario Geological Survey, Special Volume 4, Part 1, p.661-682.

Patsch, B.J.G. 1964. Report of diamond-drilling, Lucky Strike property; Lucky Strike Explorations Ltd.; Timmins Resident Geologist's office, Carscallen Township, assessment file AFRI# 42A05NE062, 9p.

Powell, W.G., Hodgson, C.J. and Carnichael, D.C. 1990. Tectono-metamorphic character of the Matachewan area, north-east Ontario; *in* Geoscience Research Grant Program, Summary of Research 1989-1990, Ontario Geological Survey, Miscellaneous Paper 150, p.56-65.

Prior, G.J., Gibson, H.L., Watkinson, D.H. and Cook, R.E. 1999. Anatomy, lithogeochemistry, and emplacement mechanisms for the QP Rhyolite, Kidd Creek Mine, Timmins, Ontario; *in* Economic Geology, Monograph 10, p.123-142.

Pyke, D.R. 1980. Geology of the Timmins Area, District of Cochrane; Ontario Geological Survey, Open File Report 5281, 396 p.

——— 1982. Geology of the Timmins Area, District of Cochrane; Ontario Geological Survey, Report 219, 141p.

Pyke, D. and Cunnison, K. 1997. Geological Interpretation, Timmins West Area; unpublished map, Prospectors Alliance Limited.

Ramsey, J.G. and Huber, M.I. 1987. The techniques of modern structural geology, volume 2: Folds and Fractures; Academic Press, Toronto, p.492.

Rollinson, H. 1993. Using geochemical data: evaluation, presentation, interpretation; Longman Singapore Publishers, Singapore, 352p.

Sun, S.S and McDonough, W.F. 1989. Chemical and isotopic systematics of oceanic basalts: Implications for mantle composition and processes; *in* Magmatism in ocean basins, Geological Society of London, Special Publication 42, p. 313-345.

Todd, E.W. 1923. Kenogamissi Lake Area, including Townships of Denton and Keefer; Ontario Department of Mines, Annual Report 32, pt. 3, p. 23-35.

Tucker, C.M. and Richard, J.A. 1983. Quaternary Geology of the Dana Lake Area, Cochrane, Timiskaming, and Sudbury Districts; Ontario Geological Survey, Map P.2582, scale 1:50 000.

Vaillancourt, C. 2000. Project Unit 00-011. New Geological Mapping and Compilation in the Timmins West Area – Bristol and Ogden Townships; *in* Summary of Field Work and Other Activities 2000, Ontario Geological Survey, Open File Report 6032, p.4-1 to 4-11.

Vaillancourt, C., Pickett, C.L. and Dinel, E. 2000. Precambrian geology, Timmins West-Bristol and Ogden townships; Ontario Geological Survey, Preliminary Map P.3436, scale 1:20 000.

This page left blank intentionally.

Appendix 1: Geochemical data for 149 rock samples taken from Denton and Carscallen townships

Abbreviations used in table to follow:
(#) – number reflects map unit designation (Map P. 3517, back pocket)
mv – mafic metavolcanic rock
fv – felsic metavolcanic rock
iv – intermediate metavolcanic rock
umv – ultramafic metavolcanic rock
fi – felsic intrusive rock
BIF – banded iron formation
CLP – Carlton Lake Pluton
KGC – Kamiskotia Gabbroic Complex
umi – ultramafic intrusive rock
sill – concordant intrusive
amph – amphibolite
gab – gabbro
pd – porphyritic dike
MD – Matachewan dike
gd – syntectonic granodiorite dike; sample for U/Pb geochronological analysis
ad – alkalic dike
mylonite – highly strained rock, protolith unknown
sed – metasedimentary rock
alt. – altered, extreme silica depletion

N.D. – not detected
LOI – loss on ignition

[1] Wavelength dispersive X-ray fluorescence (fused glass disk)
[2] Wavelength dispersive X-ray fluorescence (pressed pellet)
[3] Inductively coupled plasma emission mass spectrometry
[4] Lead fire assay
[5] Inductively coupled plasma atomic emission spectoscopy
[6] Cold vapour atomic fluorescence spectrometry

Sample #	01LAH-0002	01LAH-0003A	01LAH-0004A	01LAH-0004B	01LAH-0004C	01LAH-0006	01LAH-0008	01LAH-0010	01LAH-0012	01LAH-0026
UTM East	448285	456982	448897	449240	446394	452214	446394	449240	449240	449449
UTM North	5353025	5352684	5353817	5353944	5361939	5355772	5361939	5353944	5353944	5351880
Rock type	umi (12c)	fv (2)	fv (2)	iv (2)	mv (1)	iv (8)	mv (7)	fv (8)	CLP	mv (1)
[1]SiO2 (%)	33.84	71.87	79.99	66.01	48.71	49.87	41.87	44.1	63.82	50.65
[1]TiO2 (%)	0.03	0.15	0.07	0.32	0.94	0.92	0.5	0.61	0.58	1.22
[1]Al2O3 (%)	0.55	9.6	10.19	13.54	17.83	19.1	10.03	15.98	15.8	13.81
[1]Fe2O3 (%)	6.91	8.7	3.8	11.13	10.32	11.05	9.51	8.96	6.81	14.99
[1]MnO (%)	0.09	0.09	0.08	0.2	0.17	0.19	0.19	0.2	0.01	0.22
[1]MgO (%)	39.75	0.94	0.52	2.1	4.66	3.65	8.86	6.4	1.49	6.67
[1]CaO (%)	N.D.	5.18	2.61	3.15	11.42	9.65	9.5	10.69	0.2	7.77
[1]Na2O (%)	0.02	0.03	0.43	0.05	2.58	1.94	2.99	2.53	0.64	3.69
[1]K2O (%)	N.D.	0.09	0.94	0.89	0.04	0.03	0.01	0.18	4.98	0.61
[1]P2O5 (%)	N.D.	0.06	N.D.	0.09	0.06	0.05	0.05	0.04	0.13	0.08
LOI	18.01	3.07	1.64	3.07	3.05	3.6	16.42	10.43	4.39	0.94
TOTAL	99.15	99.77	100.28	100.55	99.78	100.04	99.93	100.12	98.85	100.65
[2]As (ppm)	29	31	N.D.	N.D.	23	N.D.	367	6	4627	N.D.
[2]Ag (ppm)	N.D.	N.D.	N.D.	N.D.	N.D.	N.D.	N.D.	N.D.	N.D.	N.D.
[2]Cr (ppm)	1553	63	10	14	415	178	1308	360	37	172
[2]Ni (ppm)	2958	4	3	14	143	177	311	245	14	50
[2]Co (ppm)	109	N.D.	N.D.	N.D.	59	70	54	53	16	53
[2]Sc (ppm)	N.D.	9	N.D.	11	56	54	39	41	N.D.	62
[2]V (ppm)	16	N.D.	N.D.	N.D.	342	349	228	248	72	467
[2]Cu (ppm)	8	33	N.D.	N.D.	191	115	73	25	37	94
[2]Pb (ppm)	N.D.	33	6	N.D.	15	N.D.	N.D.	N.D.	67	N.D.
[2]Bi (ppm)	N.D.	N.D.	N.D.	N.D.	N.D.	N.D.	N.D.	N.D.	N.D.	N.D.
[2]Zn (ppm)	39	202	49	150	96	69	76	67	86	115
[2]W (ppm)	N.D.	N.D.	N.D.	N.D.	N.D.	N.D.	N.D.	N.D.	N.D.	N.D.
[2]Mo (ppm)	N.D.	N.D.	N.D.	N.D.	N.D.	N.D.	N.D.	N.D.	N.D.	N.D.
[2]Rb (ppm)	1.14	143.4	28.07	25.07	0.72	0.67	0.33	5.07	143.4	16.33
[2]Cs (ppm)	0.20	2.73	1.45	1.04	0.12	0.08	0.12	0.14	2.73	0.79
[2]Ba (ppm)	N.D.	74	173	436	46	N.D.	N.D.	38	673	156
[2]Sr (ppm)	N.D.	146	143	118	229	151	63	82	31	102
[2]Ga (ppm)	3	33	23	31	25	29	16	19	29	25
[3]Ta (ppm)	N.D.	0.4	0.74	0.7	N.D.	N.D.	N.D.	N.D.	0.4	N.D.
[2]Nb (ppm)	0.08	5.63	13.36	11.99	2.95	2.45	2	1.49	5.63	3.21
[3]Hf (ppm)	N.D.	1.7	4.83	8.62	1.72	1.48	1.23	0.87	1.7	2.01
[2]Zr (ppm)	N.D.	140	146	387	55	49	43	31	210	70
[3]Th (ppm)	N.D.	4.59	3.34	2.14	0.38	0.24	0.4	0.1	4.59	0.37
[3]U (ppm)	0.02	0.87	0.8	0.56	0.09	0.08	0.11	0.03	0.87	0.10
[2]Sb (ppm)	N.D.	N.D.	N.D.	N.D.	N.D.	N.D.	N.D.	N.D.	N.D.	N.D.
[2]Se (ppm)	N.D.	N.D.	N.D.	N.D.	N.D.	N.D.	N.D.	N.D.	N.D.	N.D.
[2]Sn (ppm)	N.D.	8	N.D.	N.D.	9	N.D.	N.D.	N.D.	N.D.	N.D.
[3]La (ppm)	N.D.	18.93	38.44	15.32	3.33	2.56	3.1	1.82	18.93	4.08
[3]Ce (ppm)	0.31	43.01	84.64	40.64	9.52	7.21	7.44	5.15	43.01	10.69
[3]Pr (ppm)	0.04	5.21	13.45	6.08	1.54	1.18	1.01	0.84	5.21	1.63
[3]Nd (ppm)	N.D.	18.71	58.03	25.7	7.11	6.37	4.68	4.1	18.71	8.38
[3]Sm (ppm)	0.05	2.86	15.66	6.65	2.3	2.05	1.38	1.33	2.86	2.78
[3]Eu (ppm)	0.02	0.38	2.18	1.93	0.86	0.84	0.46	0.52	0.38	0.84
[3]Gd (ppm)	0.06	1.9	17.35	7.41	2.91	2.78	1.95	1.75	1.9	3.70
[3]Tb (ppm)	0.02	0.28	2.64	1.41	0.5	0.5	0.33	0.31	0.28	0.66
[3]Dy (ppm)	0.09	1.59	13.62	8.69	3.41	3.17	2.22	2	1.59	4.34
[3]Ho (ppm)	0.02	0.3	2.57	1.97	0.73	0.66	0.47	0.44	0.3	0.96
[3]Er (ppm)	0.06	0.87	6.29	5.64	2.1	1.97	1.46	1.25	0.87	2.85
[3]Tm (ppm)	0.01	0.13	0.92	0.93	0.32	0.28	0.22	0.2	0.13	0.44
[3]Yb (ppm)	0.05	0.88	5.33	5.85	2.09	1.77	1.36	1.21	0.88	2.94
[3]Lu (ppm)	0.011	0.125	0.84	0.987	0.32	0.294	0.205	0.194	0.125	0.453
[3]Y (ppm)	0.53	7.68	65.04	47.91	18.82	18.43	12.67	11.18	7.68	23.97
[1]CO2 (%)	0.08	N.D.	N.D.	0.6						
[1]S (%)	2.28	0.01	N.D.	0.02			14.4	6.8	N.D.	
[5]Hg (ppb)							0.02	0.01	3.47	
[4]Ag (oz/ton)	N.D.									
[4]Au (oz/ton)	N.D.								N.D.	
[5]Au (ppb)									0.02	
[5]Pd (ppb)										
[5]Pt (ppb)										

Sample #	01LAH-0029A	01LAH-0029B	01LAH-0032	01LAH-0034	01LAH-0041A	01LAH-0041B	01LAH-0041C	01LAH-0042	01LAH-0043A	01LAH-0043B
UTM East	448285	452876	449421	448872	446485	448649	452645	449518	453196	447243
UTM North	5353025	5351937	5351960	5352638	5361140	5361933	5358676	5364172	5351936	5349138
Rock type	mv (1)	fv (2)	mv (1)	mv (1)	fv (2)	BIF	mv (1)	fv (2)	fv (2)	fv (2)
[1]SiO2 (%)	49.6	72.59	46.48	53.39	68.96	85	49.25	65.5	69.53	65.68
[1]TiO2 (%)	1.08	0.48	1.43	0.62	0.9	0.01	0.97	0.39	0.49	0.44
[1]Al2O3 (%)	17.06	12.3	15.9	14.6	17.21	0.6	14.79	12.61	16.01	14.13
[1]Fe2O3 (%)	12.32	4.52	17.09	9.76	2.86	12.87	18.54	4.28	3.09	8.41
[1]MnO (%)	0.24	0.08	0.23	0.24	0.04	0.19	0.43	0.12	0.09	0.34
[1]MgO (%)	3.28	0.42	5.33	4.84	1.77	1.88	7.71	1.15	0.75	1.5
[1]CaO (%)	8.59	2.05	10.99	5.33	0.76	0.08	2.39	4.67	0.95	1.48
[1]Na2O (%)	2.37	3.36	2.25	3.53	0.17	N.D.	1.22	3.03	3.72	4.74
[1]K2O (%)	1.18	1.98	0.19	0.94	4.96	0.02	0.45	2.2	3.26	0.63
[1]P2O5 (%)	0.09	0.07	0.1	0.09	0.06	N.D.	0.06	0.08	0.1	0.09
LOI	4.66	1.88	1.33	7.38	2.9	0.67	5.03	5.91	2.19	2.44
TOTAL	100.45	99.73	101.32	100.73	100.6	101.08	100.84	99.94	100.19	99.87
[2]As (ppm)	N.D.	N.D.	N.D.	N.D.	8	10	4	N.D.	N.D.	N.D.
[2]Ag (ppm)	N.D.	N.D.	N.D.	N.D.	N.D.	N.D.	N.D.	N.D.	N.D.	N.D.
[2]Cr (ppm)	297	10	107	235	45	18	410	11	N.D.	14
[2]Ni (ppm)	52	N.D.	60	100	7	12	144	N.D.	N.D.	N.D.
[2]Co (ppm)	53	N.D.	56	28	N.D.	N.D.	42	N.D.	N.D.	N.D.
[2]Sc (ppm)	50	9	53	30	12	7	40	13	10	9
[2]V (ppm)	409	8	479	193	137	16	423	N.D.	N.D.	N.D.
[2]Cu (ppm)	148	8	101	N.D.	5	14	59	12	3	7
[2]Pb (ppm)	7	N.D.	N.D.	N.D.	N.D.	N.D.	N.D.	N.D.	N.D.	N.D.
[2]Bi (ppm)	N.D.	N.D.	N.D.	N.D.	N.D.	N.D.	N.D.	N.D.	N.D.	N.D.
[2]Zn (ppm)	128	35	130	63	41	30	124	31	41	117
[2]W (ppm)	N.D.	N.D.	N.D.	N.D.	N.D.	N.D.	N.D.	N.D.	N.D.	N.D.
[2]Mo (ppm)	N.D.	N.D.	N.D.	N.D.	N.D.	N.D.	N.D.	N.D.	N.D.	N.D.
[2]Rb (ppm)	50.26	43.61	7.07	32.13	110.61	0.77	7.83	50.03	56.95	16.29
[2]Cs (ppm)	2.30	0.82	0.14	0.47	2.06	0.31	1.02	0.89	1.32	0.42
[2]Ba (ppm)	291	460	71	211	395	N.D.	64	372	729	160
[2]Sr (ppm)	166	76	309	112	32	N.D.	40	67	78	104
[2]Ga (ppm)	25	27	32	22	29	N.D.	29	23	30	28
[2]Ta (ppm)	N.D.	1.26	N.D.	0.31	0.6	N.D.	N.D.	0.78	0.96	0.89
[2]Nb (ppm)	3.18	19.85	4.07	4.24	9.46	0.15	2.47	11.62	14.32	12.8
[2]Hf (ppm)	1.91	11.98	2.34	2.47	5.46	0.1	1.35	7.49	8.4	7.46
[2]Zr (ppm)	62	496	78	99	209	5	46	288	360	299
[2]Th (ppm)	0.35	4.68	0.37	1.48	2.44	N.D.	0.25	4.15	4.97	4.47
[2]U (ppm)	0.10	1.24	0.09	0.36	0.57	0.1	0.24	0.72	1.15	1.06
[2]Sb (ppm)	N.D.	N.D.	N.D.	N.D.	N.D.	N.D.	N.D.	N.D.	N.D.	N.D.
[2]Se (ppm)	N.D.	N.D.	N.D.	N.D.	N.D.	N.D.	N.D.	N.D.	N.D.	N.D.
[2]Sn (ppm)	N.D.	N.D.	N.D.	N.D.	N.D.	N.D.	N.D.	N.D.	N.D.	N.D.
[3]La (ppm)	3.90	33.95	5.00	9.54	15.15	2.14	59.25	28.46	35.16	29.67
[3]Ce (ppm)	10.07	75.81	13.02	20.15	35.46	3.83	121.08	61.08	75.28	65.52
[3]Pr (ppm)	1.54	10.3	2.02	2.54	4.73	0.5	16.44	8.16	9.85	8.37
[3]Nd (ppm)	7.34	42.5	10.16	10.48	18.87	2.21	68.82	31.6	38.67	32.92
[3]Sm (ppm)	2.25	9.95	3.26	2.38	4.43	0.52	11.25	6.63	7.89	6.92
[3]Eu (ppm)	0.92	2.11	1.18	0.81	0.73	0.26	1.71	1.4	1.48	1.38
[3]Gd (ppm)	2.85	10.29	4.39	2.47	3.92	0.62	5.69	6.52	8.1	7.31
[3]Tb (ppm)	0.52	1.66	0.78	0.40	0.64	0.11	0.52	1.09	1.34	1.21
[3]Dy (ppm)	3.27	10.37	5.06	2.42	3.82	0.76	2.38	6.77	7.89	7.75
[3]Ho (ppm)	0.74	2.19	1.10	0.51	0.79	0.19	0.45	1.52	1.67	1.65
[3]Er (ppm)	2.08	6.46	3.24	1.50	2.27	0.61	1.2	4.32	4.92	4.84
[3]Tm (ppm)	0.33	0.97	0.50	0.22	0.32	0.09	0.17	0.68	0.74	0.76
[3]Yb (ppm)	2.14	6.2	3.23	1.45	2.08	0.57	1.05	4.37	4.56	4.98
[3]Lu (ppm)	0.346	1.012	0.531	0.233	0.309	0.101	0.16	0.717	0.744	0.785
[3]Y (ppm)	19.00	57.42	28.10	13.39	19.4	6.07	11.12	38.45	45.6	44.86
[1]CO2 (%)					0.05	N.D.	N.D.			
[1]S (%)					0.01	0.38	0.2			
[5]Hg (ppb)										
[4]Ag (oz/ton)					N.D.	0.8	N.D.			
[4]Au (oz/ton)					N.D.	N.D.	N.D.			
[5]Au (ppb)										
[5]Pd (ppb)										
[5]Pt (ppb)										

Sample #	01LAH-0044A	01LAH-0044B	01LAH-0045A	01LAH-0045B	01LAH-0046	01LAH-0048A	01LAH-0048B	01LAH-0051	01LAH-0051B	01LAH-0051C
UTM East	448285	447243	449015	451407	449518	449708	454447	452645	448285	449522
UTM North	5353025	5349138	5352625	5358425	5364172	5365040	5365891	5358676	5353025	5362870
Rock type	mv (1)	fv (2)	mv (1)	KGC	fv (2)	fv (2)	iv (2)	mv (1)	mv (1)	mv (1)
[1]SiO2 (%)	48.37	67.99	55.61	48.44	75	73.36	64.17	36.12	49.44	56.2
[1]TiO2 (%)	1.04	0.47	0.79	1.15	0.11	0.12	0.5	0.2	1.36	1.51
[1]Al2O3 (%)	16.72	15.17	15.75	13.76	13.31	11.42	15.04	5.02	14.32	13.92
[1]Fe2O3 (%)	12.39	4.22	9.12	12.19	3.91	3.73	5.75	39.1	14.51	12.27
[1]MnO (%)	0.18	0.08	0.21	0.18	0.08	0.06	0.1	2.35	0.56	0.24
[1]MgO (%)	5.91	1.11	3.11	7.86	1	0.99	2.68	4.84	5.68	2.75
[1]CaO (%)	4.38	2.25	11.91	8.42	2.33	2.13	4.3	4.78	7.43	5.13
[1]Na2O (%)	4.68	0.74	0.34	3.04	0.46	2.25	3.8	0.05	4.43	3.37
[1]K2O (%)	0.2	3.78	0.21	0.12	2.6	1.98	1.56	1.16	0.22	0.31
[1]P2O5 (%)	0.09	0.09	0.07	0.23	N.D.	0.04	0.09	0.04	0.12	0.25
LOI	7.04	4.82	2.75	4.32	2.21	3.2	1.71	6.26	2.98	3.67
TOTAL	100.98	100.72	99.87	99.69	101.02	99.29	99.7	99.93	101.04	99.62
[2]As (ppm)	9	7	9	N.D.	N.D.	N.D.	2	N.D.	29	4
[2]Ag (ppm)	N.D.	N.D.	N.D.	N.D.	N.D.	N.D.	N.D.	N.D.	N.D.	N.D.
[2]Cr (ppm)	135	12	248	592	11	4	105	101	200	37
[2]Ni (ppm)	51	N.D.	129	210	N.D.	14	37	38	55	10
[2]Co (ppm)	47	N.D.	46	52	N.D.	N.D.	19	N.D.	46	27
[2]Sc (ppm)	52	13	35	34	N.D.	N.D.	18	10	53	32
[2]V (ppm)	368	8	267	239	N.D.	N.D.	101	62	437	256
[2]Cu (ppm)	90	5	91	83	N.D.	N.D.	30	30	4	31
[2]Pb (ppm)	N.D.	N.D.	N.D.	N.D.	N.D.	N.D.	N.D.	N.D.	7	N.D.
[2]Bi (ppm)	N.D.	N.D.	N.D.	N.D.	N.D.	N.D.	N.D.	N.D.	N.D.	N.D.
[2]Zn (ppm)	138	61	89	103	92	118	80	82	76	96
[2]W (ppm)	N.D.	N.D.	N.D.	N.D.	N.D.	24	N.D.	N.D.	N.D.	N.D.
[2]Mo (ppm)	N.D.	N.D.	N.D.	N.D.	4	24	N.D.	N.D.	N.D.	N.D.
[2]Rb (ppm)	5.95	69.28	5.89	2.51	44.03	47.64	40.49	51.07	3.48	8.40
[2]Cs (ppm)	0.13	1.13	0.16	0.10	1.25	1.32	0.97	>5.00	0.18	0.53
[2]Ba (ppm)	80	502	72	64	362	665	310	96	83	107
[2]Sr (ppm)	87	51	242	522	80	29	148	56	309	242
[2]Ga (ppm)	24	28	25	25	35	28	23	8	27	28
[3]Ta (ppm)	N.D.	0.92	N.D.	N.D.	1.93	1.67	0.54	N.D.	N.D.	0.58
[2]Nb (ppm)	3.22	13.75	2.99	2.45	28.64	23.73	7.26	1.76	4.65	9.24
[3]Hf (ppm)	2.10	7.89	1.78	2.32	9.86	11.35	4.24	0.93	2.91	5.13
[2]Zr (ppm)	71	301	64	68	271	313	180	35	93	185
[3]Th (ppm)	0.51	4.44	0.94	0.97	7.29	5.87	2.68	0.59	0.71	1.84
[3]U (ppm)	0.15	1.42	0.25	0.20	2.3	12.98	0.64	0.31	0.19	0.50
[2]Sb (ppm)	N.D.	N.D.	N.D.	N.D.	N.D.	N.D.	N.D.	N.D.	N.D.	N.D.
[2]Se (ppm)	N.D.	N.D.	N.D.	N.D.	N.D.	N.D.	N.D.	N.D.	N.D.	N.D.
[2]Sn (ppm)	N.D.	N.D.	N.D.	N.D.	N.D.	N.D.	N.D.	N.D.	N.D.	N.D.
[3]La (ppm)	4.47	33.56	7.04	19.98	49.86	46.75	18.92	6.49	6.49	13.47
[3]Ce (ppm)	11.04	71.06	15.58	49.19	114.54	102.04	40.6	12.89	16.62	32.40
[3]Pr (ppm)	1.69	9.61	2.02	7.10	17.86	15.33	4.88	1.53	2.46	4.55
[3]Nd (ppm)	7.85	37.65	8.65	29.10	76.98	65.15	19.2	6.3	11.26	19.42
[3]Sm (ppm)	2.33	7.69	2.18	5.49	19.8	17.87	3.79	1.41	3.50	5.06
[3]Eu (ppm)	0.83	1.52	0.84	1.78	3.1	2.84	0.94	0.74	1.40	1.62
[3]Gd (ppm)	3.05	8.05	2.82	4.44	22.28	26.98	3.62	1.62	4.49	5.60
[3]Tb (ppm)	0.57	1.29	0.46	0.65	4	>5.00	0.59	0.28	0.82	1.00
[3]Dy (ppm)	3.75	8.36	3.08	3.60	24.77	>40.00	3.56	1.83	5.21	6.35
[3]Ho (ppm)	0.84	1.71	0.65	0.73	5.46	>10.00	0.73	0.41	1.16	1.43
[3]Er (ppm)	2.39	5.14	1.88	1.95	15.75	>20.00	2.17	1.29	3.22	4.18
[3]Tm (ppm)	0.36	0.77	0.27	0.29	2.51	>5.00	0.31	0.19	0.51	0.65
[3]Yb (ppm)	2.18	4.85	1.65	1.74	15.79	>20.00	2.06	1.23	3.16	4.11
[3]Lu (ppm)	0.325	0.765	0.263	0.272	2.458	>5.000	0.335	0.203	0.527	0.645
[3]Y (ppm)	21.44	47.96	17.83	18.79	128.62	>200.00	20.08	13.51	28.67	35.85
[1]CO2 (%)								3.11		
[1]S (%)								0.19		
[5]Hg (ppb)										
[4]Ag (oz/ton)								N.D.		
[4]Au (oz/ton)								N.D.		
[5]Au (ppb)				N.D.				N.D.		N.D.
[5]Pd (ppb)				N.D.				N.D.		N.D.
[5]Pt (ppb)				N.D.				N.D.		N.D.

Sample #	01LAH-0051D	01LAH-0056A	01LAH-0056B	01LAH-0057	01LAH-0059A	01LAH-0059B	01LAH-0060A	01LAH-0060C	01LAH-0061A	01LAH-0061B
UTM East	450430	454147	454202	449081	455675	447682	450509	449081	447694	455869
UTM North	5363746	5365747	5365378	5352203	5364576	5350313	5363736	5352203	5350372	5366521
Rock type	fv (2)	iv (2)	iv (2)	mv (1)	fv (2)	fv (2)	fv (2)	mv (1)	fv (2)	BIF
[1]SiO2 (%)	75.52	59.65	70.08	44.53	76.97	69.22	73.93	58.63	62.87	78.93
[1]TiO2 (%)	0.13	1.19	0.3	0.56	0.2	0.29	0.2	0.63	1.15	0.03
[1]Al2O3 (%)	12.93	18.32	16.07	13.81	12.24	15.87	12.24	15.33	17.42	1.32
[1]Fe2O3 (%)	2.24	6.26	2.96	22.86	2.27	2.96	3.23	6.31	4.66	15.27
[1]MnO (%)	0.04	0.11	0.05	1	0.04	0.05	0.05	0.17	0.13	0.71
[1]MgO (%)	0.87	1.35	1.72	4.58	0.24	1.7	0.4	3.77	1.12	2.22
[1]CaO (%)	0.35	5.43	0.62	7.9	1.08	0.6	0.89	4.28	6.24	0.98
[1]Na2O (%)	4.6	4.45	2.03	2.52	2.31	2.02	0.34	5.44	3.21	0.03
[1]K2O (%)	1.64	0.68	3.99	0.71	2.56	3.99	5.3	0.73	1.31	0.03
[1]P2O5 (%)	N.D.	0.15	0.1	0.08	0.02	0.1	0.02	0.09	0.15	0.02
LOI	1.28	1.4	2.46	1.55	1.42	2.49	2.28	5.29	2.02	0.67
TOTAL	99.6	98.97	100.38	100.1	99.37	99.29	98.89	100.66	100.28	100.2
[2]As (ppm)	N.D.	N.D.	16	N.D.	N.D.	3	N.D.	N.D.	7	11
[2]Ag (ppm)	N.D.	N.D.	N.D.	N.D.	N.D.	N.D.	N.D.	N.D.	N.D.	N.D.
[2]Cr (ppm)	9	208	209	225	9	18	4	258	8	25
[2]Ni (ppm)	N.D.	81	61	102	N.D.	2	N.D.	98	21	34
[2]Co (ppm)	N.D.	50	40	23	N.D.	N.D.	N.D.	23	23	N.D.
[2]Sc (ppm)	N.D.	39	29	26	N.D.	N.D.	N.D.	22	21	6
[2]V (ppm)	N.D.	283	248	163	N.D.	30	N.D.	146	164	18
[2]Cu (ppm)	N.D.	59	93	27	N.D.	13	4	17	3	14
[2]Pb (ppm)	N.D.	N.D.	N.D.	6	N.D.	N.D.	N.D.	N.D.	8	N.D.
[2]Bi (ppm)	N.D.	N.D.	N.D.	N.D.	N.D.	N.D.	N.D.	N.D.	N.D.	N.D.
[2]Zn (ppm)	33	39	31	67	38	50	38	135	62	163
[2]W (ppm)	N.D.	N.D.	N.D.	N.D.	N.D.	N.D.	N.D.	N.D.	N.D.	N.D.
[2]Mo (ppm)	N.D.	N.D.	N.D.	N.D.	N.D.	N.D.	N.D.	N.D.	N.D.	N.D.
[2]Rb (ppm)	35.34	26.05	84.41	18.96	56.71	111.15	90.21	16.32	39.84	1.01
[2]Cs (ppm)	0.52	0.95	1.6	1.76	1.23	1.83	2.19	0.28	1.72	0.47
[2]Ba (ppm)	550	208	299	149	458	831	607	137	605	N.D.
[2]Sr (ppm)	70	201	134	171	90	143	26	135	196	7
[2]Ga (ppm)	32	29	26	20	28	26	27	20	27	N.D.
[3]Ta (ppm)	2.04	0.32	N.D.	0.30	0.68	0.7	0.69	0.34	0.46	N.D.
[2]Nb (ppm)	33.33	5.84	4.11	4.11	9.64	8.07	9.62	4.56	7.96	0.48
[3]Hf (ppm)	12.52	2.56	2.2	2.35	7.16	4.95	7.83	2.78	3.63	0.19
[2]Zr (ppm)	331	102	87	97	296	192	293	103	151	7
[3]Th (ppm)	7.98	0.8	1.19	1.44	3.59	3.78	4.26	1.19	1.19	0.08
[3]U (ppm)	1.64	0.24	0.3	0.45	0.64	1.16	0.5	0.44	0.26	0.17
[2]Sb (ppm)	N.D.	N.D.	N.D.	N.D.	N.D.	N.D.	N.D.	N.D.	N.D.	N.D.
[2]Se (ppm)	N.D.	N.D.	N.D.	N.D.	N.D.	N.D.	N.D.	N.D.	N.D.	N.D.
[2]Sn (ppm)	N.D.	N.D.	N.D.	N.D.	N.D.	N.D.	N.D.	N.D.	N.D.	N.D.
[3]La (ppm)	50.69	8.73	8.09	12.14	29.25	23.01	21.69	8.94	15.26	4.89
[3]Ce (ppm)	108.2	21.45	18.39	24.38	59.54	41.56	48.35	19.15	34.4	10.84
[3]Pr (ppm)	16.19	2.98	2.4	2.94	7.52	4.61	6.56	2.48	4.65	1.4
[3]Nd (ppm)	67.61	12.91	9.44	11.65	27.61	15.64	26	9.88	18.86	5.71
[3]Sm (ppm)	16.56	3.22	2.31	2.56	5.9	2.84	6.35	2.17	3.99	1.34
[3]Eu (ppm)	1.94	1.15	0.9	1.07	1.25	0.78	1.56	0.66	1.31	1.15
[3]Gd (ppm)	16.68	3.58	2.53	2.86	6.05	2.52	7.09	2.24	3.78	1.48
[3]Tb (ppm)	2.94	0.56	0.46	0.47	0.97	0.36	1.24	0.35	0.59	0.23
[3]Dy (ppm)	17.89	3.48	2.92	2.90	6.2	2.18	7.49	2.20	3.42	1.48
[3]Ho (ppm)	3.85	0.71	0.62	0.62	1.36	0.44	1.64	0.48	0.68	0.34
[3]Er (ppm)	10.79	1.95	1.73	1.94	3.98	1.25	4.7	1.36	1.93	1
[3]Tm (ppm)	1.69	0.28	0.26	0.29	0.61	0.18	0.74	0.20	0.29	0.16
[3]Yb (ppm)	10.59	1.75	1.59	1.94	3.82	1.21	4.78	1.27	1.85	1.02
[3]Lu (ppm)	1.647	0.255	0.243	0.303	0.619	0.189	0.775	0.218	0.29	0.175
[3]Y (ppm)	85.73	18.52	16.44	19.26	36.11	13.49	40.53	11.74	18.53	9.48
[1]CO2 (%)										
[1]S (%)										
[5]Hg (ppb)										N.D
[4]Ag (oz/ton)						N.D.	N.D.			0.03
[4]Au (oz/ton)						N.D.	N.D.			
[5]Au (ppb)										
[5]Pd (ppb)										
[5]Pt (ppb)										

Sample #	01LAH-0065	01LAH-0066	01LAH-0069A	01LAH-0069B	01LAH-0069C	01LAH-0069D	01LAH-0074	01LAH-0077A	01LAH-0077B	01LAH-0078
UTM East	448625	448625	455049	452447	450356	450286	448560	447054	447963	452110
UTM North	5362831	5362831	5352209	5349452	5351149	5351578	5362862	5363382	5363286	5356455
Rock type	KGC	KGC	mv (1) sill	KGC	fv (2)	iv (2)	mv (1)	amph (12b)	amph (12b)	mv (7)
[1]SiO2 (%)	84.33	74.01	46.34	47.08	75.99	68.53	55.29	48.62	51.83	49.85
[1]TiO2 (%)	0.14	0.02	0.75	0.73	0.07	0.32	0.04	0.54	0.74	0.68
[1]Al2O3 (%)	5.73	0.59	15.82	16.25	13.67	14.37	1.04	12.87	15.22	15.06
[1]Fe2O3 (%)	4.91	20.57	11.05	11.11	2.18	5.78	29.28	11.36	11.91	12.29
[1]MnO (%)	0.08	0.2	0.18	0.18	0.02	0.09	0.52	0.18	0.23	0.26
[1]MgO (%)	0.92	2.05	8.6	7.15	0.21	0.97	2.94	10.86	7.12	7.42
[1]CaO (%)	0.43	3	11.14	12.72	2.37	5.61	3.36	11.98	11.15	10.95
[1]Na2O (%)	0.45	0.06	0.85	0.86	4.44	1.98	0.03	1.51	1.83	1.88
[1]K2O (%)	1.01	0.06	0.14	0.03	0.75	0.26	0.16	0.22	0.16	0.31
[1]P2O5 (%)	0.04	0.06	0.05	0.05	N.D.	0.1	0.01	0.03	0.05	0.04
LOI	1.86	0.36	3.6	4.26	1.2	1.68	7.52	1.44	0.64	1.53
TOTAL	99.89	100.98	98.53	100.41	100.92	99.68	100.19	99.62	100.88	100.28
[2]As (ppm)	4	N.D.	9	N.D.	N.D.	N.D.	N.D.	N.D.	N.D.	N.D.
[2]Ag (ppm)	N.D.	N.D.	N.D.	N.D.	N.D.	N.D.	N.D.	N.D.	N.D.	N.D.
[2]Cr (ppm)	22	23	255	169	9	16	90	721	201	367
[2]Ni (ppm)	N.D.	26	163	146	N.D.	N.D.	122	136	51	84
[2]Co (ppm)	N.D.	N.D.	59	49	N.D.	N.D.	25	56	44	51
[2]Sc (ppm)	N.D.	N.D.	52	40	N.D.	15	9	70	67	65
[2]V (ppm)	5	14	282	251	N.D.	N.D.	35	316	358	343
[2]Cu (ppm)	16	87	72	52	N.D.	N.D.	182	120	120	69
[2]Pb (ppm)	6	N.D.	N.D.	N.D.	N.D.	N.D.	N.D.	N.D.	N.D.	N.D.
[2]Bi (ppm)	N.D.	N.D.	N.D.	N.D.	N.D.	N.D.	N.D.	N.D.	N.D.	N.D.
[2]Zn (ppm)	117	79	94	124	30	78	154	63	81	77
[2]W (ppm)	N.D.	N.D.	N.D.	N.D.	N.D.	N.D.	N.D.	N.D.	N.D.	N.D.
[2]Mo (ppm)	N.D.	N.D.	N.D.	N.D.	N.D.	N.D.	N.D.	N.D.	N.D.	N.D.
[2]Rb (ppm)	34.12	1.74	4.75	0.36	21.4	7.73	7.85	5.56	2.72	9.43
[2]Cs (ppm)	0.66	0.4	0.38	0.04	1.17	0.3	3.5	0.2	0.07	0.2
[2]Ba (ppm)	383	37	44	36	280	76	49	56	67	143
[2]Sr (ppm)	24	3	167	181	94	139	3	73	73	83
[2]Ga (ppm)	8	N.D.	23	22	30	31	5	17	24	20
[3]Ta (ppm)	N.D.	N.D.	N.D.	N.D.	1.16	0.96	N.D.	N.D.	N.D.	N.D.
[2]Nb (ppm)	3.35	0.2	2.28	2.5	17.84	15.4	0.43	1.22	1.72	1.63
[3]Hf (ppm)	1.49	0.2	1.33	1.33	6.57	8.87	0.24	0.92	1.24	1.15
[2]Zr (ppm)	47	11	43	43	159	288	12	28	41	37
[3]Th (ppm)	3.71	0.12	0.25	0.32	3.74	3.32	0.11	0.13	0.2	0.18
[3]U (ppm)	0.77	0.04	0.06	0.08	0.86	0.72	0.16	0.04	0.05	0.05
[2]Sb (ppm)	N.D.	N.D.	N.D.	N.D.	N.D.	N.D.	N.D.	N.D.	N.D.	N.D.
[2]Se (ppm)	N.D.	N.D.	N.D.	N.D.	N.D.	N.D.	N.D.	N.D.	N.D.	N.D.
[2]Sn (ppm)	N.D.	N.D.	N.D.	N.D.	N.D.	N.D.	N.D.	N.D.	N.D.	N.D.
[3]La (ppm)	16.58	1.82	3.31	4.06	21.84	14.29	1.37	2.42	2.35	2.08
[3]Ce (ppm)	35.34	3.99	8.35	10.18	53.61	38.24	3.11	4.86	6.48	5.72
[3]Pr (ppm)	4.22	0.52	1.27	1.5	7.56	5.54	0.43	0.86	1.05	0.96
[3]Nd (ppm)	15.62	2.22	6.12	7.32	34.09	24.53	2.05	4.38	5.36	4.77
[3]Sm (ppm)	3.28	0.56	1.92	2.16	9.74	6.76	0.58	1.42	1.83	1.68
[3]Eu (ppm)	1.26	0.14	0.76	0.87	1.79	2.04	0.3	0.5	0.63	0.59
[3]Gd (ppm)	3.22	0.71	2.61	2.56	11.59	8.41	0.88	1.97	2.44	2.33
[3]Tb (ppm)	0.5	0.12	0.45	0.46	2.09	1.51	0.16	0.34	0.48	0.42
[3]Dy (ppm)	3.23	0.77	2.99	2.91	13.17	10.23	1.16	2.5	3.24	2.87
[3]Ho (ppm)	0.68	0.17	0.64	0.62	2.83	2.24	0.27	0.54	0.71	0.64
[3]Er (ppm)	1.95	0.54	1.88	1.76	8.53	6.91	0.87	1.62	2.21	2.06
[3]Tm (ppm)	0.31	0.08	0.28	0.26	1.32	1.08	0.13	0.25	0.34	0.32
[3]Yb (ppm)	1.83	0.51	1.67	1.55	8.51	7.11	0.86	1.66	2.23	2.02
[3]Lu (ppm)	0.298	0.077	0.267	0.264	1.333	1.123	0.151	0.265	0.351	0.33
[3]Y (ppm)	18.94	5.26	17.98	16.34	81.55	62.58	8.19	14.54	18.72	17.59
[1]CO2 (%)										
[1]S (%)										
[5]Hg (ppb)										
[4]Ag (oz/ton)	N.D.	N.D.					N.D.			
[4]Au (oz/ton)	N.D.	N.D.					N.D.			
[5]Au (ppb)	N.D.	N.D.					21.61	N.D.		
[5]Pd (ppb)	N.D.	N.D.					N.D.	N.D.		
[5]Pt (ppb)	N.D.	N.D.					N.D.	N.D.		

Sample #	01LAH-0081B	01LAH-0083	01LAH-0085	01LAH-0092	01LAH-0093	01LAH-0096	01LAH-0097	01LAH-0102A	01LAH-0102B	01LAH-0103B
UTM East	446456	447882	446456	447882	452928	448819	451724	447675	447675	448655
UTM North	5362885	5362586	5362885	5362586	5349603	5352596	5356908	5362522	5362522	5362551
Rock type	umv (6)	KGC	KGC	mv (1)	CLP	CLP	CLP -pd	umv (6)	gab (12a)	mv (7)
[1]SiO2 (%)	45.06	47.71	62.36	41.21	65.65	64.93	65.77	45.56	46.22	53.42
[1]TiO2 (%)	2.16	0.81	0.58	0.86	0.37	0.37	0.44	0.27	1.91	1.29
[1]Al2O3 (%)	16.43	15.57	14.73	16.11	16.99	7.72	16.58	6.15	15	13.52
[1]Fe2O3 (%)	15.04	12.62	9.43	14.96	3	14.23	3.41	10.54	16.02	13.63
[1]MnO (%)	0.19	0.19	0.12	0.23	0.04	0.03	0.03	0.15	0.2	0.23
[1]MgO (%)	3.81	7.36	1.89	10.99	1.16	1.16	1.27	24.2	6.84	7.39
[1]CaO (%)	3.96	11.21	4.59	8.83	3.27	0.27	2.54	7.67	7.73	3.62
[1]Na2O (%)	6.15	1.13	2.6	1.81	5.6	N.D.	1.86	0.04	3.5	1.67
[1]K2O (%)	0.29	0.11	0.69	0.14	1.62	1.54	4.11	N.D.	0.03	0.29
[1]P2O5 (%)	0.16	0.05	0.09	0.05	0.1	0.21	0.11	0.01	0.14	0.09
LOI	5.38	2.79	2.84	3.79	1.79	5.66	3.94	5.86	2.79	5.87
TOTAL	98.64	99.55	99.92	98.97	99.58	94.31	100.06	100.44	100.4	101.02
[2]As (ppm)	1398	35	N.D.	N.D.	N.D.	159	6	36	N.D.	N.D.
[2]Ag (ppm)	N.D.	N.D.	N.D.	N.D.	N.D.	109	N.D.	N.D.	N.D.	N.D.
[2]Cr (ppm)	115	390	13	472	20	25	18	3153	135	255
[2]Ni (ppm)	92	148	N.D.	185	5	239	4	1439	103	38
[2]Co (ppm)	58	53	N.D.	58	N.D.	47	N.D.	102	64	48
[2]Sc (ppm)	42	58	14	54	6	N.D.	6	35	38	45
[2]V (ppm)	431	318	26	345	49	39	60	189	385	407
[2]Cu (ppm)	219	90	88	140	3	30855	76	11	107	116
[2]Pb (ppm)	N.D.	N.D.	N.D.	N.D.	N.D.	109	N.D.	N.D.	N.D.	N.D.
[2]Bi (ppm)	N.D.	N.D.	N.D.	N.D.	N.D.	81	N.D.	N.D.	N.D.	N.D.
[2]Zn (ppm)	71	90	63	113	40	380	25	73	129	100
[2]W (ppm)	22	N.D.	N.D.	N.D.	N.D.	N.D.	N.D.	N.D.	N.D.	N.D.
[2]Mo (ppm)	N.D.	N.D.	N.D.	N.D.	N.D.	469	N.D.	N.D.	N.D.	N.D.
[2]Rb (ppm)	3.79	2.85	22.26	4.48	45.21	35.63	110.2	0.38	0.42	5.31
[2]Cs (ppm)	0.61	0.07	0.92	0.26	0.87	0.92	2.7	0.1	0.09	0.06
[2]Ba (ppm)	212	36	176	72	576	431	551	N.D.	43	101
[2]Sr (ppm)	72	113	109	135	368	24	70	5	160	34
[2]Ga (ppm)	36	23	27	21	27	17	31	13	30	24
[3]Ta (ppm)	0.55	N.D.	0.54	N.D.	0.38	N.D.	N.D.	N.D.	0.51	N.D.
[2]Nb (ppm)	10.23	2.14	8.01	2.1	5.15	3.71	3.48	0.59	9.2	3.97
[3]Hf (ppm)	3.47	1.08	3.56	1.34	3.19	2.57	3.23	0.41	3.06	2.16
[2]Zr (ppm)	134	35	126	40	104	112	135	12	113	78
[3]Th (ppm)	0.71	0.13	2.65	0.18	5.12	15.6	2.42	N.D.	0.63	0.44
[3]U (ppm)	0.18	0.03	0.67	0.05	1.1	1.34	0.65	0.01	0.16	0.11
[2]Sb (ppm)	N.D.	N.D.	N.D.	N.D.	N.D.	N.D.	N.D.	N.D.	N.D.	N.D.
[2]Se (ppm)	N.D.	N.D.	N.D.	N.D.	N.D.	11	N.D.	N.D.	N.D.	N.D.
[2]Sn (ppm)	N.D.	N.D.	N.D.	N.D.	N.D.	N.D.	N.D.	N.D.	N.D	N.D.
[3]La (ppm)	9.22	2.5	14.97	2.3	28.54	>100.00	15.53	0.48	8.79	4.45
[3]Ce (ppm)	25.25	6.85	33.55	6.49	53.34	>200.00	30.64	1.13	23.93	12.5
[3]Pr (ppm)	3.87	1.12	4.23	1.08	5.87	>25.00	3.66	0.2	3.65	1.93
[3]Nd (ppm)	18.47	5.65	16.62	5.7	20.3	>100.00	12.75	1	17.8	9.72
[3]Sm (ppm)	5.16	1.92	3.92	1.89	2.98	9.25	2.16	0.39	4.9	2.89
[3]Eu (ppm)	1.43	0.7	1.27	0.74	0.96	1.95	0.54	0.06	1.53	1
[3]Gd (ppm)	5.94	2.63	3.9	2.73	2.15	4.09	1.48	0.61	5.36	3.49
[3]Tb (ppm)	0.91	0.45	0.64	0.46	0.28	0.48	0.21	0.11	0.9	0.57
[3]Dy (ppm)	5.81	3.08	4.17	3.07	1.46	1.72	0.98	0.77	5.26	3.87
[3]Ho (ppm)	1.13	0.68	0.87	0.68	0.3	0.26	0.2	0.18	1.05	0.79
[3]Er (ppm)	3.26	1.98	2.62	2.06	0.86	0.57	0.49	0.52	2.87	2.34
[3]Tm (ppm)	0.46	0.3	0.4	0.32	0.12	0.08	0.08	0.08	0.44	0.34
[3]Yb (ppm)	2.97	1.88	2.48	2.01	0.86	0.45	0.47	0.57	2.57	2.01
[3]Lu (ppm)	0.434	0.301	0.397	0.316	0.127	0.073	0.07	0.084	0.405	0.305
[3]Y (ppm)	29.37	17.75	24.92	17.64	8.4	6.64	5.09	4.54	27.32	19.91
[1]CO2 (%)										
[1]S (%)										
[5]Hg (ppb)										
[4]Ag (oz/ton)	N.D.		N.D.			N.D.	N.D.	N.D.		
[4]Au (oz/ton)	N.D.		N.D.			0.02	N.D.	N.D.		
[5]Au (ppb)	390.52		N.D.					N.D.		
[5]Pd (ppb)	N.D.		N.D.					N.D.		
[5]Pt (ppb)	N.D.		N.D.					N.D.		

Sample #	01LAH-0105A	01LAH-0105B	01LAH-0105C	01LAH-0107	01LAH-0109	01LAH-0111B	01LAH-0111C	01LAH-0111D	01LAH-0111E	01LAH-0113D
UTM East	447675	447675	446487	447054	446487	446494	446436	446436	446573	450286
UTM North	5362522	5362522	5362586	5363382	5362586	5362756	5362859	5362859	5360411	5351578
Rock type	fv (8)	fv (8)	mv (7)	mv (7)	MD (15)	mv (7)	amph (12b)	gab (12a)	gd - geochron	ad (14b)
[1]SiO2 (%)	67.02	72.41	44.26	50.55	41.61	49.2	49.7	66.1	73.82	56.4
[1]TiO2 (%)	0.48	0.24	1.01	0.67	0.33	0.7	1.27	0.37	0.03	0.67
[1]Al2O3 (%)	18.31	7.63	13.31	15.06	6.17	15.39	14.11	13.81	14.87	14.84
[1]Fe2O3 (%	3.85	10.17	13.28	10.54	10.3	14.36	15.12	3	0.43	6.8
[1]MnO (%)	0.01	0.04	0.26	0.23	0.14	0.2	0.26	0.04	0.02	0.1
[1]MgO (%)	0.99	0.96	5.93	6.17	27.76	6.73	7.11	2.25	0.04	4.98
[1]CaO (%)	0.09	0.91	9.24	12.42	5.61	8.35	8.34	3.79	0.93	5.76
[1]Na2O (%)	0.83	2.08	0.92	1.58	0.2	4.14	3.29	8.49	5	4.53
[1]K2O (%)	4.62	0.79	0.91	0.23	0.01	0.71	1.02	0.03	4.53	2.77
[1]P2O5 (%)	0.05	0.06	0.09	0.05	0.02	0.15	0.06	0.06	N.D.	0.48
LOI	4.23	4.31	10.86	2.86	7.64	0.89	1.18	1.87	0.47	2.29
TOTAL	100.49	99.59	100.08	100.35	99.78	100.81	101.46	99.8	100.15	99.61
[2]As (ppm)	19	24	5	N.D.	4	N.D.	N.D.	N.D.	N.D.	N.D.
[2]Ag (ppm)	N.D	N.D	N.D.	N.D.	N.D.	N.D.	N.D.	N.D.	N.D.	N.D.
[2]Cr (ppm)	19	54	94	372	2411	263	75	18	6	151
[2]Ni (ppm)	14	59	68	76	1382	107	45	15	N.D.	80
[2]Co (ppm)	N.D	55	35	47	105	30	57	12	N.D.	29
[2]Sc (ppm)	N.D	10	54	70	34	34	64	9	N.D.	17
[2]V (ppm)	35	54	370	339	166	213	507	40	N.D.	156
[2]Cu (ppm)	72	464	4	106	31	6	214	14	6	29
[2]Pb (ppm)	6	19	N.D.	N.D.	N.D.	N.D.	N.D.	10	16	10
[2]Bi (ppm)	N.D	N.D	N.D.	N.D.	N.D.	N.D.	N.D.	N.D.	N.D.	N.D.
[2]Zn (ppm)	124	4788	142	70	56	44	108	31	13	85
[2]W (ppm)	N.D	N.D	N.D.	N.D.	N.D.	N.D.	N.D.	N.D.	N.D.	N.D.
[2]Mo (ppm)	N.D	3	N.D.	N.D.	N.D.	N.D.	N.D.	N.D.	N.D.	N.D.
[2]Rb (ppm)	90.14	27.94	47.46	3.81	1.61	15	35.78	0.44	87.79	53.6
[2]Cs (ppm)	2.41	0.47	0.75	0.1	1.63	0.96	0.26	0.05	0.45	0.37
[2]Ba (ppm)	535	117	129	83	N.D.	235	405	N.D.	466	1604
[2]Sr (ppm)	99	67	87	87	24	170	229	33	129	994
[2]Ga (ppm)	34	28	22	21	11	27	24	20	25	29
[3]Ta (ppm)	0.97	N.D	N.D.	N.D	N.D	N.D	N.D	0.48	N.D.	0.42
[2]Nb (ppm)	14.7	3.01	3.69	1.6	0.44	4.05	2.48	6.84	2.5	7.29
[3]Hf (ppm)	9.07	1.96	1.92	1.12	0.54	2.3	1.49	3.27	1.42	5.46
[2]Zr (ppm)	368	80	71	35	16	90	43	127	39	176
[3]Th (ppm)	5.75	1.53	0.5	0.17	N.D	1.34	0.22	3.15	0.8	7.25
[3]U (ppm)	2.34	0.52	0.13	0.05	0.01	0.33	0.09	1.18	0.66	1.95
[2]Sb (ppm)	N.D	N.D	N.D	N.D	N.D	N.D	N.D	N.D	N.D	N.D
[2]Se (ppm)	N.D	7	N.D.	N.D	N.D	N.D	N.D	N.D	N.D	N.D
[2]Sn (ppm)	N.D	N.D	N.D	N.D	N.D	N.D	N.D	N.D	N.D	N.D
[3]La (ppm)	4.44	12.38	4.83	2.1	0.53	12.18	3.96	8.82	2.76	47.96
[3]Ce (ppm)	10.53	27.05	12.03	5.79	1.58	27.54	9.56	25.38	6.28	99.83
[3]Pr (ppm)	1.24	3.3	1.81	0.92	0.27	3.6	1.5	3.43	0.79	13.04
[3]Nd (ppm)	4.45	12.9	8.61	4.85	1.52	14.64	7.43	13.64	2.83	53.4
[3]Sm (ppm)	0.99	2.59	2.71	1.66	0.59	2.9	2.3	2.83	0.6	10.84
[3]Eu (ppm)	0.29	0.84	1.05	0.61	0.25	0.9	0.98	0.64	0.2	2.94
[3]Gd (ppm)	1.16	2.18	3.27	2.27	1.03	2.78	3.24	2.76	0.56	8.77
[3]Tb (ppm)	0.24	0.31	0.61	0.42	0.19	0.43	0.56	0.46	0.09	1.14
[3]Dy (ppm)	1.88	1.85	3.99	2.81	1.29	2.65	3.71	2.72	0.54	5.84
[3]Ho (ppm)	0.48	0.36	0.88	0.63	0.28	0.55	0.76	0.57	0.13	1.04
[3]Er (ppm)	1.58	1.02	2.57	1.91	0.84	1.63	2.38	1.79	0.42	2.83
[3]Tm (ppm)	0.27	0.15	0.4	0.3	0.13	0.24	0.35	0.27	0.07	0.38
[3]Yb (ppm)	1.97	1.01	2.46	1.93	0.76	1.65	2.3	1.76	0.53	2.31
[3]Lu (ppm)	0.308	0.165	0.362	0.294	0.125	0.242	0.357	0.255	0.1	0.349
[3]Y (ppm)	12.91	9.48	23.06	17	7.5	14.79	20.09	16.76	4.01	30.2
[1]CO2 (%)										
[1]S (%)										
[4]Hg (ppb)										
[4]Ag (oz/ton)	N.D	N.D								
[4]Au (oz/ton)	N.D	N.D								
[4]Au (ppb)										
[4]Pd (ppb)										
[4]Pt (ppb)										

Sample #	01LAH-0114A	01LAH-0115B	01LAH-0119	01LAH-0120A	01LAH-0120B	01LAH-0122	01LAH-0123	01LAH-0124	01LAH-0125	01LAH-0126
UTM East	452855	455628	452113	447598	452640	447909	453702	447909	452424	450233
UTM North	5352670	5357692	5356450	5363295	5353210	5353603	5350397	5353603	5353631	5356769
Rock type	fi (13)	fi (13)	gab (12a)	gab (12a)	mylonite	mv (7)	iv (8)	mv (7)	iv (8)	gab (12a)
[1]SiO2 (%)	67.15	69.7	49.44	55.05	54.26	42	60.97	47.21	61.7	62.3
[1]TiO2 (%)	0.33	0.2	0.83	0.65	0.64	0.47	0.81	0.6	0.49	0.56
[1]Al2O3 (%)	15.99	16.87	13.42	15.7	15.94	9.53	19.81	11.31	15.32	14.5
[1]Fe2O3 (%)	2.86	1.27	13.23	7.02	8.65	12.78	7.23	10.87	4.25	5.8
[1]MnO (%)	0.05	0.02	0.23	0.14	0.17	0.1	0.03	0.16	0.06	0.17
[1]MgO (%)	1.87	0.52	8.59	4.88	5.26	24.71	2.73	11.61	1.56	1.97
[1]CaO (%)	2.23	2.7	11.08	11.63	12.39	0.75	0.28	7.13	5.57	10.42
[1]Na2O (%)	5.11	5.93	2.24	1.42	0.71	0.32	2.71	2.97	1.92	2.62
[1]K2O (%)	3.02	1.77	0.76	1.37	0.87	N.D.	1.75	0.08	2.57	0.3
[1]P2O5 (%)	0.15	0.07	0.05	0.13	0.12	0.03	0.14	0.05	0.15	0.15
LOI	1.3	0.51	1.06	1.24	1.21	7.98	4.03	7.17	6.42	1.03
TOTAL	100.08	99.56	100.95	99.24	100.22	98.67	100.5	99.17	100.02	99.81
[2]As (ppm)	N.D.	N.D.	N.D.	N.D.	N.D.	11	12	9	N.D.	N.D.
[2]Ag (ppm)	N.D.	N.D.	N.D.	N.D.	N.D.	N.D.	N.D.	N.D.	N.D.	N.D.
[2]Cr (ppm)	22	N.D.	200	674	721	3833	246	1185	38	95
[2]Ni (ppm)	11	N.D.	102	128	221	1261	125	227	9	45
[2]Co (ppm)	N.D.	N.D.	57	40	31	121	34	60	17	18
[2]Sc (ppm)	N.D.	N.D.	67	42	44	40	27	47	17	22
[2]V (ppm)	49	13	376	224	225	289	224	271	67	158
[2]Cu (ppm)	6	N.D.	140	39	64	127	45	100	16	26
[2]Pb (ppm)	11	11	N.D.	N.D.	N.D.	N.D.	N.D.	N.D.	N.D.	N.D.
[2]Bi (ppm)	N.D.	N.D.	N.D.	N.D.	N.D.	N.D.	N.D.	N.D.	N.D.	N.D.
[2]Zn (ppm)	63	47	106	75	82	75	91	70	65	81
[2]W (ppm)	N.D.	N.D.	N.D.	N.D.	N.D.	N.D.	N.D.	N.D.	N.D.	N.D.
[2]Mo (ppm)	N.D.	N.D.	5	N.D.	N.D.	N.D.	N.D.	N.D.	N.D.	N.D.
[2]Rb (ppm)	62.12	48.63	19.45	42.27	27.67	0.45	38.72	1.7	65.71	8.88
[2]Cs (ppm)	0.46	1.34	0.19	0.64	1.41	0.23	3.87	0.63	1.11	0.08
[2]Ba (ppm)	1533	784	125	872	649	N.D.	380	N.D.	398	235
[2]Sr (ppm)	719	696	139	237	192	6	338	47	118	371
[2]Ga (ppm)	28	25	21	21	24	17	34	18	24	24
[3]Ta (ppm)	0.37	N.D.	N.D.	N.D.	N.D.	N.D.	0.39	N.D.	0.73	N.D.
[2]Nb (ppm)	5.9	1.48	2.17	4.1	4.2	0.62	6.22	2.38	10.16	4.58
[3]Hf (ppm)	3.48	2.63	1.19	2.14	2.23	0.96	3.92	1.49	4.26	2.59
[2]Zr (ppm)	101	83	36	80	82	31	135	51	165	86
[3]Th (ppm)	4.31	1.7	0.21	1.16	1.24	0.15	3.75	0.41	3.5	2.25
[3]U (ppm)	0.81	0.39	0.07	0.29	0.3	0.03	1.06	0.11	0.88	0.65
[2]Sb (ppm)	N.D.	N.D.	N.D.	N.D.	N.D.	N.D.	N.D.	N.D.	N.D.	N.D.
[2]Se (ppm)	N.D.	N.D.	N.D.	N.D.	N.D.	N.D.	N.D.	N.D.	N.D.	N.D.
[2]Sn (ppm)	N.D.	N.D.	N.D.	N.D.	N.D.	N.D.	N.D.	N.D.	N.D.	N.D.
[3]La (ppm)	30.44	12.49	2.89	11.16	12.06	2.53	24.4	3.46	20.53	15.17
[3]Ce (ppm)	62.14	25.32	7.66	24.35	26.41	6.01	53.55	8.69	43.96	31.68
[3]Pr (ppm)	7.46	2.9	1.15	3.05	3.32	0.92	6.65	1.29	5.23	3.92
[3]Nd (ppm)	28.81	10.69	6.09	12.57	13.52	4.37	25.8	5.92	20	15.43
[3]Sm (ppm)	5.32	1.71	1.98	2.41	2.73	1.06	4.42	1.84	4.07	2.96
[3]Eu (ppm)	1.36	0.5	0.76	0.78	0.8	0.14	1.13	0.59	0.97	0.84
[3]Gd (ppm)	3.82	1.08	2.5	2.2	2.56	1.11	3.29	2.49	3.9	2.43
[3]Tb (ppm)	0.46	0.11	0.46	0.33	0.39	0.19	0.45	0.44	0.6	0.36
[3]Dy (ppm)	2.28	0.52	3.16	2.04	2.42	1.18	2.62	2.92	3.69	2.02
[3]Ho (ppm)	0.38	0.08	0.69	0.41	0.49	0.27	0.5	0.62	0.74	0.41
[3]Er (ppm)	0.96	0.22	2.12	1.24	1.46	0.86	1.42	1.82	2.04	1.16
[3]Tm (ppm)	0.14	0.03	0.31	0.19	0.22	0.14	0.21	0.28	0.3	0.18
[3]Yb (ppm)	0.82	0.18	2.05	1.32	1.47	0.92	1.45	1.84	1.91	1.18
[3]Lu (ppm)	0.122	0.034	0.302	0.196	0.214	0.147	0.217	0.277	0.3	0.176
[3]Y (ppm)	10.71	2.48	18	11.67	13.5	7.39	13.39	16.94	20.75	11.38

[1]CO2 (%)
[1]S (%)
[4]Hg (ppb)
[4]Ag (oz/ton)
[4]Au (oz/ton)
[4]Au (ppb)
[4]Pd (ppb)
[4]Pt (ppb)

Sample #	01LAH-0127	01LAH-0130	01LAH-0131	01LAH-0133A	01LAH-0133B	01LAH-0139	01LAH-0141	01LAH-0143	01LAH-0145A	01LAH-0145B
UTM East	452274	453702	453996	455119	452214	447909	453996	448620	449522	447680
UTM North	5358589	5350397	5351847	5352162	5355772	5353603	5352193	5352051	5362870	5350310
Rock type	gab (12a)	mv (7)	mv (7)	mylonite	mylonite	amph (12b)	iv (8)	mv (7)	mv (7)	iv (8)
[1]SiO2 (%)	48.24	50.34	50.88	59.95	69.77	50.45	63.17	52.65	47.7	63.53
[1]TiO2 (%)	1.04	0.84	0.97	0.7	0.31	0.91	0.33	1.62	0.39	0.44
[1]Al2O3 (%)	10.25	16.2	19.93	16.4	16.32	14.96	17.02	14.19	7.86	15.27
[1]Fe2O3 (%	12.64	10.31	11.04	6.84	2.49	14.17	3.3	15.08	10.47	4.15
[1]MnO (%)	0.39	0.23	0.21	0.11	0.03	0.23	0.05	0.28	0.22	0.08
[1]MgO (%)	6.34	3.17	3.57	3.48	1.28	6.98	2.31	2.32	14.92	1.49
[1]CaO (%)	19.33	6.8	6.65	7.33	3.23	8.55	3.69	11.76	10.32	4.94
[1]Na2O (%)	0.23	2.94	2.79	2.12	5.36	2.67	5.23	0.79	1.81	1.56
[1]K2O (%)	0.09	0.83	0.73	1.54	0.99	1.06	2.52	0.36	0.13	2.64
[1]P2O5 (%)	0.15	0.04	0.05	0.14	0.1	0.07	0.17	0.13	0.02	0.12
LOI	1.49	5.75	3.99	2.24	0.89	1.33	1.81	1.89	5.46	6
TOTAL	100.18	99.45	100.79	100.85	100.78	101.38	99.61	101.06	99.3	100.22
[2]As (ppm)	N.D.	4	25	N.D.	N.D.	N.D.	3	N.D.	5	8
[2]Ag (ppm)	N.D.	N.D.	N.D.	N.D.	N.D.	N.D.	N.D.	N.D.	N.D.	N.D.
[2]Cr (ppm)	779	272	187	246	43	118	60	43	2935	32
[2]Ni (ppm)	290	158	186	110	17	51	40	26	994	4
[2]Co (ppm)	70	57	73	41	N.D.	57	N.D.	53	100	N.D.
[2]Sc (ppm)	40	40	48	27	9	64	N.D.	59	44	12
[2]V (ppm)	196	300	357	193	45	365	57	464	224	64
[2]Cu (ppm)	97	77	111	46	21	191	5	77	82	29
[2]Pb (ppm)	N.D.	N.D.	N.D.	5	8	5	12	N.D.	N.D.	13
[2]Bi (ppm)	N.D.	N.D.	N.D.	N.D.	N.D.	N.D.	N.D.	N.D.	N.D.	N.D.
[2]Zn (ppm)	90	81	79	73	46	121	55	143	74	54
[2]W (ppm)	N.D.	N.D.	N.D.	N.D.	N.D.	N.D.	N.D.	N.D.	N.D.	N.D.
[2]Mo (ppm)	N.D.	N.D.	N.D.	N.D.	N.D.	N.D.	N.D.	N.D.	N.D.	N.D.
[2]Rb (ppm)	2.32	22.38	24.11	47.82	41.96	49	48.8	7.55	4.44	42.65
[2]Cs (ppm)	0.05	0.47	0.31	0.59	2.11	0.35	0.64	0.17	0.63	0.54
[2]Ba (ppm)	47	207	209	519	720	274	1819	118	81	365
[2]Sr (ppm)	321	103	154	306	678	228	1008	105	75	150
[2]Ga (ppm)	24	24	30	24	29	24	28	30	14	24
[2]Ta (ppm)	0.6	N.D.	N.D.	N.D.	N.D.	N.D.	N.D.	0.30	N.D.	0.73
[2]Nb (ppm)	10.72	2.76	2.45	4.7	2.91	3.07	5.48	4.72	0.62	9.18
[2]Hf (ppm)	2.9	1.48	1.52	2.61	3.43	1.64	3.71	2.71	0.66	3.91
[2]Zr (ppm)	131	49	47	100	102	52	114	101	18	162
[2]Th (ppm)	1.97	0.29	0.23	1.72	3.81	0.32	6.96	0.44	0.07	3.42
[2]U (ppm)	0.55	0.08	0.07	0.4	0.98	0.08	1.06	0.11	0.03	0.84
[2]Sb (ppm)	N.D.	N.D.	N.D.	N.D.	N.D.	N.D.	N.D.	N.D.	N.D.	N.D.
[2]Se (ppm)	N.D.	N.D.	N.D.	N.D.	N.D.	N.D.	N.D.	N.D.	N.D.	N.D.
[2]Sn (ppm)	N.D.	N.D.	N.D.	N.D.	N.D.	N.D.	N.D.	N.D.	N.D.	N.D.
[3]La (ppm)	19.5	2.98	2.02	12.65	11.7	3.86	51.95	5.81	0.96	18.08
[3]Ce (ppm)	42.64	8.29	6.12	27.55	26.69	10.48	96.08	15.47	2.61	38.18
[3]Pr (ppm)	5.56	1.32	1.04	3.43	2.91	1.64	10.88	2.40	0.45	4.74
[3]Nd (ppm)	23.44	6.73	5.77	13.94	10.54	8.2	39.33	12.42	2.39	17.45
[3]Sm (ppm)	4.66	2.04	2.03	2.7	1.88	2.56	6.31	4.04	0.90	3.5
[3]Eu (ppm)	1.59	0.74	0.87	0.82	0.69	0.91	1.58	1.34	0.50	0.86
[3]Gd (ppm)	4.11	2.6	2.67	2.53	1.31	3.34	4.03	5.15	1.37	3.2
[3]Tb (ppm)	0.56	0.44	0.51	0.38	0.18	0.57	0.45	0.91	0.25	0.51
[3]Dy (ppm)	3.2	2.92	3.23	2.43	1.01	3.95	2.1	6.09	1.68	3.01
[3]Ho (ppm)	0.61	0.6	0.7	0.46	0.2	0.83	0.35	1.28	0.38	0.61
[3]Er (ppm)	1.68	1.77	2.08	1.43	0.52	2.49	0.85	3.87	1.10	1.72
[3]Tm (ppm)	0.23	0.26	0.31	0.21	0.08	0.39	0.13	0.58	0.17	0.26
[3]Yb (ppm)	1.32	1.75	1.97	1.35	0.54	2.58	0.7	3.72	1.00	1.69
[3]Lu (ppm)	0.207	0.267	0.297	0.221	0.086	0.407	0.11	0.583	0.169	0.255
[3]Y (ppm)	16.95	15.97	18.39	13.11	5.32	22.93	10.06	32.77	9.78	16.94
[1]CO2 (%)										
[1]S (%)										
[5]Hg (ppb)										
[4]Ag (oz/ton)										
[4]Au (oz/ton)										
[5]Au (ppb)						N.D.				
[5]Pd (ppb)						N.D.				
[5]Pt (ppb)						N.D.				

Sample #	01LAH-0146	01LAH-0147	01LAH-0149	01LAH-0150	01LAH-0151	01LAH-0152	01LAH-0153	01LAH-0154	01LAH-0155	01LAH-0160
UTM East	455858	447601	449556	448385	448048	452206	447351	449556	447746	452206
UTM North	5365874	5350431	5362905	5352145	5360210	5352604	5349665	5362905	5350781	5352604
Rock type	sed (9)	iv (8)	umv (6)	mv (7)	umv (6)	umv (6)	pd (14a)	mv (7)	fi (13)	gab (12a)
[1]SiO2 (%)	66.11	63.58	41.54	50.11	41.64	39.67	71.09	50.82	63.98	50.02
[1]TiO2 (%)	0.32	0.47	0.33	0.72	0.34	0.23	0.27	0.72	0.55	0.51
[1]Al2O3 (%)	15.52	15.88	6.2	14.99	6.59	5	14.69	14.44	14.92	15.32
[1]Fe2O3 (%)	2.27	4.33	10.67	11.59	11.53	10.86	2.57	12.52	4.42	9.61
[1]MnO (%)	0.05	0.06	0.16	0.21	0.14	0.14	0.04	0.18	0.06	0.18
[1]MgO (%)	1.17	1.52	26.73	6.07	25.35	29.63	1.06	7.24	2.91	8.64
[1]CaO (%)	2.64	3.99	7.08	12.82	6.77	3.67	3.1	10.23	4.51	10.94
[1]Na2O (%)	5.5	2.46	0.22	1.79	0.5	0.12	4.5	2.81	4.91	2.96
[1]K2O (%)	2.11	2.58	N.D.	0.23	0.04	N.D.	1.2	0.36	0.77	0.59
[1]P2O5 (%)	0.08	0.14	0.01	0.05	0.02	N.D.	0.07	0.05	0.22	0.03
LOI	3.87	5.08	7.05	1.29	5.8	9.2	1.59	0.77	1.61	1.44
TOTAL	99.63	100.11	100	99.87	98.71	98.53	100.18	100.13	98.86	100.25
[2]As (ppm)	7	N.D.	N.D.	N.D.	3	N.D.	N.D.	N.D.	N.D.	N.D.
[2]Ag (ppm)	N.D.	N.D.	N.D.	N.D.	N.D.	N.D.	N.D.	N.D.	N.D.	N.D.
[2]Cr (ppm)	34	30	2801	199	3101	2672	23	206	72	794
[2]Ni (ppm)	6	6	1370	56	1272	1671	3	62	54	95
[2]Co (ppm)	N.D.	N.D.	106	48	113	118	N.D.	49	14	42
[2]Sc (ppm)	10	13	35	69	34	23	N.D.	67	10	64
[2]V (ppm)	60	70	181	368	193	140	27	365	92	287
[2]Cu (ppm)	12	18	33	70	1408	125	N.D.	94	18	52
[2]Pb (ppm)	N.D.	N.D.	N.D.	N.D.	69	N.D.	N.D.	N.D.	11	N.D.
[2]Bi (ppm)	N.D.	N.D.	N.D.	N.D.	N.D.	N.D.	N.D.	N.D.	N.D.	N.D.
[2]Zn (ppm)	31	62	59	72	139	66	37	62	59	96
[2]W (ppm)	N.D.	N.D.	N.D.	N.D.	N.D.	N.D.	N.D.	N.D.	N.D.	N.D.
[2]Mo (ppm)	N.D.	N.D.	N.D.	N.D.	N.D.	N.D.	N.D.	N.D.	N.D.	N.D.
[2]Rb (ppm)	41.48	46.38	0.38	4.28	0.99	0.77	31.28	7.92	13.93	17.16
[2]Cs (ppm)	0.72	0.79	0.11	0.07	0.25	0.20	0.42	0.14	0.54	0.26
[2]Ba (ppm)	595	492	N.D.	94	N.D.	N.D.	367	76	899	134
[2]Sr (ppm)	128	137	36	103	14	114	325	89	821	130
[2]Ga (ppm)	28	25	11	21	13	9	25	23	29	16
[3]Ta (ppm)	N.D.	0.73	N.D.	N.D.	N.D.	N.D.	N.D.	N.D.	N.D.	N.D.
[2]Nb (ppm)	2.9	9.71	0.44	1.69	0.47	0.34	1.72	1.63	3.9	1.03
[3]Hf (ppm)	2.96	3.95	0.48	1.19	0.56	0.29	2.69	1.23	3.78	0.76
[2]Zr (ppm)	104	174	12	40	17	5	96	38	131	22
[3]Th (ppm)	2.78	3.58	N.D.	0.19	0.06	N.D.	0.6	0.19	8.45	0.09
[3]U (ppm)	0.89	0.86	0.01	0.05	0.02	0.03	0.16	0.05	1.79	0.03
[2]Sb (ppm)	N.D.	N.D.	N.D.	N.D.	N.D.	N.D.	N.D.	N.D.	N.D.	N.D.
[2]Se (ppm)	N.D.	N.D.	N.D.	N.D.	N.D.	N.D.	N.D.	N.D.	N.D.	N.D.
[2]Sn (ppm)	N.D.	N.D.	N.D.	N.D.	75	N.D.	N.D.	N.D.	N.D.	N.D.
[3]La (ppm)	11.63	20.5	0.41	3.00	0.56	0.47	8.24	2.14	36.26	1.37
[3]Ce (ppm)	23.21	43.3	1.24	7.32	1.75	1.15	17.07	5.93	77.78	3.70
[3]Pr (ppm)	2.77	5.21	0.22	1.13	0.31	0.18	1.94	0.98	10.03	0.62
[3]Nd (ppm)	10.16	18.91	1.29	5.45	1.70	0.95	6.69	4.95	37.27	3.34
[3]Sm (ppm)	1.99	3.77	0.55	1.82	0.65	0.37	1.2	1.71	6.46	1.17
[3]Eu (ppm)	0.59	0.92	0.21	0.66	0.27	0.12	0.35	0.70	1.57	0.43
[3]Gd (ppm)	1.54	3.55	0.89	2.43	1.06	0.61	0.89	2.41	4.17	1.61
[3]Tb (ppm)	0.2	0.54	0.17	0.44	0.20	0.12	0.12	0.45	0.48	0.30
[3]Dy (ppm)	1.03	3.15	1.11	3.09	1.32	0.76	0.64	3.07	2.45	2.12
[3]Ho (ppm)	0.18	0.66	0.26	0.68	0.30	0.17	0.11	0.72	0.42	0.47
[3]Er (ppm)	0.52	1.85	0.75	2.05	0.88	0.51	0.31	2.12	1.1	1.39
[3]Tm (ppm)	0.07	0.28	0.11	0.31	0.13	0.08	0.05	0.34	0.15	0.21
[3]Yb (ppm)	0.52	1.71	0.66	2.09	0.80	0.52	0.32	2.17	0.99	1.41
[3]Lu (ppm)	0.081	0.287	0.105	0.346	0.118	0.079	0.045	0.344	0.142	0.231
[3]Y (ppm)	5.08	19.18	6.28	18.11	7.87	4.26	3.47	17.78	11.93	12.26
[1]CO2 (%)					0.22	0.82				0.05
[1]S (%)					0.06	0.06				0.03
[5]Hg (ppb)					9.59	0.6				
[4]Ag (oz/ton)										
[4]Au (oz/ton)										
[5]Au (ppb)			N.D.					N.D.		
[5]Pd (ppb)			N.D.					12.77		
[5]Pt (ppb)			N.D.					16.39		

Sample #	01LAH-0163	01LAH-0167A	01LAH-0167B	01LAH-0171	01LAH-0176	01LAH-0182	01LAH-0184	01LAH-0186A	01LAH-0186B	01LAH-0186D
UTM East	452222	452328	450509	452025	448891	452234	454147	454202	452351	452626
UTM North	5352786	5352786	5363736	5351894	5364153	5351882	5365747	5365378	5351732	5351450
Rock type	mv (7)	mv (7)	ad (14b)	KGC	pd (14a)	umv (6)	sed (9)	sed (9)	umv (6)	gab (12a)
[1]SiO2 (%)	51.19	52.77	52.95	51.93	65.77	44.15	58.32	49.22	42.34	47.58
[1]TiO2 (%)	0.67	1.03	0.87	1.14	0.44	0.7	1.07	0.86	0.82	0.73
[1]Al2O3 (%)	15.02	15.38	15.37	13.15	14.51	19.11	16.3	15.63	17.44	16.08
[1]Fe2O3 (%)	11.16	9.2	7.97	15.23	7.38	9.68	8.98	15.28	12.37	10.44
[1]MnO (%)	0.23	0.19	0.14	0.27	0.13	0.15	0.15	0.34	0.11	0.18
[1]MgO (%)	6.81	5.37	5.14	4.9	0.59	6.28	3.94	3.58	7.2	7.96
[1]CaO (%)	11.08	6.23	6.84	9.64	3.57	10.38	4.58	5.13	5.58	11.15
[1]Na2O (%)	1.77	4.03	4.97	3.15	5.71	3.15	3.68	4.33	2.82	2.08
[1]K2O (%)	0.19	0.36	2.43	0.26	0.63	0.05	0.03	0.03	0.56	0.02
[1]P2O5 (%)	0.05	0.07	0.54	0.09	0.14	0.05	0.16	0.1	0.05	0.05
LOI	1.01	5.93	2.22	0.34	1.36	5.96	3.39	6.33	12.05	3.68
TOTAL	99.17	100.57	99.42	100.1	100.21	99.66	100.6	100.84	101.34	99.95
[2]As (ppm)	N.D.	N.D.	3	N.D.	N.D.	8	4	12	94	64
[2]Ag (ppm)	N.D.	N.D.	N.D.	N.D.	N.D.	N.D.	N.D.	N.D.	N.D.	N.D.
[2]Cr (ppm)	371	147	128	134	14	113	54	85	290	516
[2]Ni (ppm)	77	99	63	58	N.D.	132	49	95	184	97
[2]Co (ppm)	46	70	23	43	N.D.	40	40	52	51	46
[2]Sc (ppm)	71	52	21	46	17	39	25	33	51	52
[2]V (ppm)	344	435	171	367	N.D.	217	222	237	314	302
[2]Cu (ppm)	104	79	22	40	N.D.	66	65	79	N.D.	129
[2]Pb (ppm)	N.D.	N.D.	11	N.D.	N.D.	N.D.	N.D.	5	N.D.	8
[2]Bi (ppm)	N.D.	N.D.	N.D.	N.D.	N.D.	N.D.	N.D.	N.D.	N.D.	N.D.
[2]Zn (ppm)	72	92	97	110	120	75	89	97	162	79
[2]W (ppm)	N.D.	N.D.	N.D.	N.D.	N.D.	N.D.	N.D.	N.D.	N.D.	N.D.
[2]Mo (ppm)	N.D.	N.D.	N.D.	N.D.	N.D.	N.D.	N.D.	N.D.	N.D.	N.D.
[2]Rb (ppm)	5.08	8.04	60.13	2.92	16.63	0.90	0.66	0.9	14.23	N.D.
[2]Cs (ppm)	0.06	0.28	1.51	0.13	0.71	0.04	0.06	0.15	1.01	0.06
[2]Ba (ppm)	93	136	1890	180	194	N.D.	39	45	97	N.D.
[2]Sr (ppm)	78	250	1144	87	157	175	175	50	98	161
[2]Ga (ppm)	21	23	28	25	31	23	25	23	23	24
[3]Ta (ppm)	N.D.	N.D.	0.42	N.D.	0.75	N.D.	0.38	N.D.	N.D.	N.D.
[2]Nb (ppm)	1.48	2.31	8.76	3.19	11.58	2.06	6.32	4.33	2.18	2.14
[3]Hf (ppm)	1.13	1.62	5.5	1.96	8.75	1.22	3.26	2.16	1.30	1.32
[2]Zr (ppm)	37	50	180	66	329	40	125	79	44	42
[3]Th (ppm)	0.16	0.24	6.95	0.31	3.01	0.23	1.17	0.84	0.22	0.24
[3]U (ppm)	0.04	0.06	2.14	0.08	0.62	0.06	0.32	0.22	0.06	0.06
[2]Sb (ppm)	N.D.	N.D.	N.D.	N.D.	N.D.	N.D.	N.D.	N.D.	N.D.	N.D.
[2]Se (ppm)	N.D.	N.D.	N.D.	N.D.	N.D.	N.D.	N.D.	N.D.	N.D.	N.D.
[2]Sn (ppm)	N.D.	N.D.	N.D.	N.D.	N.D.	N.D.	N.D.	N.D.	N.D.	N.D.
[3]La (ppm)	1.97	2.24	48.87	4.25	21	2.85	11.84	6.78	2.98	3.09
[3]Ce (ppm)	5.52	6.52	105.27	11.16	50.34	7.49	26.09	16.02	7.83	8.04
[3]Pr (ppm)	0.89	1.06	16	1.70	7.58	1.16	3.5	2.19	1.18	1.23
[3]Nd (ppm)	4.59	5.39	67.84	8.59	33.6	5.62	14.77	9.25	5.70	6.02
[3]Sm (ppm)	1.55	1.84	13.96	2.79	8.35	1.75	3.42	2.49	1.58	1.80
[3]Eu (ppm)	0.58	0.72	3.77	0.90	2.1	0.73	1.21	0.84	0.41	0.68
[3]Gd (ppm)	2.23	2.50	10.46	3.74	8.84	2.21	3.6	2.79	2.06	2.40
[3]Tb (ppm)	0.42	0.44	1.24	0.66	1.52	0.38	0.58	0.48	0.38	0.42
[3]Dy (ppm)	2.82	2.89	5.82	4.41	9.53	2.44	3.33	3.01	2.62	2.74
[3]Ho (ppm)	0.60	0.62	1.04	0.97	2.16	0.52	0.69	0.67	0.58	0.57
[3]Er (ppm)	1.83	1.87	2.56	2.82	6.28	1.49	1.92	1.97	1.61	1.66
[3]Tm (ppm)	0.28	0.27	0.36	0.43	0.98	0.22	0.28	0.3	0.25	0.26
[3]Yb (ppm)	1.82	1.74	2.09	2.85	6.38	1.38	1.9	1.96	1.51	1.63
[3]Lu (ppm)	0.312	0.280	0.303	0.434	1.05	0.218	0.286	0.33	0.241	0.249
[3]Y (ppm)	16.33	16.52	26.47	25.38	54.15	13.64	17.8	18.49	14.50	15.37
[1]CO2 (%)	0.48	2.85		0.07		2.48			7.92	1
[1]S (%)	0.02	0.02		0.02		0.04			0.02	0.26
[5]Hg (ppb)				1.99						
[4]Ag (oz/ton)			N.D.							
[4]Au (oz/ton)			N.D.							
[5]Au (ppb)			N.D.							
[5]Pd (ppb)			N.D.							
[5]Pt (ppb)			N.D.							

Sample #	01LAH-0187	01LAH-0205	01LAH-0211	01LAH-0213	01LAH-0214	01LAH-0219A	01LAH-0219B	01LAH-0220	01LAH-0221	01LAH-0225
UTM East	447980	447980	448285	452610	449556	450017	455858	452691	448893	449187
UTM North	5353445	5353445	5353025	5350362	5362905	5354811	5365874	5351862	5363993	5348524
Rock type	sed (9)	sed (9)	sed (9)	KGC	umv (6)	fv (4)	mv (5)	fi (13b)	mv (5)	fv (4)
[1]SiO2 (%)	61.6	59.43	62.61	58.26	59.24	73.14	46.07	59.9	50.14	74.45
[1]TiO2 (%)	0.59	0.85	0.52	1.76	0.67	0.24	0.45	0.9	1.72	0.2
[1]Al2O3 (%)	16.67	16.63	17.09	15.88	16.31	13.12	14.16	14.79	15.48	12.3
[1]Fe2O3 (%)	5.79	6.59	4.68	8.86	11.03	2.94	7.47	8.6	10.23	2.88
[1]MnO (%)	0.06	0.13	0.05	0.18	0.18	0.05	0.13	0.1	0.09	0.06
[1]MgO (%)	3.42	2.6	2.2	2.92	2.56	0.62	7.93	2.71	4.03	0.25
[1]CaO (%)	2.93	4.69	4.24	6.43	2.99	0.98	6.8	5.14	7.21	1.17
[1]Na2O (%)	6.88	1.63	5.41	3.92	1.87	6.21	3.32	4.22	5.62	4.34
[1]K2O (%)	0.59	1.13	1.01	0.65	0.49	0.81	1.72	1.18	0.06	2.55
[1]P2O5 (%)	0.1	0.15	0.08	0.26	0.13	0.03	0.04	0.15	0.29	0.03
LOI	2.03	6.85	2.55	1.96	5.73	1.86	12.87	2.51	5.99	2.01
TOTAL	100.65	100.67	100.44	101.08	101.19	100	100.96	100.2	100.86	100.24
[2]As (ppm)	N.D.	N.D.	N.D.	N.D.	N.D.	N.D.	N.D.	N.D.	N.D.	N.D.
[2]Ag (ppm)	N.D.	N.D.	N.D.	N.D.	N.D.	N.D.	N.D.	N.D.	N.D.	N.D.
[2]Cr (ppm)	93	85	266	8	363	10	513	34	225	7
[2]Ni (ppm)	48	37	49	N.D.	113	N.D.	199	22	107	N.D.
[2]Co (ppm)	19	20	16	16	17	N.D.	48	28	44	N.D.
[2]Sc (ppm)	15	32	17	23	25	N.D.	37	27	37	N.D.
[2]V (ppm)	123	238	119	169	184	N.D.	188	157	258	N.D.
[2]Cu (ppm)	18	14	N.D.	5	28	N.D.	N.D.	N.D.	11	3
[2]Pb (ppm)	N.D.	N.D.	N.D.	N.D.	N.D.	N.D.	N.D.	N.D.	N.D.	N.D.
[2]Bi (ppm)	N.D.	N.D.	N.D.	N.D.	N.D.	N.D.	N.D.	N.D.	N.D.	N.D.
[2]Zn (ppm)	60	65	34	88	76	28	48	41	54	79
[2]W (ppm)	N.D.	N.D.	N.D.	N.D.	N.D.	N.D.	N.D.	N.D.	N.D.	N.D.
[2]Mo (ppm)	N.D.	N.D.	N.D.	N.D.	N.D.	N.D.	N.D.	N.D.	N.D.	N.D.
[2]Rb (ppm)	7.38	31.83	33.47	17.38	10.78	19.22	44.44	37.90	1.95	60.09
[2]Cs (ppm)	0.31	1.7	1.01	1.23	0.84	0.24	0.56	1.52	0.07	1.31
[2]Ba (ppm)	375	276	223	180	161	305	386	255	48	601
[2]Sr (ppm)	218	175	183	149	149	51	104	246	340	63
[2]Ga (ppm)	27	25	24	25	25	28	19	27	23	30
[3]Ta (ppm)	0.31	0.42	N.D.	0.4	0.30	1.86	0.30	0.62	0.98	1.89
[2]Nb (ppm)	4.46	6.46	4.3	7.3	5.20	31.12	3.55	9.36	19.29	28.81
[3]Hf (ppm)	2.97	3.38	2.46	3.22	2.93	10.43	1.82	5.45	3.24	11.51
[2]Zr (ppm)	117	138	93	120	112	396	60	207	112	363
[3]Th (ppm)	1.54	1.68	1.24	1.09	1.34	6.49	1.62	2.70	1.90	6.72
[3]U (ppm)	0.4	0.42	0.32	0.33	0.41	1.25	0.40	0.65	0.46	1.47
[2]Sb (ppm)	N.D.	N.D.	N.D.	N.D.	N.D.	N.D.	N.D.	N.D.	N.D.	N.D.
[2]Se (ppm)	N.D.	N.D.	N.D.	N.D.	N.D.	N.D.	N.D.	N.D.	N.D.	N.D.
[2]Sn (ppm)	N.D.	N.D.	N.D.	N.D.	N.D.	N.D.	N.D.	N.D.	N.D.	N.D.
[3]La (ppm)	12.73	14.36	8.72	12.7	10.36	51.09	7.93	20.72	26.66	51.21
[3]Ce (ppm)	26.57	28.69	18.86	30.62	23.31	109.99	17.64	47.34	61.45	110.5
[3]Pr (ppm)	3.26	3.79	2.33	4.42	3.03	15.69	2.28	6.22	8.55	16.41
[3]Nd (ppm)	12.73	15.08	9.19	19.35	11.80	61.73	9.07	25.68	32.86	66.69
[3]Sm (ppm)	2.62	3.31	2.02	4.42	2.58	13.09	2.20	5.91	6.28	15.07
[3]Eu (ppm)	0.82	1.07	0.66	1.56	0.92	2.62	0.55	1.43	2.22	3.12
[3]Gd (ppm)	2.53	3.14	1.94	4.46	2.60	13.02	2.44	6.30	5.60	14.3
[3]Tb (ppm)	0.38	0.49	0.31	0.7	0.44	2.06	0.41	1.02	0.86	2.32
[3]Dy (ppm)	2.18	2.9	1.76	4.17	2.75	12.67	2.64	6.40	4.89	13.67
[3]Ho (ppm)	0.44	0.59	0.36	0.89	0.62	2.58	0.54	1.32	0.98	2.81
[3]Er (ppm)	1.26	1.69	1.06	2.42	1.83	7.18	1.62	3.94	2.66	7.67
[3]Tm (ppm)	0.18	0.24	0.15	0.36	0.29	1.05	0.26	0.56	0.40	1.16
[3]Yb (ppm)	1.17	1.66	0.97	2.18	1.84	6.66	1.58	3.77	2.33	7.14
[3]Lu (ppm)	0.186	0.253	0.155	0.349	0.293	1.026	0.260	0.582	0.367	1.111
[3]Y (ppm)	12.01	15.52	9.69	22.83	17.59	64.82	14.56	36.35	25.40	66.76
[1]CO2 (%)							9.56	0.8		
[1]S (%)							0.01	N.D.		
[5]Hg (ppb)										
[4]Ag (oz/ton)										
[4]Au (oz/ton)										
[5]Au (ppb)										
[5]Pd (ppb)										
[5]Pt (ppb)										

Sample #	01LAH-0226	01LAH-0501A	01LAH-0501B	01LAH-0504A	01LAH-0504B	01LAH-0504C	01LAH-0504D	01LAH-0504E	01LAH-0517	01LAH-0521B
UTM East	450857	448867	448655	448978	452645	448659	448649	448649	453702	452583
UTM North	5354106	5352761	5362551	5352709	5358676	5362164	5362249	5362249	5350397	5349463
Rock type	fv (4) pd	fv (2)	mv (1)	umv (6)	mv (7)	mv (7)	umv (6)	mv (7)	CLP	CLP
[1]SiO2 (%)	73.56	75.31	49.63	43.48	54.02	53.32	43.62	51.82	65.8	65.98
[1]TiO2 (%)	0.18	0.07	0.88	0.86	1.11	1.03	0.96	0.96	0.53	0.33
[1]Al2O3 (%)	11.39	13.66	15.3	16.18	16.01	16.3	17.43	18.12	16.22	16.13
[1]Fe2O3 (%	4.2	1.86	11.49	10.6	9.85	9.67	18.47	14.68	4.31	2.64
[1]MnO (%)	0.07	0.03	0.19	0.34	0.16	0.14	0.46	0.3	0.06	0.04
[1]MgO (%)	1.64	0.18	7.36	3.02	5.69	6.46	3.4	3.35	1.55	1.51
[1]CaO (%)	2.16	0.89	10.26	10.35	7.13	4.71	8.91	7.31	3.87	3.53
[1]Na2O (%)	2.94	6.19	1.82	1.06	3.68	3.41	0.92	1.84	4.34	5.61
[1]K2O (%)	1.18	0.74	0.3	2.14	0.27	1.08	0.37	1.13	2.06	0.9
[1]P2O5 (%)	0.03	N.D.	0.07	0.14	0.15	0.15	0.09	0.1	0.14	0.16
LOI	3.32	0.92	2.91	10.83	2.69	3.91	6.17	0.75	1.34	2.57
TOTAL	100.67	99.87	100.22	99	100.76	100.2	100.78	100.36	100.22	99.41
[2]As (ppm)	N.D.	N.D.	N.D.	59	14	3	36	N.D.	N.D.	N.D.
[2]Ag (ppm)	N.D.	N.D.	N.D.	N.D.	N.D.	N.D.	N.D.	N.D.	N.D.	N.D.
[2]Cr (ppm)	13	12	85	74	120	154	91	225	17	22
[2]Ni (ppm)	N.D.	N.D.	95	86	29	28	119	88	10	8
[2]Co (ppm)	N.D.	N.D.	39	36	32	36	47	50	12	N.D.
[2]Sc (ppm)	N.D.	N.D.	41	41	34	33	45	46	10	N.D.
[2]V (ppm)	N.D.	N.D.	266	255	267	267	271	310	70	50
[2]Cu (ppm)	N.D.	N.D.	57	53	41	60	77	48	11	N.D.
[2]Pb (ppm)	6	N.D.	N.D.	19	N.D.	N.D.	N.D.	N.D.	N.D.	N.D.
[2]Bi (ppm)	N.D.	N.D.	N.D.	N.D.	N.D.	N.D.	N.D.	N.D.	N.D.	N.D.
[2]Zn (ppm)	127	30	100	245	59	65	128	93	59	60
[2]W (ppm)	N.D.	N.D.	N.D.	N.D.	N.D.	N.D.	N.D.	N.D.	N.D.	N.D.
[2]Mo (ppm)	N.D.	N.D.	N.D.	N.D.	N.D.	N.D.	N.D.	N.D.	N.D.	N.D.
[2]Rb (ppm)	46.79	17.95	9.37	53.9	5.84	33.08	11.72	32.3	55.15	25.22
[2]Cs (ppm)	1.17	0.51	0.7	2.66	0.66	2.9	3.49	2.16	1.74	0.62
[2]Ba (ppm)	239	201	311	230	111	335	89	152	646	399
[2]Sr (ppm)	67	56	118	92	239	225	203	196	378	514
[2]Ga (ppm)	27	31	24	25	25	26	25	24	28	26
[2]Ta (ppm)	1.69	1.11	N.D.	0.31	0.34	0.33	0.31	N.D.	0.43	N.D.
[2]Nb (ppm)	28.24	17.18	4.04	4.91	6.37	6.31	5.4	4.82	6.74	3.49
[3]Hf (ppm)	9.25	5.81	2.44	2.16	2.81	2.9	2.47	2.33	4.53	2.47
[2]Zr (ppm)	322	156	89	86	97	101	82	86	161	74
[3]Th (ppm)	5.64	3.83	0.65	0.99	0.99	1.04	1.1	0.94	4.17	1.04
[3]U (ppm)	1.2	0.82	0.17	0.26	0.23	0.25	0.31	0.27	0.84	0.35
[2]Sb (ppm)	N.D.	N.D.	N.D.	N.D.	N.D.	N.D.	N.D.	N.D.	N.D.	N.D.
[2]Se (ppm)	N.D.	N.D.	N.D.	N.D.	N.D.	N.D.	N.D.	N.D.	N.D.	N.D.
[2]Sn (ppm)	N.D.	N.D.	N.D.	N.D.	N.D.	N.D.	N.D.	N.D.	N.D.	N.D.
[3]La (ppm)	47.86	21.36	6.21	9.04	11.2	12.11	9.32	8.3	33.57	7.94
[3]Ce (ppm)	97.04	50.69	15.36	20.79	27.2	28.48	23.06	19.78	69.72	17.52
[3]Pr (ppm)	14.63	7.73	2.25	2.92	3.78	3.87	3.28	2.68	8.18	2.27
[3]Nd (ppm)	58.14	32.4	10.25	12.12	16.64	16.64	14.5	11.94	29.88	9.37
[3]Sm (ppm)	12.74	9.25	2.86	2.92	3.95	3.85	3.65	2.85	4.75	1.91
[3]Eu (ppm)	2.44	1.73	0.97	0.93	1.17	1.23	1.27	0.97	1.19	0.5
[3]Gd (ppm)	12.87	10.75	3.61	3.3	4.17	4.14	4.06	3.22	3.35	1.36
[3]Tb (ppm)	2.07	2	0.61	0.55	0.69	0.65	0.66	0.52	0.45	0.18
[3]Dy (ppm)	12.17	11.97	4	3.07	4.23	4.17	4.21	3.41	2.71	0.8
[3]Ho (ppm)	2.47	2.68	0.82	0.71	0.88	0.88	0.86	0.72	0.51	0.13
[3]Er (ppm)	6.73	7.67	2.42	1.92	2.52	2.53	2.5	2.1	1.47	0.36
[3]Tm (ppm)	0.98	1.22	0.36	0.31	0.37	0.38	0.36	0.32	0.22	0.05
[3]Yb (ppm)	5.99	7.74	2.3	1.93	2.36	2.48	2.3	1.97	1.37	0.36
[3]Lu (ppm)	0.929	1.231	0.366	0.309	0.386	0.376	0.366	0.325	0.224	0.049
[3]Y (ppm)	61.79	67.86	21.38	18.24	23.5	23.19	21.73	19.21	14.66	3.93
[1]CO2 (%)										
[1]S (%)										
[5]Hg (ppb)										
[4]Ag (oz/ton)				N.D.	N.D.	N.D.	N.D.	N.D.		
[4]Au (oz/ton)				N.D.	N.D.	N.D.	N.D.	N.D.		
[5]Au (ppb)					N.D.			N.D.		
[5]Pd (ppb)					N.D.			N.D.		
[5]Pt (ppb)					N.D.			N.D.		

Sample #	01LAH-0521C	01LAH-0522A	01LAH-0522B	01LAH-0522C	01LAH-0528	01LAH-0533A	01LAH-0533B	01LAH-0544	01LAH-0547	01LAH-0548A
UTM East	449357	447909	452865	453722	452579	448626	453702	446456	453783	449575
UTM North	5354764	5353603	5352837	5354117	5351951	5354096	5350397	5362885	5354312	5354929
Rock type	mv (1)	mv (1)	BIF	mv (1)	fv (4)	KGC	CLP	KGC	fv (2)	KGC
[1]SiO2 (%)	52.28	55.67	82.28	61.2	73.52	51.25	69.23	34.97	74.98	49.45
[1]TiO2 (%)	0.87	0.63	0.01	0.56	0.35	0.43	0.46	2.24	0.25	0.83
[1]Al2O3 (%)	15.33	15.1	0.97	15.84	13.87	16.05	14.54	14.14	9.83	15.32
[1]Fe2O3 (%)	11.55	11.08	10.74	6.29	4.04	10.47	4.54	14.3	3.63	12.02
[1]MnO (%)	0.22	0.47	0.52	0.11	0.05	0.19	0.05	0.23	0.05	0.22
[1]MgO (%)	5.89	4.95	1.16	3.62	0.25	7.91	1	3.88	1.24	7
[1]CaO (%)	9.1	6.44	1.18	3.35	0.1	8.54	3.65	7.71	3.34	10.72
[1]Na2O (%)	2.29	2.78	N.D.	4.24	0.23	2.02	3.9	0.35	0.89	1.58
[1]K2O (%)	0.47	0.09	0.03	2.83	4.09	1.49	1.7	3.63	2.14	0.07
[1]P2O5 (%)	0.09	0.1	N.D.	0.11	0.06	0.02	0.08	0.21	0.06	0.06
LOI	2.53	2.84	3.31	2.15	2.94	2.46	1.33	17.35	4.5	2.81
TOTAL	100.62	100.13	100.2	100.29	99.51	100.84	100.5	99.03	100.9	100.07
[2]As (ppm)	2	N.D.	2	N.D.	6	N.D.	N.D.	47	N.D.	7
[2]Ag (ppm)	N.D.	N.D.	N.D.	N.D.	N.D.	N.D.	N.D.	N.D.	N.D.	N.D.
[2]Cr (ppm)	211	251	21	44	7	161	28	45	10	135
[2]Ni (ppm)	77	110	N.D.	30	N.D.	115	9	15	N.D.	55
[2]Co (ppm)	38	26	N.D.	21	N.D.	53	N.D.	60	N.D.	51
[2]Sc (ppm)	40	26	N.D.	15	9	56	9	56	17	61
[2]V (ppm)	281	164	11	118	N.D.	243	34	237	51	323
[2]Cu (ppm)	67	11	37	4	10	112	N.D.	11	N.D.	100
[2]Pb (ppm)	N.D.	9	8	N.D.	N.D.	N.D.	N.D.	N.D.	N.D.	9
[2]Bi (ppm)	N.D.	N.D.	N.D.	N.D.	N.D.	N.D.	N.D.	N.D.	N.D.	N.D.
[2]Zn (ppm)	90	147	50	88	34	83	36	55	32	89
[2]W (ppm)	N.D.	N.D.	N.D.	N.D.	N.D.	N.D.	N.D.	14	N.D.	N.D.
[2]Mo (ppm)	N.D.	N.D.	N.D.	N.D.	N.D.	N.D.	N.D.	N.D.	N.D.	N.D.
[2]Rb (ppm)	16.38	2.53	1.53	78.05	89.27	60.17	41.75	73.74	59.13	1.33
[2]Cs (ppm)	0.44	0.2	0.69	1.26	1.29	0.93	0.33	0.54	0.7	0.06
[2]Ba (ppm)	94	38	N.D.	1292	831	279	593	746	288	39
[2]Sr (ppm)	241	190	3	107	28	125	154	85	31	195
[2]Ga (ppm)	25	24	4	26	31	24	26	31	17	25
[3]Ta (ppm)	N.D.	0.35	N.D.	0.48	0.68	N.D.	0.96	0.55	0.4	N.D.
[2]Nb (ppm)	4.91	5.18	0.24	6.74	10.12	1.49	15.83	7.91	6.26	2.75
[3]Hf (ppm)	2.54	2.73	N.D.	3.7	7.10	0.84	8.26	2.88	5.38	1.61
[2]Zr (ppm)	89	105	N.D.	155	293	22	279	97	196	47
[3]Th (ppm)	1.01	1.67	0.06	2.39	3.37	0.44	4.58	1.41	3.28	0.38
[3]U (ppm)	0.26	0.45	0.13	0.57	0.69	0.11	1.08	0.38	0.66	0.09
[2]Sb (ppm)	N.D.	N.D.	N.D.	N.D.	N.D.	N.D.	N.D.	N.D.	N.D.	N.D.
[2]Se (ppm)	N.D.	N.D.	N.D.	N.D.	N.D.	N.D.	N.D.	N.D.	N.D.	N.D.
[2]Sn (ppm)	N.D.	N.D.	N.D.	N.D.	N.D.	N.D.	N.D.	N.D.	N.D.	N.D.
[3]La (ppm)	9.35	12.09	2.28	16.48	23.78	3.51	33.72	12.83	29.8	4.27
[3]Ce (ppm)	21.58	26.27	4.14	35.16	52.92	8.29	70.75	31.1	64.93	10.5
[3]Pr (ppm)	2.83	3.22	0.49	4.21	7.01	1.09	9.01	4.32	8.18	1.5
[3]Nd (ppm)	12.42	13.04	1.91	16.4	29.00	4.88	36.51	19.58	32.47	7.23
[3]Sm (ppm)	3.04	2.83	0.44	3.42	6.60	1.4	8.24	4.99	6.85	2.29
[3]Eu (ppm)	1.02	0.86	0.26	0.97	1.60	0.55	1.56	1.52	1.42	0.84
[3]Gd (ppm)	3.52	2.76	0.45	3.08	6.68	1.75	8.94	5.29	6.9	2.99
[3]Tb (ppm)	0.61	0.44	0.06	0.5	1.08	0.31	1.46	0.86	1	0.5
[3]Dy (ppm)	3.93	2.75	0.46	3.12	6.90	2.11	9.08	5.29	5.58	3.41
[3]Ho (ppm)	0.84	0.57	0.1	0.62	1.41	0.47	1.94	1.11	0.98	0.73
[3]Er (ppm)	2.52	1.69	0.36	1.74	4.07	1.4	5.6	3.3	2.65	2.21
[3]Tm (ppm)	0.38	0.26	0.05	0.27	0.63	0.21	0.84	0.47	0.37	0.33
[3]Yb (ppm)	2.43	1.66	0.31	1.86	3.84	1.38	5.19	2.88	2.44	2.09
[3]Lu (ppm)	0.384	0.266	0.055	0.282	0.591	0.204	0.814	0.463	0.4	0.335
[3]Y (ppm)	22.88	15.81	3.77	17.53	36.19	12.29	52.35	29.42	26.88	19.68
[1]CO2 (%)					0.29					
[1]S (%)					0.24					
[5]Hg (ppb)										
[4]Ag (oz/ton)								N.D.		
[4]Au (oz/ton)								N.D.		
[5]Au (ppb)								N.D.		
[5]Pd (ppb)								N.D.		
[5]Pt (ppb)								N.D.		

Sample #	01LAH-0548B	01LAH-0554A	01LAH-0574	01LAH-0576A	01LAH-0576B	01LAH-0587	01LAH-0599	01LAH-0602A
UTM East	453783	455755	449085	449085	449106	455123	452214	455119
UTM North	5354312	5366329	5348694	5348694	5350449	5359546	5355772	5352162
Rock type	fv (2)	fv (4)	fi (13)	fi (13)	fi (13)	fi (13)	iv (4) - alt.	mv (7)
[1]SiO2 (%)	70.1	78.14	71.71	67.79	72.22	66.14	47.55	53.78
[1]TiO2 (%)	0.52	0.18	0.14	0.31	0.11	0.34	0.57	0.68
[1]Al2O3 (%)	13.07	12.25	15.38	15.87	15.14	16.14	13.55	16.8
[1]Fe2O3 (%)	4.83	2.25	1	2.75	0.97	3.01	7.85	8.87
[1]MnO (%)	0.05	0.05	0.02	0.05	0.02	0.05	0.12	0.17
[1]MgO (%)	0.55	0.72	0.36	1.41	0.28	1.83	5.45	4.46
[1]CaO (%)	1.54	0.73	1.55	3.21	1.34	3.68	7.11	10.38
[1]Na2O (%)	4.08	0.84	5.54	5.39	5.5	5.45	2.52	2.12
[1]K2O (%)	1.63	3.09	3.14	2.74	3.29	1.97	0.19	1.08
[1]P2O5 (%)	0.09	0.01	0.04	0.15	0.03	0.13	0.07	0.15
LOI	3.8	1.99	0.56	0.68	0.59	1.48	15.7	1.29
TOTAL	100.26	100.25	99.44	100.35	99.51	100.22	100.69	99.78
[2]As (ppm)	N.D.	N.D.	N.D.	N.D.	N.D.	N.D.	89	N.D.
[2]Ag (ppm)	N.D.	N.D.	N.D.	N.D.	N.D.	N.D.	N.D.	N.D.
[2]Cr (ppm)	14	11	5	22	N.D.	67	378	155
[2]Ni (ppm)	N.D.	N.D.	N.D.	12	N.D.	26	109	85
[2]Co (ppm)	N.D.	N.D.	N.D.	N.D.	N.D.	16	37	37
[2]Sc (ppm)	8	N.D.	N.D.	7	N.D.	N.D.	38	34
[2]V (ppm)	52	N.D.	12	47	12	57	189	209
[2]Cu (ppm)	8	N.D.	N.D.	N.D.	N.D.	N.D.	51	52
[2]Pb (ppm)	8	N.D.	15	13	26	12	N.D.	5
[2]Bi (ppm)	N.D.	N.D.	N.D.	N.D.	N.D.	N.D.	N.D.	N.D.
[2]Zn (ppm)	37	63	35	55	35	47	74	93
[2]W (ppm)	N.D.	N.D.	N.D.	N.D.	N.D.	N.D.	N.D.	N.D.
[2]Mo (ppm)	N.D.	N.D.	N.D.	N.D.	N.D.	N.D.	N.D.	N.D.
[2]Rb (ppm)	51.47	93.17	63.01	51.47	73.35	49.41	3.67	31.54
[2]Cs (ppm)	0.64	3.02	0.53	0.49	0.86	1.5	0.19	0.37
[2]Ba (ppm)	380	263	1026	1556	1209	993	70	270
[2]Sr (ppm)	72	47	501	883	582	958	151	370
[2]Ga (ppm)	28	34	26	26	26	26	22	23
[2]Ta (ppm)	1.25	1.76	N.D.	N.D.	N.D.	0.35	0.36	N.D.
[2]Nb (ppm)	19.16	29.99	2.6	4.86	2.26	5.56	5.98	4.04
[2]Hf (ppm)	8.47	13.29	2.23	3.38	2.16	3.92	3.36	2.29
[2]Zr (ppm)	284	456	58	87	49	83	122	83
[2]Th (ppm)	5.95	5.44	2.81	2.7	1.64	6.48	1.23	1.56
[2]U (ppm)	1.26	1.42	0.72	0.54	0.92	0.81	0.31	0.38
[2]Sb (ppm)	N.D.	N.D.	N.D.	N.D.	N.D.	N.D.	N.D.	N.D.
[2]Se (ppm)	N.D.	N.D.	N.D.	N.D.	N.D.	N.D.	N.D.	N.D.
[2]Sn (ppm)	N.D.	N.D.	N.D.	N.D.	N.D.	N.D.	N.D.	N.D.
[3]La (ppm)	37.23	45.34	16.32	22.46	8.19	29.09	10.36	12.56
[3]Ce (ppm)	84.26	97.94	27.02	47.52	16.64	57.07	24.16	28.86
[3]Pr (ppm)	10.81	14.46	3.66	6.34	2.08	7.12	3.22	3.62
[3]Nd (ppm)	43.79	61.02	12.82	24.8	7.45	26.03	13.98	14.88
[3]Sm (ppm)	9.88	15.16	2.22	4.96	1.39	4.46	3.5	2.99
[3]Eu (ppm)	1.81	3.69	0.58	1.36	0.42	1.17	0.94	0.9
[3]Gd (ppm)	9.84	16.86	1.43	3.73	0.93	2.97	3.94	2.76
[3]Tb (ppm)	1.7	3.02	0.17	0.47	0.11	0.37	0.65	0.45
[3]Dy (ppm)	10.85	19.24	0.79	2.23	0.55	1.76	4.25	2.63
[3]Ho (ppm)	2.25	4.25	0.14	0.4	0.1	0.32	0.9	0.55
[3]Er (ppm)	6.7	12.72	0.34	0.96	0.28	0.78	2.61	1.69
[3]Tm (ppm)	0.99	1.94	0.05	0.14	0.04	0.12	0.4	0.27
[3]Yb (ppm)	6.42	12.68	0.33	0.83	0.3	0.7	2.54	1.69
[3]Lu (ppm)	0.995	1.974	0.053	0.123	0.048	0.112	0.394	0.283
[3]Y (ppm)	62.56	101.78	4.27	10.87	3.2	8.94	24.03	15.14
[1]CO2 (%)								
[1]S (%)								
[5]Hg (ppb)								
[4]Ag (oz/ton)								
[4]Au (oz/ton)								
[5]Au (ppb)								
[5]Pd (ppb)								
[5]Pt (ppb)								

Metric Conversion Table

Conversion from SI to Imperial			Conversion from Imperial to SI		
SI Unit	*Multiplied by*	*Gives*	*Imperial Unit*	*Multiplied by*	*Gives*
		LENGTH			
1 mm	0.039 37	inches	1 inch	**25.4**	mm
1 cm	0.393 70	inches	1 inch	**2.54**	cm
1 m	3.280 84	feet	1 foot	**0.304 8**	m
1 m	0.049 709	chains	1 chain	20.116 8	m
1 km	0.621 371	miles (statute)	1 mile (statute)	**1.609 344**	km
		AREA			
1 cm^2	0.155 0	square inches	1 square inch	**6.451 6**	cm^2
1 m^2	10.763 9	square feet	1 square foot	**0.092 903 04**	m^2
1 km^2	0.386 10	square miles	1 square mile	2.589 988	km^2
1 ha	2.471 054	acres	1 acre	0.404 685 6	ha
		VOLUME			
1 cm^3	0.061 023	cubic inches	1 cubic inch	**16.387 064**	cm^3
1 m^3	35.314 7	cubic feet	1 cubic foot	0.028 316 85	m^3
1 m^3	1.307 951	cubic yards	1 cubic yard	0.764 554 86	m^3
		CAPACITY			
1 L	1.759 755	pints	1 pint	0.568 261	L
1 L	0.879 877	quarts	1 quart	1.136 522	L
1 L	0.219 969	gallons	1 gallon	**4.546 090**	L
		MASS			
1 g	0.035 273 962	ounces (avdp)	1 ounce (avdp)	28.349 523	g
1 g	0.032 150 747	ounces (troy)	1 ounce (troy)	**31.103 476 8**	g
1 kg	2.204 622 6	pounds (avdp)	1 pound (avdp)	**0.453 592 37**	kg
1 kg	0.001 102 3	tons (short)	1 ton (short)	**907.184 74**	kg
1 t	1.102 311 3	tons (short)	1 ton (short)	**0.907 184 74**	t
1 kg	0.000 984 21	tons (long)	1 ton (long)	**1016.046 908 8**	kg
1 t	0.984 206 5	tons (long)	1 ton (long)	**1.016 046 90**	t
		CONCENTRATION			
1 g/t	0.029 166 6	ounce (troy)/ ton (short)	1 ounce (troy)/ ton (short)	34.285 714 2	g/t
1 g/t	0.583 333 33	pennyweights/ ton (short)	1 pennyweight/ ton (short)	1.714 285 7	g/t

OTHER USEFUL CONVERSION FACTORS

	Multiplied by	
1 ounce (troy) per ton (short)	31.103 477	grams per ton (short)
1 gram per ton (short)	0.032 151	ounces (troy) per ton (short)
1 ounce (troy) per ton (short)	20.0	pennyweights per ton (short)
1 pennyweight per ton (short)	0.05	ounces (troy) per ton (short)

Note: Conversion factors which are in bold type are exact. The conversion factors have been taken from or have been derived from factors given in the Metric Practice Guide for the Canadian Mining and Metallurgical Industries, published by the Mining Association of Canada in co-operation with the Coal Association of Canada.

MAPS NOT FILMED

CARTES NON REPRODUITES

micromedia
a division of IHS Canada

20 Victoria Street
Toronto, Ontario M5C 2N8
Tel.: (416) 362-5211
Toll Free: 1-800-387-2689
Fax: (416) 362-6161
Email: info@micromedia.on.ca